**Article:**
Mirón-Mérida, VA, Gong, YY orcid.org/0000-0003-4927-5526 and Goycoolea, FM (2021) Aptamer-based detection of fumonisin B1: A critical review. Analytica Chimica Acta, 1160. 338395. ISSN 0003-2670

https://doi.org/10.1016/j.aca.2021.338395

# Aptamer-based detection of fumonisin B1: A critical review

Vicente Antonio Mirón-Mérida[1,*], Yun Yun Gong[1], Francisco M. Goycoolea[1,*]

[1] School of Food Science and Nutrition, University of Leeds, Leeds LS2 9JT, UK; Y.Gong@leeds.ac.uk (Y.Y.G)
* Correspondence: fsvamm@leeds.ac.uk (V.A.M.M); F.M.Goycoolea@leeds.ac.uk (F.M.G.)

**Abstract:** Mycotoxin contamination is a current issue affecting several crops and processed products worldwide. Among the diverse mycotoxin group, fumonisin B1 (FB1) has become a relevant compound because of its adverse effects in the food chain. Conventional analytical methods previously proposed to quantify FB1 comprise LC-MS, HPLC-FLD and ELISA, while novel approaches integrate different sensing platforms and fluorescently labelled agents in combination with antibodies. Nevertheless, such methods could be expensive, time-consuming and require experience. Aptamers (ssDNA) are promising alternatives to overcome some of the drawbacks of conventional analytical methods, their high affinity through specific aptamer-target binding has been exploited in various designs attaining favorable limits of detection (LOD). So far, two aptamers specific to FB1 have been reported, and their modified and shortened sequences have been explored for a successful target quantification. In this critical review spanning the last eight years, we have conducted a systematic comparison based on principal component analysis of the aptamer-based techniques for FB1, compared with chromatographic, immunological and other analytical methods. We have also conducted an *in-silico* prediction of the folded structure of both aptamers under their reported conditions. The potential of aptasensors for the future development of highly sensitive FB1 testing methods is emphasized.

**Keywords:** Biosensors; mycotoxins; fumonisin B1; aptamers; aptasensors; analytical methods

## 1. Introduction

Mycotoxins are thermoresistant low molecular weight (300-700 Da) secondary metabolites, mainly produced by fungi such as *Alternaria*, *Aspergillus*, *Claviceps*, *Fusarium* and *Penicillium*, as part of their defense mechanism [1, 2]. These biotic compounds act as hazards towards vertebrates, causing diseases when ingested, inhaled, or through skin contact. Some infectious processes, for instance, mycotoxicosis, take place after metabolization and accumulation of mycotoxins in several organs and tissues, due to immediate and progressive consumption of different contaminated food commodities [3], namely cereals, cocoa, coffee, fruit juices, milk and dairy, vegetable oils, beer, dried fruits, nuts, spices and their derived products. The presence of mycotoxins in feed affects the livestock industry by negatively impacting not only the animal health, but also the human health through the consumption of contaminated by-products (eggs, meat, milk) [4]. Similarly, the presence of mycotoxins in cereals, fruits, and nuts could prevail after beverage processing, which corresponds to their manifestation in wine, beer, fruit and vegetable juice, drinks and spirits, as well as cocoa, coffee and liquorice [5] Initially, the production of mycotoxins is determined by environmental and ecological conditions (temperature, type of substrate, moisture and humidity, water activity, physical damage, insects, fungicides) [6]. However, multiple food matrices have been considered for the mitigation of toxin contamination [7], as mycotoxin occurrence also takes place at different stages of the food chain, including field handling, storage and subsequent steps. Although the WHO estimated that 25% of the food crops worldwide were contaminated with mycotoxins, recent estimations have revealed that as high as 60 to 80% of occurrence can be detected in many food products [1].

Among the nearly 300 different mycotoxins that have been documented, the most relevant from a food safety perspective comprise aflatoxins (AFB1, AFB2, AFG1, AFG2, AFM1), citrinin, deoxynivalenol, ergot alkaloids, fumonisins (FB1, FB2), HT-2 toxin, ochratoxin A, patulin, T-2 toxin and zearalenone, whose co-occurrence in food products could reach more than 40% incidences,

which might derived in multiple toxicological effects via co-exposure [1, 2, 8, 9]. In addition to mycotoxicosis, mycotoxins are related to carcinogenic and mutagenic effects along with reproductive, immune, renal, fetal and hepatic complications [2].

Exposure to mycotoxins is more likely to arise in regions with scarce methods for manipulating and storing food products and can be related to other conditions such as malnutrition, limited regulations, and lack of protection for exposed groups [10]. These metabolites affect staple foods widely consumed in the poorest and most vulnerable areas of Africa, Asia and Latin America [11]. Likewise, high-income countries are not exempt from mycotoxin occurrence, especially those importing agricultural and processed products from developing economies. North America and Europe encounter the highest mycotoxin risk in livestock [8]. As shown in Figure 1, there has been an increasing number of mycotoxin notifications in the last five years for the European Union (EU), whereas the United Kingdom (UK) has maintained a regular number of incidences, mostly identified through alerts, and border rejections of food and feed from EU member and non-member countries. To date, products such as peanuts, pistachios, hazelnuts, groundnuts, almonds, nutmeg, chilies, maize and dried figs are the most recurrent commodities exhibiting mycotoxin contamination; with a greater incidence in goods from Africa, South Asia, South America, China, USA and the Middle East [12].

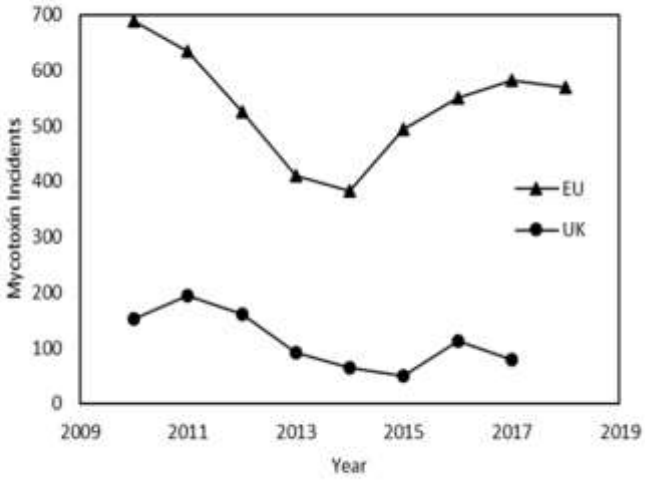


**Figure 1.** Number of mycotoxin notifications per year in the EU and the UK. Data based on the available Rapid Alert System for Food and Feed 2010-2018 by the European Commission [12] and the Incidents Annual Report 2010-2017 by the Food Standards Agency [246]

Mycotoxin contamination negatively impacts a public health and food safety level, as denoted by the economic losses in the food sector, mainly generated by a reduction on crop yields, product trade profit and livestock production. Such impact is estimated in billions of dollars and it is heightened by additional costs related to the application of control strategies and mycotoxin analysis, mostly imposed to the producers by several regulations [4, 5, 13, 14]. Likewise, prohibitions placed on contaminated products from African countries represent millionaire loses [6]. The occurrence of mycotoxins in crops modifies the fluctuations of market supply and demands, the costs in local, regional and international markets and generates public health-related costs due to interventions on medical services and support to people with mycotoxin-related disabilities [11]. For those reasons, the identification and sensitive quantification of low mycotoxin levels is a necessity for the worldwide panorama [2]. In fact, current estimations of a higher mycotoxin occurrence in food products are not only related to the effect of climate change, but also to the development of more sensitive analytical methods [1]. This was especially achieved through the advent of highly sensitive LC-MS methods, where a 200-fold improvement has allowed the analysis of multiple metabolites within the same run [8].

In developed countries such as the United Kingdom, ongoing surveillance strategies are planned for the prediction and satisfactory estimation of mycotoxins in imported goods [15]. The analytical methods utilized, namely HPLC-MS, and rapid screening methods (quantitative enzyme-linked immunosorbent assay (ELISA), fluorometric and lateral flow methods), require advanced infrastructure, electricity supply, availability of reagents, experienced technicians, instrument maintenance and validated tools. Consequently, developing countries commonly tend to utilize less complex techniques such as thin-layer chromatography (TLC) and immunological methods with semi-automated detections and minimal sample purification. TLC integrates expensive standards which are converted into perishable solutions requiring freezing and refrigeration. Similarly, antibody-based kits still present constrains regarding their refrigeration and shelf-life [11]. In this regard, even when conventional methods for mycotoxin detection, including chromatographic (HPLC, LC-MS, TLC, GC-MS) and immunological (ELISA) techniques, exhibit excellent sensitivities, their performance requires long times, expensive instrumentation and specialized operators, which limits their utilization for point-of-care and on-site analysis, and leads to the prioritization of decontamination methods [14, 16]. ELISA is a sensitive, accurate, selective and reproducible technique, which depending on its detection strategy, could be arranged in low cost, portable, and multiplex methods. This method's main disadvantages are the long incubations and its required multi-step washings, which are not suitable for its desired automatization [17, 18].

Furthermore, methods such as GC-MS and two-dimensional liquid chromatography difficult the analysis of polar metabolites, while small-sized compounds and the absence of specific biomarkers also produce analytical limitations [19, 20]. The application of chemometrics in infrared spectroscopy is still a time-consuming method due to its calibration stage [19]. Analytical methods in rural areas should be rapid, easy to implement whilst involving little transportation and a wide analytical scope [11]. Despite the indicated challenges, mycotoxin detection needs to be carried out in places with geographical and economic constrains, especially low-income countries with high mycotoxin exposure and outbreak risk [2, 13].

This goal can be achieved with advanced analytical methods, including novel biosensing techniques, which could be developed as quick yet accurate assays, with significant cost reductions. Novel methods include the innovation of previously used concepts, the development of original mechanisms and the resourceful integration of specific technology. For instance, displacement immunosensing reactions for mycotoxin detection have been studied through the role of versatile materials as pseudo haptens and nanocontainers. Particles such as mesoporous silica were loaded with glucose, whose design was scaled to a portable analysis, where the indirect measurement of the target molecule (AFB1) corresponded to the concentration of free glucose measured with a personal glucometer. Although this type of designs have been disclosed as quick, portable and low-cost detection methods comparable to commercial ELISA kits, cross reactivity was reported under the presence of analogue molecules (AFB2), while some issues related to the generation of

nanomaterials included the long synthesis time, and the lack of repeatability when a different batch was used [21].

Electrochemical methods can be coupled with competitive immunoreactions and aptamer-based detections, in which different particles and platforms (gold nanoparticles, magnetic nanoparticles, microplates) are functionalized with monoclonal antibodies (mAb) or aptamers for the achievement of low limits of detection (LODs) [22, 23]. As the use of one competitive immunoassay might not be enough for small mycotoxins, occasionally, two different reactions can be coupled within the same approach [23]. This strategy involves an initial competitive immunoreaction between the specific mycotoxin and its labeled/loaded mycotoxin conjugate, which depending on the nature of the labeling/loading agent (dopamine, L-cysteine, glucose oxide, silver nanoparticles, invertase) and the interacting nanoparticles (liposomes, magnetic beads, silica), can be followed by hydrolytic reactions [23], redox reactions [24], lysis [25, 26], and acid dissolution [27], with an indirect photoelectrochemical determination of the target concentration.

Photoelectrochemical detections portray the advantages of both electrochemical and optical assays, including high sensitivity, ease for miniaturization, and low background signals, cost and power needs [25]. However, some photoelectrochemical approaches require laborious steps, which make the determination a complex procedure [26]. In addition, the sample purity required for electrochemical biosensors increases the assay time, especially in complex food matrices [19]. Mycotoxins' enzyme-based detection can be an affordable, simple and yet a sensitive and selective option when utilized. Nevertheless, its long incubation and detection times might represent a disadvantage for a large-scale application [18]. Besides, although the use of nanomaterials results in cost-effective, rapid testing where different nanostructures (e.g. sheets, particles) increase the sensitivity, in addition to the long synthesis and modification procedures, some nanomaterial-based designs also indicate cross-reactivity (low selectivity), color interference and higher detection limits when used in colorimetric methods [18].

Fluorescent and chemiluminescent dyes and nanoparticles have been applied in bulk and paper-based detections [28, 29], which, even when sensitive in real samples, require specialized electronic and optic equipment [30]. Antibody-based tests for mycotoxin detection have been commercially developed as dipsticks in different kits [11]. Moreover, innovative biosensors have integrated the help of antibodies and colloidal gold [31], with the improved integration of smartphone-based readings [16]. Although many reported lateral flow and microfluidic-based assays, applying aptamers, enzymes or antibodies, are simple, quick, sensitive, and low-cost, in-situ arrangements, they occasionally provide qualitative results, higher LODs, and their reproducibility and stability remain undetermined [17, 18].

Other important challenges associated with detecting mycotoxins in food samples appear during sample pretreatment, where mycotoxins are commonly extracted from the food matrix with organic solvents or acidified water, followed by filtration, centrifugation and sometimes more clean-up steps. Although some solvents can affect the performance of certain bioreceptors (*e.g.* enzymes, antibodies), interfering food compounds including lipids, proteins, sugars and salts must be removed before the analysis in order to avoid peak overlap, fluorescence quenching or signal suppression in different detection methods [18, 20]. Likewise, multi-detection methods require sample cleaning within the minimum pretreatment steps and sample loss [19]. Another issue is caused by masked mycotoxins, which form through the conjugation with polar compounds (sugars), resulting in a less detectable metabolite [32]. Apart from conjugation, modified mycotoxins can also undergo hydrolysis, degradation, covalent and non-covalent binding to food matrices, which also derive in analytical underestimation [33]. In the case of fumonisins, a strong matrix interaction has been observed, in which the extraction yield is influenced by the matrix constituents and the extraction conditions, resulting in matrix dependent recoveries [33].In this critical review an exploration of the aptamer-based detection methods of FB1 was carried out by their graphical and principal component analysis comparison with different conventional and novel techniques. Additionally, different aptamers specific for FB1 were identified and separately presented according to their detection signal (fluorescence, electrochemical, colorimetric, others), with a further in-silico prediction of their folded structure.

### *1.1 Fumonisin B1*

Fumonisins are usually small alkyl amines containing two hydroxyl esterified propane tricarboxylic acids (tricarballylic acid), which are linked to adjacent carbons (Figure 2) [34]. When substituted in up to seven “R” side chains, the fumonisin aliphatic backbone serves as the basic structural unit for the conformation of different analogues. Existing fumonisin analogues can be classified in series A, B, C and P, where group B is the most abundant in nature [35]. Understanding the structure of fumonisins is critical when selecting and refining some quantification methods. For instance, group B fumonisins are soluble in water and polar solvents, therefore, they can be extracted from the food matrix with binary mixtures of water and methanol or acetonitrile [33].

Fumonisins B1 and B2 were initially studied and isolated from *Fusarium verticillioides*, formerly known as *Fusarium monoliforme*. They were discovered during the investigation of compounds responsible for leukoencephalomalacia, toxicity and hepatocarcinogenicity in some animal species [35]. Early studies reported the main role of F. *verticillioides* in the production of FB1, FB2, FB3 (iso-FB2), FB4, FA1, FA2 and FC1 [36-39], when cultivated in liquid cultures and solid matrices (maize). However, depending on the host crop and growth media, fumonisins can be generated by other fungal species such as *Alternaria alternata* on potato dextrose agar [40], stationary cultures of *Aspergillus niger* producing FB6 and FB2 [41, 42], and some strains of *Tolypocladium cylindrosporum*, T. *geodes* and T. *inflatum* which developed fumonisins in high sugar media, when incubated at 25-30 ˚C [43].

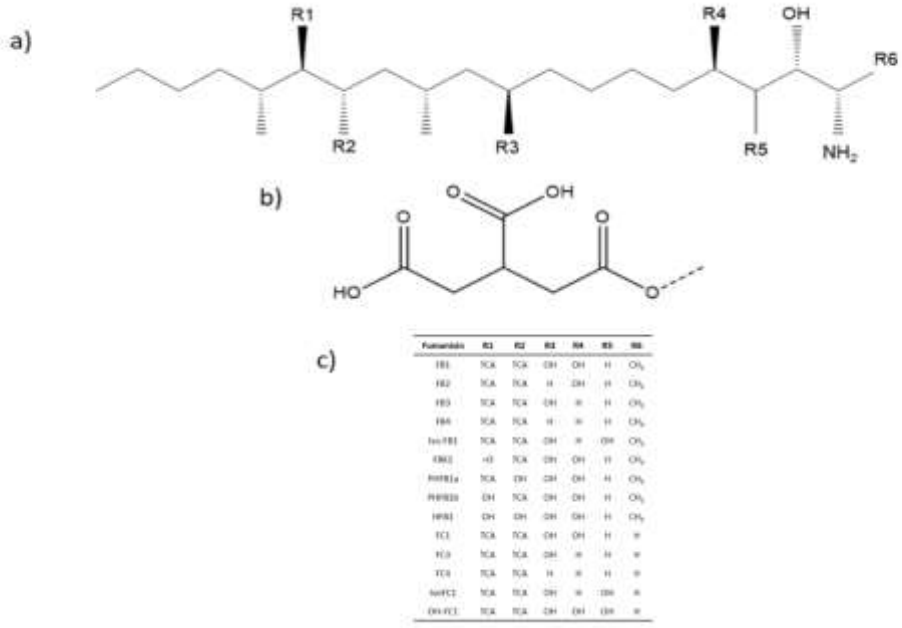


**Figure 2.** Structure representation of (a)the general fumonisin backbone, (b)tricarballylic acid (TCA) and (c)a list of alkyl amine fumonisins [35]

*1.2 Effects of fumonisin B1 on health*

Classified as group 2B hazard, fumonisins B1 and B2, are possible carcinogenic to humans [44]. Fumonisin B1 causes multiple effects on different species, its toxicity was first related to the disruption of sphingolipid metabolism, as this mycotoxin inhibits ceramide synthase, which leads to both an increase in sphinganine and a decrease in complex sphingolipids, and further cell death observed in pig kidney cells [45, 46]. Notwithstanding this frequent assumption, studies on the protective role of liver X receptor (LXR) on FB1-caused hepatotoxicity implied the presence of different pathways [47].

Another mechanism triggered by FB1 is oxidative stress, where FB1 reduces mitochondrial and cellular respiration and increases the production of reactive oxygen species, as observed in rat astrocytes and human neuroblastoma cells [48]. In the same way, FB1 reduced growth of pig iliac endothelial cells and their barrier functions, while decreased the activities of some enzymes with antioxidant effects and enhanced the formation of lipid peroxidation compounds [49]. Exposure to fumonisin could also induce epigenetic changes such as DNA methylation and hypomethylation in rat glioma cells and human intestinal and hepatoma cells [48]. Apart from neurotoxicity, hepatotoxicity, nephrotoxicity, and carcinogenicity, FB1 has also been studied in corneal infections, due to its ability to form Langmuir monolayers on liquid surfaces [50]. Besides, some geographical studies have correlated the prevalence of esophageal cancer in humans with the presence of FB1 and FB2 in regional crops [51, 52].

In addition, adverse effects from fumonisins in human health were reported for Mexican American women living in the border region between Mexico and Texas, where fumonisin exposure was associated with neural tube defects [53]. Fumonisin B1 occurrence in Tanzania was reported in breastfeeding with contaminated milk as a current issue among children under six months of age [54]. Elevated levels of dietary fumonisin were likewise related to inhibition of ceramide synthase in women from Guatemala [55], whose consumption of contaminated maize was detected in their high urinary fumonisin levels [56]. Other studies conducted in Tanzania have demonstrated the main role of fumonisin in underweight children due to breastfeeding and weaning within the first 36 months of age [57], as well as the high impact of substituting breastfeeding on the mycotoxin exposure of infants [54]. Even though fumonisin B1 is not as prioritized as other mycotoxins, its single exposure and its combination with other mycotoxins such as aflatoxins, represent an issue that needs to be addressed in deep, due to its common occurrence.

*1.3 Fumonisin occurrence in food commodities and its worldwide regulation*

The Food and Agriculture Organization (FAO) of the United Nations trough the worldwide regulations for mycotoxins in food and feed, indicated that by 2003 only 99 countries had regulations in place focused on mycotoxins. Additionally, the extent of those actions covered a brief group of different toxins among continents. As it can be noticed from Figure 3, the regulations for fumonisins in food and feed are established on either the sum of fumonisins type B1+B2+B3, B1+B2, or as total content of FB1 [58]. The maximum allowable contamination limit for the sum of FB1 and FB2 is commonly established as 2000 µg/kg and 4000 µg/kg for maize meal and raw maize, respectively, based on the Codex Alimentarius Commission [32]. However, as indicated in Table 1, this value has been lowered to 1000 µg/kg in different countries including Iran, France, Bulgaria, Switzerland, Cuba, and Brazil, not only for maize but other cereals and their derived products [5, 14]. Furthermore, more rigorous regulations have been placed for maize-based breakfast cereals, snacks (800 µg/kg) and food for infants (200 µg/kg) (Table 1). Moreover, a maximum tolerable daily intake of 2 µg/kg has been indicated, while the occurrence of FB1 in cereals (*e.g.*, corn, wheat, rye) oscillates between 40-6000 µg/kg in Europe, 11-30000 µg/kg in Africa, 0.30-18800 µg/kg in Asia and 5-15050 µg/kg in America [32].

The number of countries under fumonisin regulations is equivalent for Europe and Asia/Oceania. On the other hand, the North America region has a noticeable approach by the United States, where limits for mycotoxins are targeted not only in food, but in feed. Based on the FAO controls, Africa was overall the less active region in enforcing mycotoxin regulations, particularly for any type of fumonisin. Paradoxically, though perhaps not surprising, the highest incidence of mycotoxins in food and feed

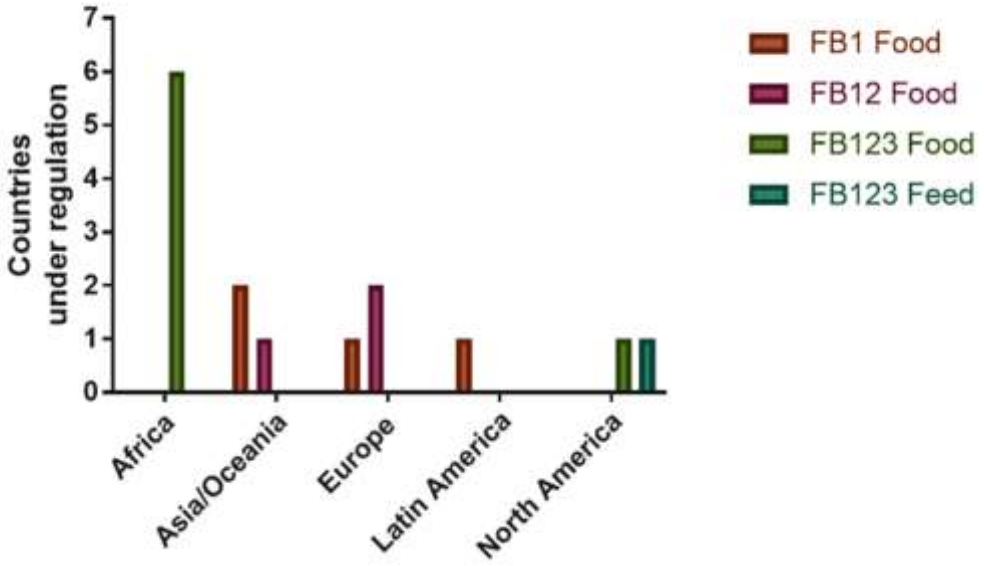


**Figure 3.** Countries regulating fumonisin in food and feed worldwide [58]

occurs in Africa [59], however since 2011 a control for aflatoxin and fumonisin was established by the East African Community (EAS), whose scope included the six member countries, with a potential application on the trade activities by the twenty COMESA member states (Table 1). Furthermore, Latin America possesses a gap in recognizing fumonisins as an important group of hazardous compounds [58].

The growth of fumonisin producing fungal species has been reported on corn seedlings, grits, meal and flour, tomato leaves, seedlings and rice [34, 38, 60-62] as well as some dried samples comprising coffee beans and vine fruits [63, 64]. Some *Fusarium* species can produce fumonisins in media based on rice, oat, carrots and malt. In contrast, *A. niger* requires low water activity media and products with high sugar content [41, 64]. Maximum levels of fumonisins in both food and feed are shown in Table 1. As previously mentioned, cereals, rice and maize food and feed products are the most common targeted commodities for possible fumonisin outbreaks. Understanding the maximum values established by regulation, along with the expected contamination levels for distinct samples, is crucial during the design of conventional and novel quantification methods. Also, it is necessary to know the scope and applicability of each technique. The focus of this systematic comparison centers in these aspects by reflecting the state of the art in the field since 2012. In this regard, a 2016 review, focused on fusarium mycotoxins, reported 8 aptasensors from the 9 disclosed until 2015 [17]. Some articles considered the existence of a single aptamer specific to FB1 [65-68], despite the disclosure of two sequences selected through SELEX [69,70], while other cases reported minimers (shortened sequences) as individual aptamers [71]. More recent articles have overlooked the total number of publications about aptamer-based biosensors for FB1 [18, 20, 72-75], likewise some other reviews only focused on one specific type of signal (*e.g.*,electrochemical, colorimetric, photoelectrochemical) for the identification of different mycotoxins, which also limited the number of reported techniques for FB1 [18, 76, 77]. Therefore, this review was necessary as the majority of aptamer applications (23 biosensors) for FB1, were reported after 2016. Additionally, this is the first review specialized in addressing all the reported aptamer sequences for detecting FB1 since the first FB1 aptamer publication in 2010 [69], with the novelty of a statistical comparison among different read-outs, and with other novel and conventional techniques. Hence, this work not only enlists existing aptamer-based biosensing techniques for FB1, but also discusses the best approaches in terms of the limit of detection, assay times and assay preparation times, with a thorough exploration of different

developments, improvements and new discoveries that occurred throughout this decade of aptasensing research for this important mycotoxin.

## 2. Methods

### *2.1 Systematic comparison*

For this systematic comparison a screening was made from results obtained after searching the words “fumonisin + aptamer” and “FB1 + aptamer” in Scopus (28, 12), Web of science (28, 14), and Google Scholar (4, 32); as well as papers containing the specific DNA sequences. As indicated in Scheme 1, from the 35 relevant papers, 32 biosensors were identified and compared with other conventional methods for FB1 detection in terms of their limit of detection (LOD), assay time, and assay preparation time. The data were plotted in GraphPad Prism 7 to show the evolution and relation of such parameters throughout the years.

### *2.2 Principal component analysis*

Aptamers are single-stranded DNA (ssDNA) or RNA, commonly formed by 20 to 220 random nucleotides. From the $10^{15}$ existing random sequences specific to different molecules, aptamers specific to fumonisin have been reported as ssDNA sequences. Aptamer-based sensors, also known as aptasensors, exploit the advantages of such oligonucleotides, including their great affinity, specificity, and applicability, which are promoted by the folded 3D structures generated by means of their complementary base pairs. Aptamer recognition occurs through hydrogen bonds, van der Waals forces, stacking and electrostatic interactions, which enable the recognition between chiral enantiomers, changes in one functional group (hydroxyl, methyl) and slight structural modifications. This is a mechanism observed as either the encapsulation of small molecules (*e.g.,* nucleotides, mycotoxins) or the insertion of large targets (*e.g.,* proteins, cells) [17, 67, 71]. Biosensors utilizing aptamers as bioreceptors, portray excellent sensitivity, selectivity and allow in-field detections with multifunctional, robust, modular and price competitive designs [78]. In some cases, aptasensors portray better results to those with other bioreceptors, for instance biosensing techniques applying surface plasmon resonance of AuNPs have been broadened and improved when aptamers were integrated, in comparison to the immunological developments of this principle [18]. To confirm the existence of such advantages from aptasensors over different methods, all the aptamer-based biosensors for FB1 detection and several conventional and novel methods published since 2012 (publication year of the first aptasensor), were combined in a principal component analysis, performed in Minitab 15 Statistical Software. Before the application of the correlation matrix, all data were treated according to the following equations:

$$LODt = \frac{LOD\ \ max}{LOD} \qquad ATt = \frac{AT\ \ max}{AT} \qquad APt = \frac{AP\ \ max}{AP}$$

Where LODt , ATt and APt are the treated limit of detection, assay time and assay preparation time, respectively; LODmax and ATmax are the maximum limit of detection and maximum assay time for all the data in this comparison (since 2012), equal to 3200 µg/L [79] and 720 min [80], respectively. The assay preparation time was calculated by adding the reported times for sample extraction, synthesis of nanoparticles, support treatment, and array assembling. The maximum preparation time per assay was calculated as 12900 min [81]. This mathematical treatment allowed to determine the maximum values' correlation to the most sensitive, fast and therefore, effective methods.

### *2.3 DNA folding*

The DNA folding forms of the four existing aptamers were predicted with mfold Web Server according to their reported folding conditions.

## 3 Conventional and novel methods for mycotoxin identification

Typical methods for identifying mycotoxins in food samples incorporate compound separation principles for the quantification through TLC, HPLC, and LC-MS [11, 75, 82]. Simultaneously, some commercial immunoassays optimized the use of antibodies for mycotoxin quantification [11, 82]. However, most of them utilize expensive and sophisticated equipment for time-consuming assays that are required to be performed by skilled operators, as they utilize complex elements and instruments [16, 83]. Novel approaches including optical [84,85], electrochemical [86] and surface-sensitive techniques (e.g., surface plasmon resonance, ion-selective field-effect transistors, surfaced-enhanced Raman spectroscopy) along with aptamer-based techniques [87-91], have been developed and found to exhibit comparable and even higher sensitivities than that of conventional procedures [92, 93].

Based on Tables 2-5, the LODs of different reported methods were plotted against their total assay times, as reflected on Figure 4a. The assay time was calculated from either the divulged times at either the injection step in chromatography, or the incubation between the antibody/aptamer/recognition region with its corresponding target molecule. This consideration excluded any pre-treatment, extraction steps and particle fabrication, as those phases were part of the assay preparation time (Figure 4b). The shortest response time for the analysis of extracted samples was achieved in seconds to minutes, when using Surface-enhanced Raman spectroscopy [94]. Nevertheless, some sensors qualified as fast required overnight steps and long incubation times for the whole system arrangement, especially when the synthesis of nanoparticles and drying phases were required. Assay times below ten minutes were achieved through chromatographic, immunoassays, and some innovative methods, nonetheless the more sensitive assays were secured with aptamer-based biosensors [89, 95, 96], immunosensors with carbon nanotubes [97, 98], and molecularly imprinted polymer nanoparticles (MIPs) [86], as indicated in Figures 4a and 4c.

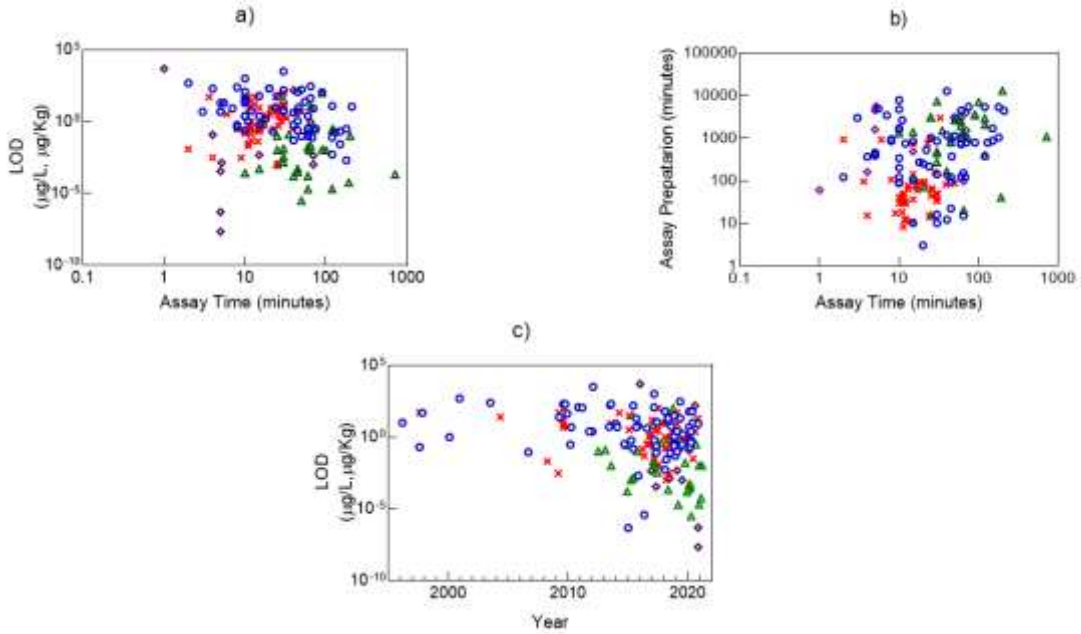


**Figure 4.** Relation of the assay time with (a) the limit of detection (LOD) and (b) assay preparation time for the approaches reported since 2012, (c) and LODs achieved over time through different methods (**O**: Immunologic, **X**:Chromatographic, **Δ**: Aptamer-based, **◊**: Other)

In addition to high specificity, the combination of minimum assay times with low limit of detections is ideal for an appropriate quantification technique. Nonetheless, an increase in the assay preparation time can complicate the achievement of on-site/point-of-care analysis and compromise the reproducibility. Even though there is high sensitivity achieved through aptasensors, such DNA-based techniques along with some immunoassays, entail long assay times with extended preparation time, due to incubation and platform preparation, respectively (Figure 4b). In those cases, the final response was normally measured as either a fluorescent or a colorimetric signal. Figure 4c portrays the LODs accomplished per year, where it can be noted that ongoing research is still focused on developing chromatographic techniques and immunoassays.

Although, over the last five years there has been an improvement on the detection limits of some protocols, especially for immunoassays whose LODs have reached the picogram scale, most of the new chromatographic and antibody-based methods still quantify values comparable to earlier findings. Conventional assays with the highest sensitivity have included electrochemical designs, electrochemiluminescent quantifications, and MS detection (Table 2-3). Of note, fluorescent, colorimetric and electrochemical aptamer-based sensors reported over the last three years, accomplished relevant LODs with a promising tendency (Figure 4).

Despite the fact that the use of antibodies with electrochemical readouts was advantageous for achieving some of the lowest LODs for fumonisin B1, equivalent to $4.6x10^{-7}$ and $3.7x10^{-6}$ µg/L [97, 98], these immunosensors were not included in the principal component analysis (PCA), as no assay time was reported in either case. Hence, as indicated in Figure 5, LC-MS [92, 93], immunoassays with optical [84, 85, 99], Raman (due to its quick procedure) [94], fluorescent readouts [100] and electrochemical MIPs [86] were correlated to the combination of low LODs with short assay times. However, such statistical analysis did not show the advantages of aptamer-based methods, which was also observed on the correlation of short assay preparation times with LC-MS, immunologic and only three aptasensors [89-91]. This was shown by PCA, where the main drawbacks from aptamer-based sensors for FB1 was their long assay and assay preparation times denoted by the absence of correlation in both components when compared to other methods.

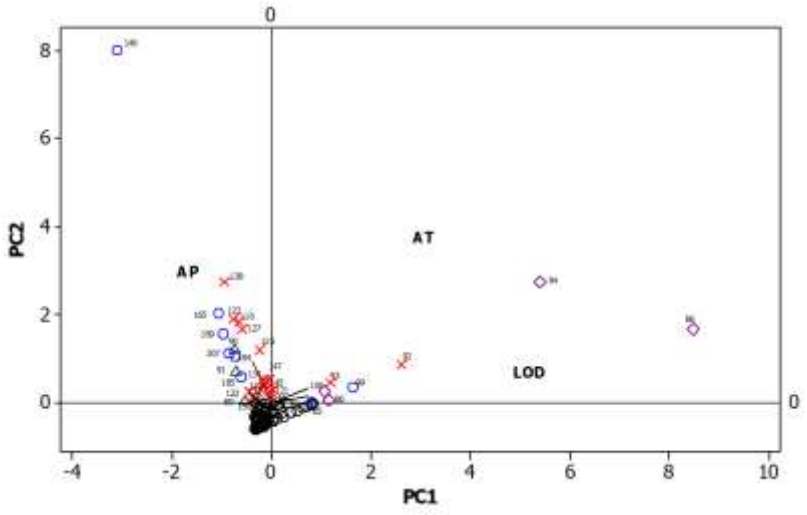


**Figure 5.** Principle component analysis for the correlation of aptasensors and conventional methods reported from 2012 to the lowest detection limits (LOD), assay time (AT) and assay preparation time (AP). (**O**: Immunologic, **X**: Chromatographic, **Δ**: Aptamer, **◊**: Other). The numbers correspond to the correlated references from Tables 2-5.

*3.1 Chromatographic detection of fumonisin B1*

Together with immunoassays, chromatographic methods for the quantification of mycotoxins, have been widely studied and optimized for the analysis of several food products as indicated in Table 2. Initial chromatographic techniques were focused on the exclusive quantification of fumonisin in corn, through the analysis of either MS/MS or fluorescence signals. Following analysis confirmed the good correlation of maize-based products expenditure with FB1 levels in human urine [101]; which consolidated its utilization as a relevant biomarker, as a portion of ingested FB1 is excreted in urine [102].

The detection of fumonisins is limited by its absence of fluorescence; therefore, the introduction of a chromophore for the derivatization of the amino groups within fumonisin is always required [103]. Initial derivatization procedures utilized maleic anhydride derivatives and fluorescamine [36,104]. Nevertheless, more sensitive detection procedures introduced and still utilize pre-column derivatization with o-phthaldialdehyde [82, 105-108], naphthalene-2,3-dicarboxaldehyde [109], and the quick and stable (9-fluorenylmethyl) chloroformate (FMOC) [110, 111].

Fluorescence detectors are restricted for the individual quantification of FB1 [106, 112, 113], the sum of FB1, FB2, FB3 [109] or the separate determination of up to three group B fumonisins [82,111]. On the other hand, one of the main advantages of mass spectrometry detectors is the possibility of performing multiplex analysis, not only for different mycotoxins [114-135], but also when combined with varied metabolites. Growth regulators, antibiotics, pesticides [93, 136, 137], and other fungal metabolites [138, 139], were simultaneously identified in analysis capable of assessing up to 74 and 90 compounds [140, 141]. Mass spectrometry has also been used for assessing mycotoxin transfer from feed to organs and tissue in poultry [134]

The importance of novel analytical methods relies on the high sensitivities achieved within a relatively short detection time. The speed of mass spectrometry signals (ESI+), was early proven to reduce the sole determination of FB1 in bovine milk to 4 minutes [142], with a half-fold time reduction on more recent assays for pig samples (plasma, urine, feces) [92]. Its limits of detection have reached 0.003 µg/kg [125, 142] for animal (bovine milk) and food samples (corn meal), and 0.001 µg/L in human urine [130]. Notwithstanding the excellent performance of conventional analytical methods, some disadvantages are related to sample pre-treatment including long extraction steps with further purification protocols, as well as method optimization of the chromatographic separation, derivatization or internal standard addition, along with its corresponding validation method. For instance, a single drying step could add two days to the total assay preparation time [117].

Sample clean-up is a key step for reducing matrix effects, where strong anion exchange (SAX) columns have been utilized as cheaper clean up cartridges in LC-MS detection, with recoveries of up to 86.6 and 106% for human hair [113] and piglet urine [92] respectively. In a similar way, immunoaffinity columns (IAC) have been proven to attain maximum recoveries of 109% for FMOC-derivatized cornmeal samples [111], and 90% in rice analyzed by LC-MS [93]. The specificity of antibodies in IAC also allowed the successful LC-MS analysis of FB1 in complex samples, such as milk [142], human urine [102] and chicken tissue [134] with peak recoveries of 88.4%, 99.1% and 95-102% respectively. Lower recoveries were found for the determination of OPA-derivatized FB1 in maize (68.5%), rice (72.4%), sorghum (75.6%) and wheat (69.4%) extracts [82]. Nonetheless, IACs increase the total assay cost, since they could account for double or triple the price of SAX cartridges, with a highly comparable performance. Besides, IACs have a limitation on the variability of analytes and could promote interaction with the matrix constituents [132]. In both cases (SAX and IAC) the total analysis time is enlarged by the conditioning, loading, washing, elution, evaporation, and reconstitution steps.

Some novel developments incorporated magnetic nanoparticles for the sorption and concentration of mycotoxins, promoting a simultaneous clean-up and sensitivity enhancement in the overall method [121]. Nonetheless, even when the performance of patented commercial clean up columns allows their utilization in single [105] and multiple mycotoxin analysis, the adsorption procedure of recent products might impede the detection of FB1 and FB2 [117]. As a replacement, novel dispersants such as nano zirconia, have been found with high extraction efficiency of FB1 [125].

Alternatively, the QuEChERS method, initially developed for pesticides, was subsequently introduced for the dispersive solid-phase extraction (SPE) of FB1 [106], and further validated for its

application in multi-target analysis due to its lower cost, less time consumption, easy procedure [116, 138, 143-145], as well as its availability in extraction kits [118] with satisfactory recoveries [122]. Likewise, sample preparation with a QuEChERS dispersive SPE was useful for minimization of matrix effects from beer, with a preconcentration step producing enhanced LODs [131]. In spite of being a favorable option for sugar reduction in the quantification of FB1 in oat, soy and rice beverages (extraction recoveries 80, 82, 85%; matrix effect: 76, 63, 75%) [123], a UPLC-MS/MS study of *Alpinia oxyphylla* revealed the unsatisfactory FB1 and FB2 recoveries from QuEChERS (~50 & 55%) and hydrophilic-lipophilic balance (HLB) cartridges (~65 & 55%), in comparison to solid-liquid extraction (~80 & 70%). Nevertheless, the three extraction methods exhibited a signal increase (80-145%) due to matrix effect [124]. By contrast, recent studies in sugarcane juice proposed the use of HLB cartridges as an alternative to QuEChERS, due to its high recoveries of 98% for FB1 [133].

Despite the expected disadvantages of the dilute and shoot method towards the complexity of some samples, which could affect the detector sensitivity and assay performance, when optimized, this procedure can be applied in the multi-target analysis of food samples without a clean-up phase [93, 123, 137, 139]. For instance, a comparison between the efficiency of dilute and IAC methods revealed that, even when lower LODs and limits of quantification (LOQs) were obtained with the clean-up step (0.5 and 1.66 against 2.3 and 4.3 µg/kg), a dilution procedure accomplished an improved regression (0.9941), high recoveries (94-106%) and reproducibility for FB1-spiked animal feed [132]. A similar situation was confirmed for matrix-match calibration [115, 137, 146], and internal standard (IS) addition [114, 126, 132] where a clean-up step was not necessary to eliminate matrix effects and run accurate determinations. Yet, the use of specific IS and a validated method for a single matrix, could reduce the scope of the determination, and increase its final cost. Notwithstanding, some approaches proposed the application of the aforementioned procedures combined with clean up techniques and QuEChERS, for a greater method validation [120, 128, 130, 147]. As previously mentioned, the use of HPLC and LC-MS methods has been widely explored mostly in developed countries, where the infrastructure and resources allow their application for mycotoxin analysis [11]. Moreover, drawbacks from chromatographic analysis comprise complex sample pre-treatment in which immunoaffinity columns increase the cost, utilization of organic solvents during sample extraction, clean-up and separation steps, derivatization if UV-Vis detection is utilized, and the need of trained users for their long and laborious procedures [148, 149]. Therefore, other alternatives should be considered for in-field assays, especially in rural areas and outbreak regions from developing countries.

### *3.2 Immunosensors for the detection of fumonisin B1*

The enzyme-linked immunosorbent assay (ELISA) for the determination of FB1 represents the foundation of different approaches. Competitive assays have been commonly employed for biosensing techniques, mostly because of the restriction produced by single epitopes on other types such as sandwich ELISA [151]. Some general procedures for a competitive immunoassay include a coating stage of antibody on the selected support, followed by the incubation with a mixture of free FB1 (sample) and functionalized toxin (horseradish peroxide (HRP)-FB1). After washing the unbound FB1 or HRP-FB1, different substrates can be added for the development of either a chemiluminescence or a colorimetric signal [152]. Some commercial kits are also based on a competitive scheme, in which capture antibodies, specific to a FB1 antibody, are coated on a well, where free FB1, enzyme-fumonisin and antibody are incubated. The bound HRP-fumonisin is then measured by incubating with a chromogen [82]. In some bulk experiments, magnetic nanobeads have been used as a support with a competitive binding role under the presence of FB1 and its biotinylated antibody [153]. Other modifications suggested the substitution of HRP with compounds such as glucose oxidase to produce hydrogen peroxide, an inducer of AuNP aggregation [154], and the application of genetically engineered antibodies [155]. A novel technique used a monoclonal antibody-rhodamine isothiocyanate (RBITC)-AuNPs probe for the competitive binding between OVA-FB1 and FB1, where cysteamine worked as a turn-on compound for revealing the degrees of fluorescence from the quenched probe [156].

This antigen-antibody interaction has been used, optimized and improved over the years; and commercially available ELISA kits and standardized ELISA protocols are still applied for method validation and comparison with novel biosensing developments [80, 95, 157-159]. As presented in Figure 4, electrochemical immunosensors have portrayed some of the lowest LODs [97, 98]. For instance, the signal of an impedance sensor was modified by depositing quantum dots-carbon nanotubes on a glassy carbon electrode (GCE) for the immobilization of the corresponding antibody. In this case, the electron transfer resistance was enhanced after target binding, allowing LODs as low as 0.46 pg/L [97]. An electrochemical indirect competitive method was also refined by modifying a GCE with nanotubes-chitosan (undefined characteristics) and FB1-bovine serum albumin (BSA). The remaining antibody after the incubation with free FB1 (sample) was able to bind FB1-BSA, as well as an alkaline phosphate-labelled anti-antibody, whose substrate triggered the electrochemical signal with lower, yet good sensitivity of 2 ng/L [160]. The reduction of conductivity promoted by the antibody-antigen reaction was again explored for the immobilization of antibodies on nanotube-modified GCE, attaining a LOD of 3.8 pg/L [98]. In addition to electrochemical methods, surface-enhanced Raman scattering (SERS) competitive immunoassays were applied by combining FB1-BSA functionalized Au nanopillars with nanotags, consisting in AuNPs simultaneously functionalized with anti-antibody and malachite green isothiocyanate (MGITC). The interaction between the primary antibody and high antigen concentrations resulted in a weak SERS signal, due to the absence of complex formation within free primary antibodies, nanopillars and nanotags, with a LOD of 0.00511 pg/L [161].

As noted in Table 3, immunosensors can be supported on different matrices, including optical fiber, well plates, glass slides, magnetic beads, magnetic nanoparticles, electrodes and chips. Yet another of the main advantages of using antibodies is the feasibility to be incorporated in paper-based biosensors. Paper matrices are presently relevant for the creation of portable, point-of-care, applicable and cheap devices [83]. The conjugation of antibodies with colloidal gold (gold nanoparticles) has been widely applied for the colorimetric detection of FB1 on nitrocellulose membranes [ 84, 99, 162-171]. Some modifications included the application of urchin-like and flower-like gold nanoparticles (AuNP), which slightly increased the sensitivity when compared to a spherical particle [84, 85].

As an alternative to color intensity measurements, a chemiluminescent substrate could be incubated with HRP for a slight improvement of the LOD [172, 173], or the application of quantum dots (QD) in which a radiometric analysis revealed a constant signal from the test line with biotin-BSA, compared to the calibration with anti-mouse IgG [174]. Nevertheless, the application of fluorescent QDs does not always result in an improved sensitivity. This has been confirmed in a nitrocellulose strip for the detection of FB1 (LOD: 60 µg/L), ZEN and OTA with a monoclonal antibody-QD probe placed on the conjugate pad, through the competitive interaction with mycotoxin-BSA at the test line [175], and a mAB-Europium fluorescent nanoparticle with FB1 (LOD: 8.26 µg/L) and FB1-BSA (Test line) [176]. An advantage of paper-based biosensors is the possibility of performing smartphone-based analysis, as already achieved on colorimetric and fluorescent signals [177]. Notwithstanding the multiple modifications, most of the differences among paper-based and other types of immunosensors can be explained in terms of the different antibodies selected and employed in each method.

Although ELISA is characterized by its simplicity, speed, reproducibility, and accuracy, its cost, equipment needs, and assay times make it unsuitable for on-site analysis, especially in developing countries [18, 67]. Compared to other immunoassays (*e.g.*, electrochemical), ELISA requires more reagent consumption, incubation times and portrays limited separation, cleaning and reproducibility [156]. Of note, the exploitation of the efficient conversion rate of HRP ($10^7$ substrate molecules/min) in sandwich-type and competitive assays results in specific and sensitive approaches. However, the prolonged incubation times along with the cost the chemicals and matched antibodies, prevents their wider application for the analysis of small mycotoxins, which might result in semi-quantitative and qualitatively results, mainly observed in immunochromatographic assays [84, 85, 99, 155, 165, 171, 178-181]. In this regard, immunochromatographic multitarget detection could result in misreading and line interference, with the subsequent detection of false positives [181]. Besides, the frequent non-linear behavior in the calibration curves from immunological assays has been linked to strenuous and long procedures [182]. In addition, compared to aptamers, the application of antibodies presents

some drawbacks, including cross-reactivity and false positives, leading to mycotoxin underestimation thus affecting the final selectivity [18, 23, 24, 25]. Apart from the reported cross-reactivity [84, 156, 167, 168, 177, 183-187], which is occasionally not tested in certain designs [98, 153, 188], antibody-based detections are susceptible to pH changes and matrix effects when inappropriately used or if matrix-matched calibrations have been omitted, which influences the observed preference for chromatographic methods, especially as regulatory analysis [11, 21]. Unlike antibodies, aptamers are chemically and pH stable, resist room temperature storage and present reversible denaturation. Furthermore, their non-biological screening allows their easy, high-purity in-vitro synthesis and modification, whose obtained sequences can be successfully combined with nanomaterials [67, 71]. In fact, attempts to replace antibodies with aptamers have originated an alternative method to ELISA, named enzyme-linked apta-sorbent assay or ELASA [18].

*3.3 Other methods*

Alternatives to the extensively known immunologic and chromatographic techniques include chemometric, electrochemical and colorimetric analysis, as shown in Table 4. In SERS, the spectral variations of extracted samples mixed with Ag dendrites were measured on a quartz plate [94], while innovative, promising and more robust techniques incorporated the use of molecularly imprinted polymer nanoparticles (MIPs). Commonly polymerized with monomers such as methacrylic acid (MAA), ethylene glycol methacrylate (EGMP), N-isopropylacrylamide (NIPAM), N,N'-methylene-bis-acrylamide (BIS), N-tert-butylacrylamide (TBAm), and N-(3-Aminopropyl) methacrylamide hydrochloride (NAPMA); MIPs have functioned as a replacement of primary antibodies; in which the utilization of FB1 as template molecule enhanced the performance, selectivity, thermal stability, and easy manufacturing of this technique. Once the MIPs are synthesized, the general procedure is similar to ELISA, where free FB1 competes with a FB1-HRP conjugate, where the latter reacts with a substrate (TMB: 3,3′,5,5′-tetramethylbenzidine), bearing a colorimetric response. Such mechanism reduces the limit of the detection to 4.4 ng/L [208] and 1.37 ng/L [159], while an improvement on the silanisation step yielded more MIPSs and allowed the quantification of FB in maize, with a lower LOD equivalent to 1 ng/L [209]. Recent alternative methods suggested the chemical modification of FB1 prior to its quantification assay, where alkaline hydrolysis with KOH was proposed to reduce steric hindrance, allowing the formation of hydrogen bonds between hydrolyzed fumonisin (HFB1) and the $NH_2$ groups in cysteamine functionalized AuNP [210]. Likewise, a derivatization step between FB1 and a fluorescent derivative was necessary for spectra acquisition on a nylon membrane [100]. Besides, as already observed for some immunoassays, electrochemical methods were combined with MIPs, for a reduction on the limit of detection. A GCE modified with AuNPs and $Ru@SiO_2$ in chitosan (undefined characteristics), was proved as favorable support to produce MIPs generating electrochemiluminescent estimations with a LOD of 0.35 ng/L [211]. In a similar approach, an iridium tin oxide (ITO) electrode modified with CdS quantum dots, chitosan (undefined characteristics) and graphene oxide worked as the UV polymerization area, in which the resulting MIPs were used for photoelectrochemical evaluation of FB1 levels as low as 4.7 ng/L [212]. The application of nanoMIPs in electrochemical measurements (EIS, DPV) allowed the achievement of LODs as low as 21.6 fg/L, which so far is the lowest value reported for FB1 [86].

On the other side capillary electrophoresis (CE) was initially reported in 1995 as a different technique with greater capability for the separation of FB1 to that from LC, where either its integration with MS detection or the quantification of fluorescent derivatives were utilized in the analysis of corn [213, 214]. Subsequent CE approaches explored the performance of fluorescein isothiocyanate for the derivatization of FB1 [215], and its application in the competitive binding of mAb by labeled (derivatized) and unlabeled FB1, for the CE of the remaining fluorescein-FB1 [216]. Despite the advantages of CE in terms of the column efficiency, speed, reduction of organic solvents [214], the high limit of detections restricted any further applications. After two decades only one recent work on the application of coated ($C_1$) and uncoated capillaries resulted in a relatively high LOD of 156 µg/L for the analysis of rice and fusarium microconidia by CE-MS [217], which denotes an opportunity for exploring, refining and optimizing more CE options for the determination of FB1 and other analogues.

## 4 Aptamer-based determination of FB1

Aptamers are single-stranded DNA or RNA with high molecular recognition towards different types of targets, including nucleic acids, cells, proteins and small molecules. Such probes exhibit diverse binding affinities and target selectivity and can discriminate even slight chiral differences [67, 69]. Due to their exceptional affinity and specificity, aptamers are often considered as comparable to antibodies, with certain advantages for in-field detection caused by their chemical synthesis, easy nucleobase and chemical modification, and exponential self-amplification [67]. Contrary to antibodies, aptamers' chemical production is less costly, laborious, more ethical (as they entail no harm to animals), and allows the obtention, modification, and labeling of large aptamer quantities under many experimental conditions without batch variations. Such benefits have allowed aptamers in diagnosis, therapeutics, drug delivery, environmental monitoring, and food safety [65, 74]. Likewise, aptamers are aimed to substitute antibodies as the gold standard in molecular recognition, where their three-dimensional folding determines their high affinity and binding capability for the development of quick, cost-effective and wide range methods [71, 65]. Aptamers are discovered and selected by a technique called Systematic Evolution of Ligands by Exponential enrichment (SELEX) in which a large DNA library is incubated with the target or other relevant molecules, followed by the amplification of potential binders after several selection and discrimination rounds [69]. Depending on the analyte, SELEX can be carried out by target immobilization in magnetic-beads by covalent and non-covalent binding, capillary electrophoresis through electric fields on the target charge and hydrodynamic radius, whole cell-SELEX, and optical surface plasmon resonance chips with mass-related refractive index changes [65].

On the other hand, innovative SELEX techniques include robotic/automated procedures, microfluidic-based chips, next-generation sequencing for the acquisition of millions of sequences, graphene oxide-SELEX, quartz crystal microbalance-SELEX for mass changes after binding, human-genome SELEX, and computer-based screening (*in silico* SELEX) [65]. Aptasensors are biosensing devices that utilize aptamers as biorecognition elements for the conversion of different signals into measurable values [75]. The outstanding performance of aptasensors depends on the sequence architecture and the way it is assembled in the biosensing design [74]. Depending on the nucleotide number and sequencing, aptamers can take different 3D conformations such as loops, triple stranded and G-quadruplex arrangements, pseudoknots and staples [68]. So far, two aptamers composed by 96 and 80 nucleotides, have been reported through SELEX and utilized in different biosensing approaches for FB1 [69,70]. The structure, sequencing and molecular docking of aptamers can be analyzed by specific software tools [65, 74, 218], from which mfold and RNA structure 4.6 software have been used for predicting the secondary structure of FB1 specific aptamers [69, 70]. The mfold web server is useful for studying aptamer-target reaction sites [219], while the determination of nucleic acid folding calculates a minimum free energy ($\Delta G$) [220]. DNA folding in mfold requires a formatted sequence, the inclusion of its optional constrains including forcing or prohibiting specific base pairs and helixes, and its folding parameters. In this regard, the specific parameters for determining a linear (default) or circular sequence include the folding temperatures (0-100 °C), ionic conditions as molar concentration ([Na+] or [Mg++]), the free energy increments, distance between pairs, and maximum number of foldings, if necessary. Once the required parameters are included, the software generates a structure plot, based on the energy dot plot for the lower $\Delta G$ in optimal conditions [220]. The folded structure of all the reported aptamers for FB1 is presented in Figure 6, where the 96 nt and 80 nt aptamers [69, 70] displayed a more complex structure, mostly expressed by the formation of multiple stem loops, in contrast with the simple folded organization of their reduced aptamers and minimers [91, 221]. In terms of the 3D conformation, a B duplex structure was confirmed for the 96 nt aptamer, through circular dichroism assays. Nevertheless, 3D representations of docking revealed the susceptibility of FB1 to be bound by the backbone of the 96 nt aptamer and its minimer, along with the 80 nt aptamer [218]. The final structure, predicted in Mfold, relied on the folding temperature, commonly varying from ice to room temperature, along with the ions present in the buffer ($Mg^{+2}$, $Na^{+}$).

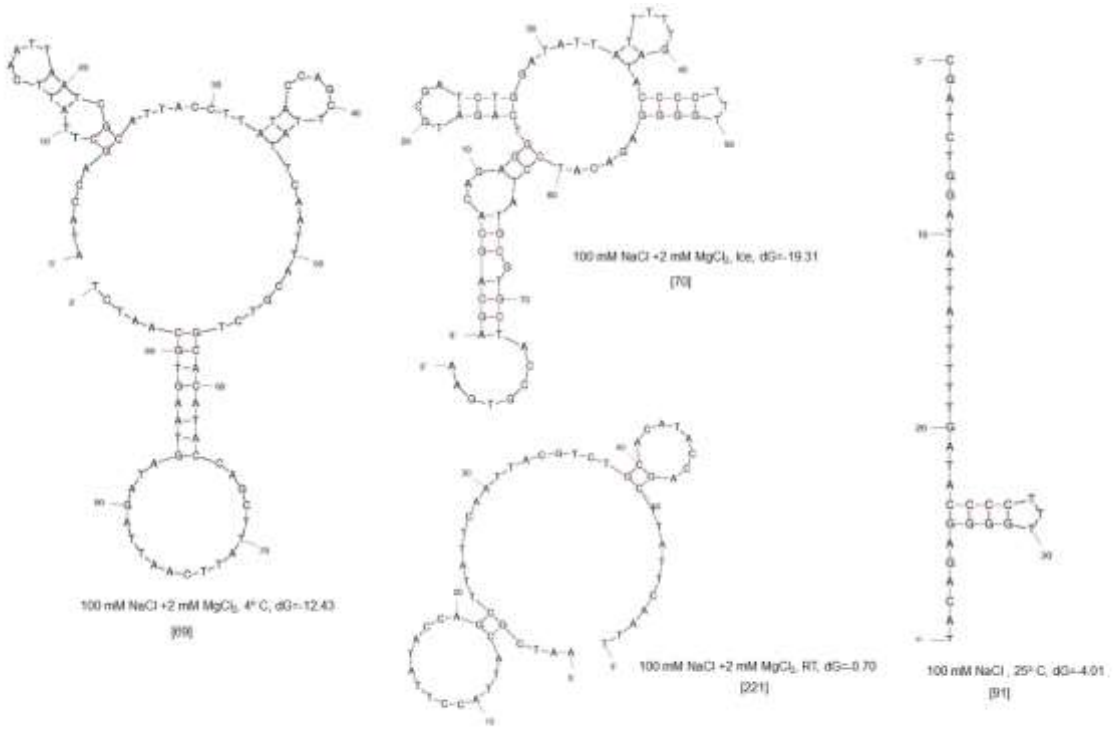


**Figure 6.** Aptamer folding forms obtained in Mfold at the specified conditions

All the aptamer-based sensors for FB1 are chronologically described in Table 5, while the binding and functionalization conditions are illustrated in Table 6. From the 32 aptasensors found in the literature, 25 utilized the 96 nt aptamer [69], one method applied a shortened version (60 nt) from this first sequence [90], one platform included the second 80 nt aptamer [222], two biosensors manipulated a condensed version (40 nt) of the second main aptamer [91,223], and three references did not specify their single-stranded (ss) DNA sequence [87, 88, 96]. From the two patented oligonucleotides, the aptamer with sequence: 5'-GCA TCA CTA CAG TCA TTA CGC ATC GCG AGG GGA CGG GAA CGC GCT GAA GGG AGG CCT AGG ATC GTG TGA AGT GCT GTC CC-3', has not been applied in any other biosensing technique [224]. A similar outcome occurred to the second patent, which reported an 80 nt aptamer with 40 non-specified random nucleotides [225], flanked by similar primer binding sites to those reported by Chen and collaborators for their 80 nt sequence [70]. The schematic representation of each type of aptamer-based biosensor is illustrated in Figures 7, 8 and 9, for the fluorescent, electrochemical, and colorimetric/other aptasensors specific for FB1, respectively. It should be noted that the most recent sequences have not replaced the first reported aptamer, and current biosensing designs still apply the 96 nt ssDNA molecule with high sensitivity and specificity. Different immobilization mechanisms support the versatility of many aptasensing techniques for FB1. In this regard, aptamer modification with thiol groups allowed Au-S covalent binding with AuNPs [226], gold and AuNPs-modified electrodes [222, 227-231], and gold-coated silicon cantilevers [148]. Likewise, biotin modified aptamers have been attached to avidin-conjugated upconversion nanoparticles (UCNPs) [81] and magnetic nanoparticles [95, 232], as well as streptavidin-magnetic beads [149], and streptavidin-coated microplates [233]. Furthermore, amino groups integrated to aptamers promoted binding to glutaraldehyde modified silica photonic crystal microspheres (PHCM) [234], isothiocyanate modified PHCM [235], GPTMS modified $TiO_2$-PSi surfaces [80], and carboxylic groups in 3-mercaptopropionic acid-capped CdTe quantum dot-coated silica spheres, activated by EDC/NHS [236]. When no end modification is required in immobilization procedures, aptamers can be adsorbed on graphene oxide and other surfaces. To this end, π-π stacking with their nucleobases [81, 91, 223, 237, 238, 239], electrostatic binding to gold nanoparticles [89], or hybridization with complementary sequences fixed to other supports including luminescent

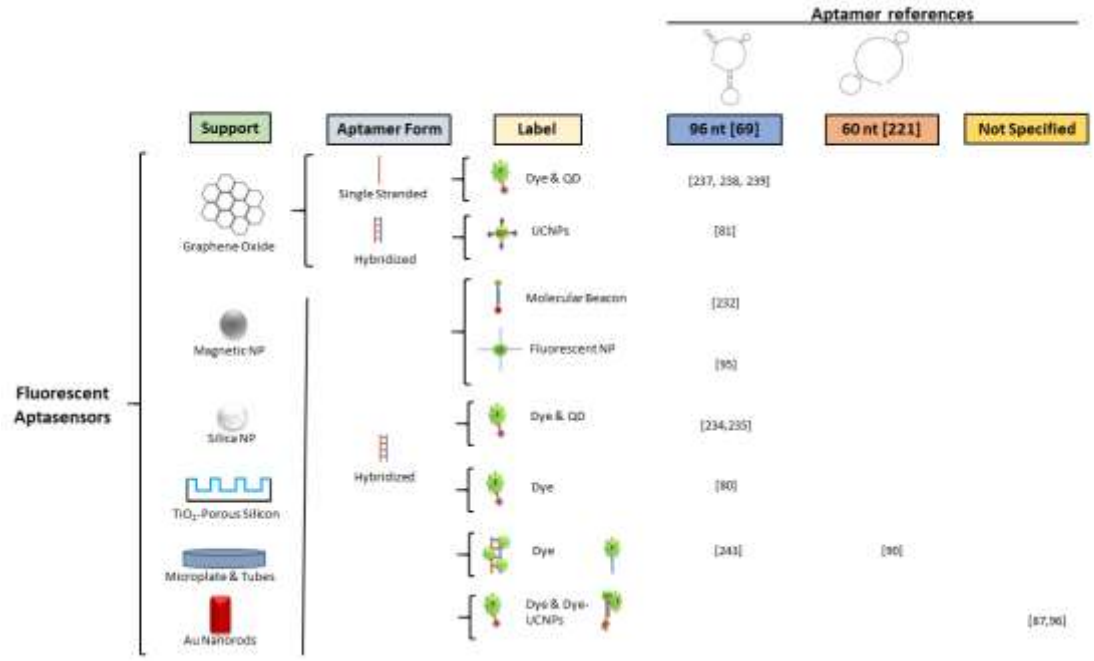


**Figure 7.** Schematic representation of the mechanisms of aptamer-based biosensors for FB1 with fluorescent detections. (Abbreviations: **NP:** Nanoparticles; **QD:** Quantum Dots; **UCNPs:** Upconversion fluorescent nanoparticles)

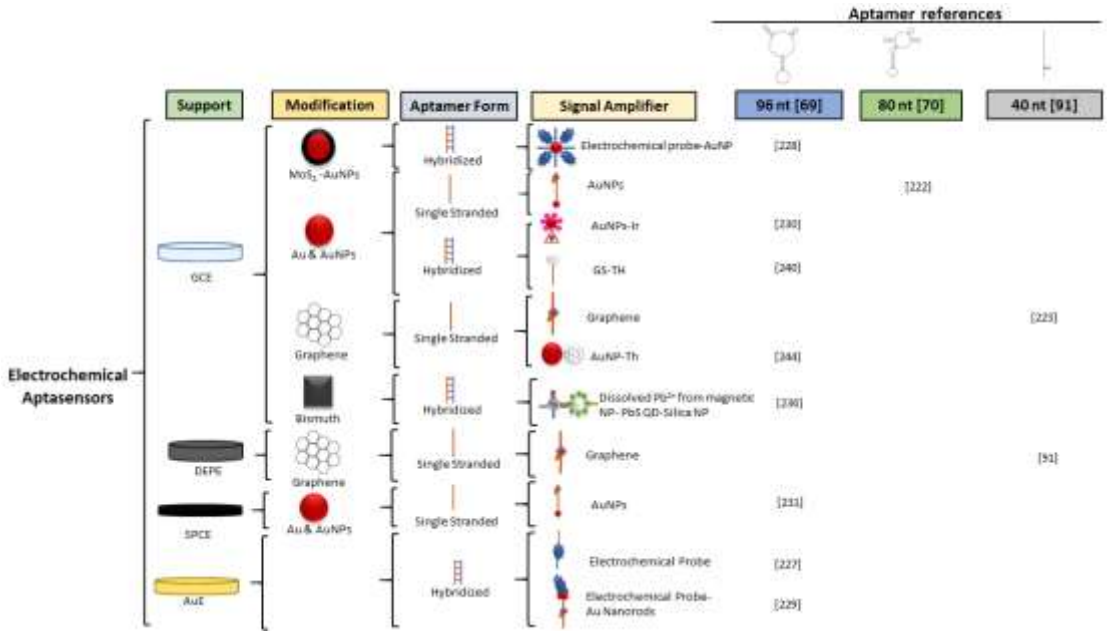


**Figure 8.** Schematic representation of the mechanisms of aptamer-based biosensors for FB1 with electrochemical detections. (Abbreviations: **AuE:** Gold electrode; **AuNPs:** Gold nanoparticles; **DEPE:** Disposable electrical printed electrode; **GCE:** Glassy carbon electrode; **GS:** Graphene sheets; **NP:** Nanoparticle; **SPCE**: Screen-printed carbon electrode; **QD:** Quantum dots; **TH:** Thionine)

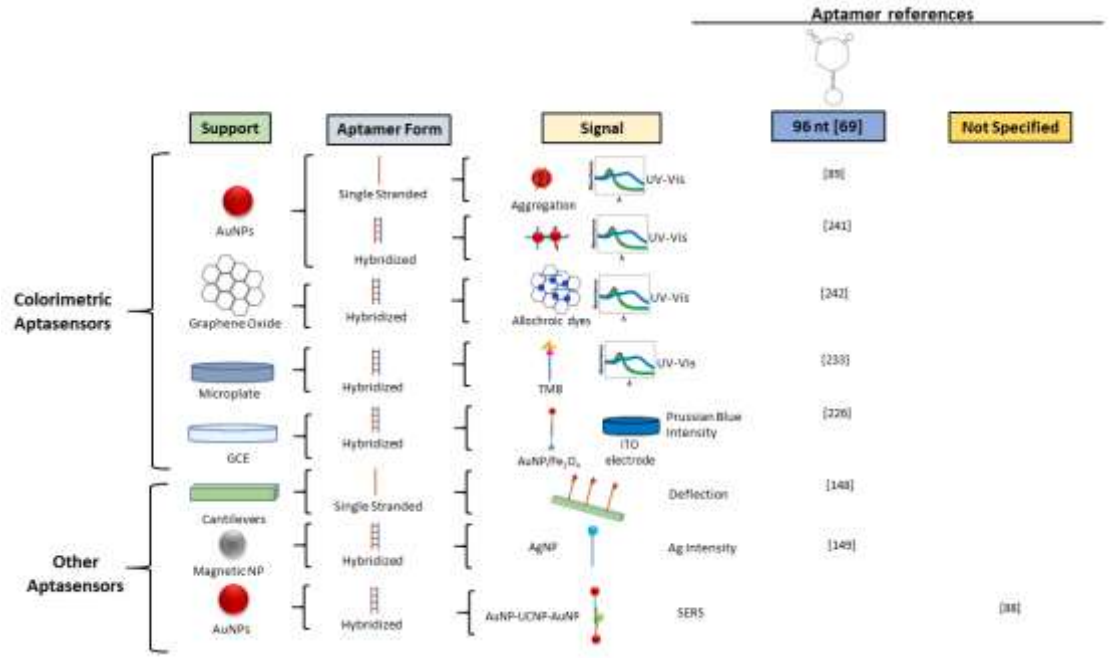


**Figure 9**. Schematic representation of the mechanisms of aptamer-based biosensors for FB1 with colorimetric and other detections. (Abbreviations: **AgNPs:** Silver nanoparticles; **AuNPs:** Gold nanoparticles; **GCE:** Glassy carbon electrode; **ITO:** Indium tin oxide; **NP:** Nanoparticles; **SERS:** Surface enhanced-Raman spectroscopy; **TMB**: 3,3′,5,5′-tetramethylbenzidine; **UCNPs**: Upconversion fluorescentμ nanoparticles)

nanoparticles [95], electrodes [240], magnetic beads [236], magnetic nanoparticles [226], quantum dots [149], gold nanoparticles [226, 241], gold nanorods [87, 96] and graphene oxide [242] have been explored.

*4.1 A 96-mer aptamer for the determination of FB1*

The first aptamer specific for FB1 was reported by McKeague [69], after 18 SELEX rounds through negative selections with unmodified and modified (L-homocysteine, L-cysteine, L-methionine and L-glutamic acid) magnetic beads. From the six sequences initially studied, the sequence with the lowest G content (8 %) was selected due to its greatest binding affinity, confirmed by its low dissociation constant (Kd=100 nM). This sequence consisted in 60 random nucleotides (bold letters), surrounded by two primer binding sites: 5'-ATA CCA GCT TAT TCA ATT **AAT CGC ATT ACC TTA TAC CAG CTT ATT CAA TTA CGT CTG CAC ATA CCA GCT TAT TCA ATT** AGA TAG TAA GTG CAA TCT-3' [69]. A good binding affinity (Kd= 42.9 pM) was confirm for this aptamer by fluorescent microscale thermophoresis (MST), which differed from the value obtained through magnetic bead assays (2.11 pM) due to differences in their target and aptamer mobilities [218].

*4.1.1 Fluorescent detection with the 96 nt aptamer*

From all the biosensing designs applying the 96 nt aptamer (Figure 7), the most sensitive were those transduced into fluorescent [80, 95, 234], and electrochemical [227-229] signals. The first fluorescent method described the application of avidin-modified fluorescent nanoparticles and graphene oxide (GO), as donor/acceptor pair in Förster resonance energy transfer (FRET). A biotin modified aptamer was attached to upconversion fluorescent particles (UCNPs); and under the presence of an increasing fumonisin concentration, the particles were not quenched by GO, thus exhibiting a linear increment on the fluorescence intensity [81]. A very simple bulk fluorometric method

was developed through the hybridization of aptamers with a FAM-labelled complementary DNA, and its displacement upon FB1 binding [243]. The surface of reduced GO (RGO)/platinum nanoparticles (PtNPs) and RGO/Ni/PtNPs micromotors were also used as a quencher of fluorescein amidine (FAM)-aptamers, with a direct increase on its fluorescence intensity produced by target biding [237, 238]. A similar mechanism was developed by immobilization of red CdTe quantum dots-$NH_2$-modified aptamers on GO/$Fe_3O_4$ nanocomposites (energy acceptor), where the quenched fluorescence was restored after target binding with a reduction of the background interference by magnetic separation [239]. Another procedure was proposed for the FRET-quenching effect between AuNP and UCNPs attached to a molecular beacon (MB), although the measured signal intensity was an indirect analysis of the fumonisin content. To this end, a biotinylated aptamer (linked to avidin modified magnetic particles), was hybridized with its complementary DNA, which was also able to hybridize and open the MB, thus forming a fluorescent double-stranded DNA arrangement [232].

In the most sensitive development with this long sequence (LOD: $1.9x10^{-5}$ µg/L), the functionalization of magnetic nanoparticles with biotinylated aptamers and time-resolved fluorescent nanoparticles ($NaYF_4$:Ce/Tb) with biotinylated complementary DNA, resulted in the formation of capture and signal probes, respectively. The DNA hybridization step derived to a magnetic/fluorescent biocomplex, whose dehybridization and magnetic separation at rising concentrations of FB1 resulted in a reduction of the fluorescence intensity [95]. Similarly, amino modified aptamers hybridized with their fluorescein isothiocyanate (FTIC)- modified complementary DNA, were coupled to silica photonic crystal microspheres (SPCMs), with an inhibitory effect on the fluorescent signal caused by an increasing target concentration [234]. In fact, good sensitivity can be achieved with SPCM suspensions, when bound to a hybridized duplex structure formed by a black hole quencher (BHQ2)-labelled antiaptamer (quencher) and a $NH_2$(5')/Cy3(3') modified aptamer. An increasing FB1 concentration enlarged the separation between the dye and its corresponding quencher, promoting a higher fluorescent signal [235]. Moreover, the hybridization between a $NH_2$/Cy3 modified aptamer and its BHQ2-antiaptamer was examined when immobilized to a $TiO_2$ modified silicon wafer, where the increment of fluorescence was triggered by the addition of FB1 [80].

*4.1.2 Electrochemical detection with the 96 nt aptamer*

As already stated, electrochemical methods have also been applicable to sensitive FB1 aptasensors, and their precise completion can be enhanced by the addition of materials such as AuNP and graphene-thionine (GS-TH) (Figure 8). Electrodes functionalized with AuNP are convenient for DNA attachment, and the complexity of its fabrication depends on the aptamer structure. For instance, the unmodified 96-mer molecule was docked to a AuNP modified glassy carbon electrode (GCE) through a thiolated capture DNA. A higher sensitivity was promoted by the addition of GS-TH, due to its competition against FB1 for binding the aptamer, which also generated a decrease in the redox peak. Under this approach, GS-TH are integrated as a peak current enhancer for the Au-modified GCE, because of its ideal stability, surface area, biocompatibility and electrical conductivity reported through cyclic voltammetry (CV, -0.6 to 0.1 V), in which the presence of FB1 diminishes the signal [240]. GCEs modified with GS-AuNPs-TH have also been used as signal amplifiers and anchor sites for the single quantification of FB1 with a thiolated aptamer, harnessing the π-π interactions among TH and GS, as well as the SH-Au bonds between aptamers and AuNPs. The cyclic voltammetry characterization denoted the redox reduction of TH, which is diminished after the immobilization of aptamers, with a higher decrease under the presence of FB1 due to electrode impedance [244]. Efforts for reducing the costs and increasing the capacity of aptasensors have focused on a combination of powerful electrochemical techniques with portable devices. A screen-printed carbon electrode (auxiliary, reference and working electrodes included) modified with polydimethylsiloxane was selected for the electrodeposition of AuNP, and further attachment of a thiolated aptamer. The coil to G-quadruplex conformational transition, supported by the presence of FB1, was applied to strengthen the electron transfer resistance (ΔI), reflected as a reduction in the electrochemical impedance spectroscopy (EIS) response. The principle behind this approach was based on the inhibition of the electron transfer between the redox probe $[Fe(CN)_6]^{3-/4-}$ and the electrode surface, promoted by the electrostatic repulsion from the negative FB1-aptamer complex

towards the negative redox probe [231]. While the previous methods were able to quantify FB1 in a ng/L scale, upcoming electrochemical assays are reaching limits of detection in the pg/L range.

Gold electrodes worked as ideal supports for combined DNA structures, as verified for double-stranded DNA (aptamer-cDNA). The incubation with different concentrations of FB1 in this assay left some free and hybridized cDNA on the electrode, from which free cDNA was subsequently digested with exonuclease I. The remaining double-stranded DNA interacted with methylene blue (MB) whose electrochemical signal reached a LOD of 0.00015 µg/L. In this type of array, double-stranded DNA enriched with MB acted as a signal amplifier during the differential pulse voltammetry (DPV) and EIS measurements, where FB1 promoted the release of aptamers; thus, less double-stranded DNA was formed, and less MB could intercalate, which resulted in higher $\Delta I$ [227]. A Y-shaped hybridized structure was also conjugated on a gold electrode. This approach included a DNA sequence complementary on different segments to two aptamers and the addition of gold nanorods for signal enlargement related to concentrations of FB1 as low as 0.00026 µg/L. It is worth mentioning that AuNRs denoted greater conductivity, biocompatibility, and surface area to that of AuNPs. Therefore, they were used for the thiolated immobilization of Fc-SH in order to increase the current, which was inhibited by the presence of FB1 as reported by EIS in a $Fe(CN)_6]^{3-/4-}$/KCl solution and DPV (-500 to 600 mV). Additionally, the Y-shaped DNA structure allowed the simultaneous analysis of OTA and FB1 [229]. Another technique in the pg/L scale (0.0005 µg/L) was designed on a glassy carbon electrode modified with molybdenum disulfide ($MoS_2$) and gold nanoparticles for the attachment of aptamers and further immobilization with labelled cDNA, whose differential pulse voltammetry (DPV) decreased with the addition of FB1. In this case, the reduction of $MoS_2$ nanosheets improved the conductivity, electrochemical activity, and electron transfer of GCE as indicated through DPV (-0.6 to 0.6 V) and CV (-0.2 to 0.6 V) in $Fe(CN)_6]^{3-/4-}$ /KCl. Besides, this material worked as a support for AuNPs-aptamers, their hybridization with cDNA-AuNPs, and their labelling with 6-(Ferrocenyl) hexanethiol and thionine probes for a dual well-resolved determination [228].

Occasionally, electrochemical determinations are indirect measurements of labels and other compounds derived from the incubation with FB1. For instance, $Fe_3O_4$@Au magnetic beads were coupled with a thiolated complementary DNA, for the hybridization of amino-modified aptamers, conjugated with $SiO_2$@PbS hybrid spheres. An increasing concentration of FB1 produced a reduction on the number of hybridized labels, which after a magnetic separation were dissolved in acid for the square wave voltammetry of the remaining $Pb^{2+}$ in a bismuth film modified GCE [236]. A colorimetric method coupled with an electrochemical mechanism, was designed through a GCE modified with silver enhanced AuNP-aptamer-cDNA-$Fe_3O_4$ nanocomposites and cDNA-$Fe_3O_4$ at different degrees due to aptamer-cDNA dehybridization by FB1. To achieve the closed bipolar electrode reaction (BPE), the modified GCE (cathode), a Pt wire (counter electrode) and a AgCl/Ag wire (reference electrode), were submerged in a $H_2O_2$/SDS solution. In turn, another Pt wire (anode), connected to the GCE, along with an ITO electrode, were placed in a different electrochemical cell filled with HCl, $K_3[Fe(CN)_6]$ and $FeCl_3$. In this design, varying target concentrations resulted in different GCE effective areas and current flow, reported as Prussian blue (PB) deposition on the ITO electrode. This indirect electrochemical procedure was translated into a colorimetric signal by means of the smartphone detection of deposited PB at the ITO electrode, submerged in the reporting solution along with the BPE anode [226]. Unlike other techniques, a less sensitive electrochemiluminescent (ECL) assay resulted from AuNPs modified with a thiolated aptamer and an iridium complex, when fixed to an Au electrode by a partial complementary DNA. As the AuNP/Ir complex enhanced the electrode conductivity, the addition of FB1 decreased its ECL signal [230]. Additionally, three aptasensors also explored the modification of electrodes with AuNP-thiolated aptamers [222] and graphene-aptamers [91, 223], however they integrated the 80 nt aptamer [70] and its derived 40 nt sequence. These are discussed in Section 4.3.

### *4.1.3 Alternative and colorimetric detection with the 96 nt aptamer*

As illustrated in Figure 9, alternative aptasensors comprised gold-modified microcantilevers, capable of containing thiolated aptamers, in which the differential deflection linearly increased with higher FB1 concentrations [148]. A different approached was proposed for aptamers functionalized with magnetic beads, whose hybridization with cDNA-silver nanoparticles (AgNPs) was diminished

by the presence of the target, with further inductively coupled plasma mass spectrometry of the Ag released as cDNA-AgNPs [149].

In order to reduce the assay complexity, five colorimetric methods have been proposed for the unmodified version of this aptamer, which are converted into optical determinations of either the color intensity or the UV-Vis spectral properties of nanoparticles, labels and chromogenic substrates. On the first system, gold nanoparticles were functionalized with either a thiolated short-strand (DNA1) complementary to the unmodified aptamer or a thiolated short-strand complementary to DNA1 (DNA2). The association of the aptamer and DNA1 was interrupted by the addition of FB1, which also permitted the hybridization of AuNP-DNA1 and AuNP-DNA2, causing aggregation and color shift from red to blue, detected by the naked eyed and analyzed by UV-Vis absorption [241]. For the second approach, thymolphthalein was adsorbed on the surface of GO nanoparticles modified with a semi complementary DNA. The use of the unmodified 96-mer aptamer as a DNA linker, allowed the conjugation of the labelled GO with $Fe_3O_4$/GO, previously modified with a second semi complementary DNA. After target incubation, the $Fe_3O_4$/GO particles were magnetically removed, and a colorimetric detection (UV-Vis absorption) was revealed by adjusting the pH of the remaining solution containing labelled GO [242]. Another colorimetric assay was proposed through the competition between HRP-cDNA and FB1 for binding an aptamer immobilized on a streptavidin-coated microplate. Depending on the amount of FB1, a colorless TMB solution was catalyzed by the hybridized HRP-cDNA to obtain the blue oxTMB, whose yellow color was exposed by the stopping solution (sulfuric acid) and recorded as absorption at 450 nm [233]. As denoted on the previous section, the FB1-regulated electrodeposition of Prussian blue on an ITO electrode was converted into smartphone-based colorimetric detection of the red, green and blue channels in Image J [226]. In contrast to previous reports, the sole application of the unmodified sequence (96 nt) was reported by our research group through an aptamer-FB1-AuNPs conjugate under the presence of $MgCl_2$, which indicated stability to salt-induced aggregation at an increasing target concentration. A critical finding was the role of the detectors on the final sensitivity on a same biosensing system. In this regard, a high LOD was reported when the UV-Vis absorption peaks were analyzed (LOD: 0.003 µg/mL). Recent studies in our laboratory have shown a refined particle separation, innovatively carried out by Asymmetric Flow Field-Flow Fractionation (AF4), in which the analysis of UV-Vis (LOD: 0.000000056 µg/mL) and multiangle light scattering (LOD: 0.00000016 µg/mL) fractograms were comparable to the most sensitive approaches [89].

*4.2 Shorter sequences and minimers derived from the 96 nt aptamer*

Five years after the dissemination of the first aptamer specific to FB1 [69], the same research group explored the affinity of minimers (truncated aptamers) from the initial 96 nt aptamer. The different structures included the whole sequence, and its subsequent chains created by preserving the 3' stem loop motif, and removing the 3', 5', or both primer binding regions (PBR).

Larger melting temperatures from minimers containing the 3' region, suggested their role on the stability and complete formation of hairpins [221]. The same study compared the binding affinity through the calculation of the dissociation constant (Kd) by two assays: DNase I and magnetic beads. The DNase I assay indicated similar affinities between the minimer without the two PBR and the full-length oligonucleotide (Table 6); however, this method also carried considerable errors and denoted binding towards FB2. In contrast, the magnetic beads confirmation assay proved the high affinity of minimers lacking the 3' and both PBR, as well as their overall upgraded binding, due to primary amine masking by the beads, suggesting a most favorable interaction with the tricarballylic acid regions [221]. In silico and docking studies of the minimer without the 3' end, denoted poor and no binding when MST (Kd=3 nM) and magnetic beads (Kd=No binding) were utilized for the assessment of its affinity [218]. A reduction on the sequence length might lead to the development of simpler, yet more sensitive biosensors. The interaction within the shorter 60 nt strand without PBR and its complementary DNA was tested under the presence of different concentrations of FB1, in which the rate of double-stranded DNA formation was identified with the fluorescent dye PicoGreen [90]. Regardless of the specificity issues presented by Frost [221], the truncated sequence studied by Gui [90] was capable of discriminating ochratoxin A (OTA) aflatoxin B1 (AFB1), citrinin (CTN) and zearalenone (ZEN). The specificity of the original long length aptamer was already confirmed for the

null interaction with OTA, AFB1, AFB2, AFG1, AFG2, FB2, ZEN, L-cysteine, BSA, T-2 toxin and deoxynivalenol (DON)(Table 5). Still, even when this 60 nt aptamer-based method was correlated to a reduction on the assay and assay preparation times, its depicted LOD was higher than the values achieved with the full 96 nt sequence.

*4.3 A novel oligonucleotide (80 nt) for the determination of FB1*

Four years after the first reported sequence, a new aptamer selection was presented by using a library of single stranded DNA designed with 80 nt sequences, in which 40 random nucleotides (bold letters) were edged by 20 nt on each side. The SELEX process was executed with the aid of magnetic beads, and included negative (magnetic beads), positive (FB1 modified magnetic beads) and counter (free glycine, AFB1, AFB2, ZEN) selection rounds, which also served to confirm the aptamer selectivity. The selected aptamer: 5'-AGC AGC ACA GAG GTC AGA TG **C GAT CTG GAT ATT ATT TTT GAT ACC CCT TTG GGG AGA CAT** CCT ATG CGT GCT ACC GTG AA-3', showed a lower Kd (62 nM), hence a greater affinity to FB1 was expected for the development of more sensitive aptasensors than that with the 96 nt aptamers [70]; however, this was not the case and the aptasensors so far reported using this aptamer have not shown the expected superior sensitivity, which was also confirmed by its fewer applications. In this regard, although this sequence indicated good binding affinity in MST assays (Kd=224 pM), no binding was detected through the assay with magnetic beads, which might suggest a variability of affinity in close relation to the target freedom or immobilization state [218].

After its introduction, the full-length thiolated version was docked on glassy carbon electrodes in order to enhance its electron transfer resistance, whose decrement was caused by the addition of the target mycotoxin [222]. This electrochemical arrangement derived in a sensitive method, with a similar LOD (0.0014 µg/L) to previous electrochemical aptasensors for FB1 (0.0034 µg/L) [222, 231]. Furthermore, a shorter version, consisting on its 40 random nucleotides, was casted on doped (B or N) and undoped graphene modified GCE, from which boron-doped graphene helped immobilize a higher amount of FB1, improving the impedimetric signal thus the sensitivity of the electrochemical sensor. The Nyquist plot characterization revealed the steric hindrance from the aptamer layer and the repulsion between the aptamer phosphate backbone and the negative redox probe, hence a higher electron transfer resistance of $[Fe(CN)_6]^{3-/4-}$ was observed, especially after the incubation with higher FB1 concentrations [223]. This 40 nt aptamer was also immobilized on graphene oxide nanocolloids (GONCs), causing a reduction on the electroactivity from the oxygen containing groups. The addition of FB1 prompted the full detachment of the aptamer and the partial reestablishment of electroactivity, with potential for biosensing purposes and verified sensitivity under the presence of OTA and thrombin [91]. Although the latter corresponded to low assay and assay preparation times, both biosensors were not comparable to the applications with longer chains. Further research is needed to reveal the affinity mechanism for this aptamer to understand its sensitivity constrains and fully develop highly sensitive aptamer-based sensors.

*4.4 Not specified sequences and alternative methods*

Three studies published by the same research group did not specify the aptamers sequence for the detection of FB1. The first approach relied on the hybridization of Cy5.5-aptamer and its cDNA on gold nanorods, with a further measurement of their SERS (LOD: 0.0003 µg/L) and fluorescent (LOD:0.0005 µg/L) signals under the presence of the target mycotoxin [87]. The second work, which so far is the most sensitive aptasensor for FB1, was reported with a LOD of 0.000003 µg/L. In this arrangement, the inner filter effect between UCNPs and gold nanorods, both linked by a hybridized aptamer, was reduced by disrupting the biocomplex through target incubation and stimulating fluorescence under excitation (980 nm) [96]. The third biosensor combined the modification of AuNPs with aptamers and 4-mercaptobenzoic acid as a Raman reporter, whose signal was reduced after target incubation through dehybridization from a cDNA-AuNP-(4-MBA) complex, with an LOD of 0.00002 µg/L [88]. The effect of the electrochemical interaction between FB1 and fish sperm double-stranded DNA was examined on the impedimetric detection with a pencil graphite electrode, which provides a promising biosensing technique with other DNA structures apart from aptamers [245].

Nevertheless, the addition of five FB1 concentrations did not portray differentiated responses; therefore, more optimization would be ideal for the application of this type of non-specific sequences.

*4.5 Multiplex detection*

Aptasensors are not restricted to the sole determination of single mycotoxins, multiplex analysis can be accomplished with different arrays. Fluorescent [81] and magnetic [149, 236] nanoparticles, as well as their association [95, 239], were applied for the multiple detection of FB1 and OTA. Moreover, photonic crystal microspheres were able to support double (FB1, OTA) and triple (FB1, OTA, AFB1) mycotoxin quantification [234, 235]. In a similar way to fluorescent particles, the application of fluorescent labels favored the establishment of optimum $\lambda_{em}$ in combination with their specific reading methods (filters), for the detection of FB1 and OTA [237]. The specific allocation of a cy3 aptamer and its BHQ antiaptamer on $TiO_2$ modified silicon wafers, was also suitable for the linear quantification of multiple mycotoxins (OTA, AFB1, FB1), where the fluorescence increment was spotted on a defined area of a wafer surface [80]. The combination of two different fluorescent compounds with UCNPs induced two resolved responses under the presence of ZEN and FB1 [96], while the functionalization of UCNPs and AuNPs with aptamers along with aptamer labelling were exploited in the multiplex SERS and fluorescence detection of ZEN, OTA and FB1, through a triple hybridization with a cDNA-AuNPs complex [88]. Likewise, as previously mentioned, the combination of different allochroic dyes with magnetic and GO nanoparticles, was also convenient for the colorimetric detection of FB1, OTA, AFB1 and microcystin-LR [242].

Recent improved electrochemical methods also allowed multiplex analysis, as in the case of glassy carbon electrodes modified with enhancers of electron mobility such as $MoS_2$ and AuNP. These were utilized for the simultaneous quantification of FB1 and ZEN produced by the different reduction peaks from FC6S and thionine, respectively, which functioned as labels for cDNA when simultaneously immobilized on colloidal gold [228]. Likewise, gold electrodes modified with a Y-shaped DNA conformation were efficient for detecting OTA and FB1 due to immobilization of thiolated thionine and ferrocene on gold nanorods, which in addition of enhanced electron transfer, exhibited distinctive peak currents [229].

*4.6 Comparison between aptaensors for FB1: advantages, disadvantages and future perspectives*

A principal component analysis (PCA) specific to all the aptamer-based biosensors for FB1 is indicated in Figure 10, by using LODmax, ATmax and APmax values of 100 µg/L [242], 720 minutes [80] and 12900 minutes [81], respectively. As already noted, assays with a hybridized 96 nt aptamer were mainly correlated to the lowest LODs through fluorescent [80, 81, 95, 232, 235], electrochemiluminescent [230], optical [242] and MS [149] detections, along with fluorescent and SERS signals obtained from non-specified hybridized aptamers [88, 96]. On the other hand, the shortest assay times were correlated to applications with the 96 nt aptamer in its end-modified [148, 231, 237, 238, 244] and hybridized forms [228, 229, 240, 243], as well as electrochemical designs with shorter sequences including the thiol modified 80 nt aptamer [222] and an unmodified 40 nt sequence [223]. Likewise, the shortest assay preparation times showed high correlation to the 60 nt fluorescent [90], 40 nt electrochemical [91], and 96 nt colorimetric [89] aptasensors. Nevertheless, as already stated, the high correlation of the 96 nt aptamer with a high sensitivity (low LODs) in combination with its convenient specificity, were relevant for the existence of more biosensors based on this long length sequence. The most sensitive aptasensors for FB1 have reported LODs equivalent to $1.9x10^{-5}$ µg/L for the utilization of fluorescent nanoparticles [95], $3x10^{-6}$ µg/L from Au nanorods-fluorescent UCNPs [96], and $5.6x10^{-5}$ µg/L for an aptamer-FB1-AuNP complex analyzed by AF4-UV-Vis [89]. UCNPs, fluorescent and ECL particles have suitable optical and chemical properties, precisely their lack of autofluorescence, background noise and absorption by biological samples, along with their lower toxicity, greater stability, and higher photoresistance, when compared to organic fluorophores [81, 232] and fluorescent dyes, indicating fluorescence bleaching and overlap [235]. Even when sensitive, the assay times of many fluorescent aptasensors for FB1 exceeded 100 minutes [80, 81, 88, 232], whose assay preparation time occasionally surpassed 24 h [81, 95, 230, 232, 234 235]. Moreover, this type of methods requires fluorescence spectrophotometers, which might limit their on-site application.

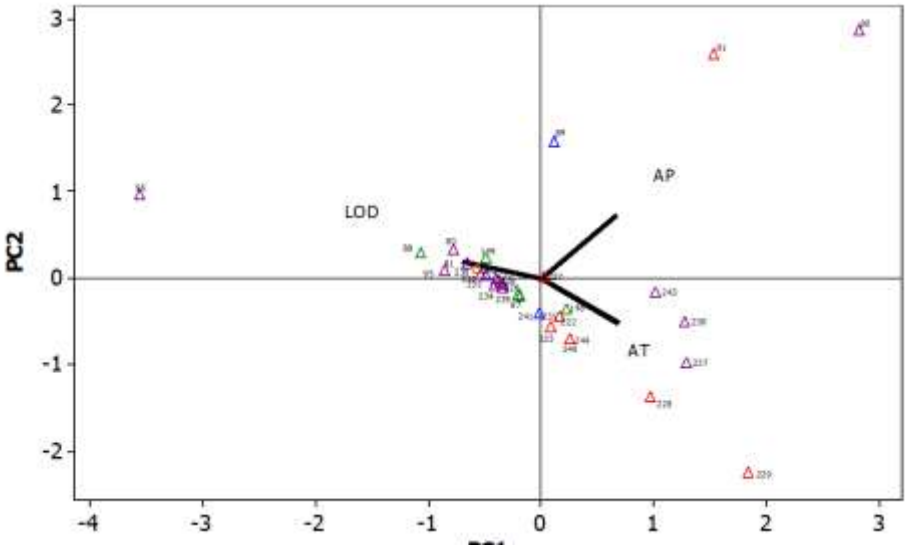


**Figure 10.** Principle component analysis for the correlation of all the reported aptasensors for optical (Δ), fluorescent (Δ), chemiluminescent (Δ), electrochemical (Δ), and other signals (Δ). The numbers correspond to the correlated references from Table 5.

Although, electrochemical aptasensors have indicated low costs, simple operation, good selectivity, affinity, miniaturization and stability, their polishing and other modification steps increase their assay preparation times [227-230], as already observed in some biosensing platforms [226, 236, 240, 244]. In this matter, SPCEs could function as a cheaper and time-effective alternative to methods with modified electrodes [228]. Furthermore, the use of different nanoparticles enhances the applicability of aptamers, however, their long synthesis and washing steps generate an increment on the assay preparation times [241, 242]. In addition, more robust techniques might be ideal for increasing the sensitivity of nanoparticle-based aptasensors. Precisely, as already discussed, the LODs of the signals from the unique complex produced by the incubation of the 96 nt aptamer, FB1 and AuNP in particular buffer conditions ($MgCl_2$ 1mM), was enhanced through the application of AF4 for resolving those complexes [89]. Nevertheless, this analytical technique portrays long assay times and has the same constrains found in chromatographic methods. On the other hand, it is worth noting that no paper-based aptasensor has been developed for the quantification of FB1, whose application could reduce the cost and extend the applicability of such sensitive conformations.

Despite the similar scope of application between aptamers and antibodies, aptasensors are more versatile than immunosensors in terms of their lower sample volumes, simplicity, and absence of washing steps in the majority of the aptamer-based detections [237]. As previously mentioned, contrary to aptasensors, immunochemical methods required high reagent volumes and normally result in the analysis of single mycotoxins where cross-reactivity is observed towards matrix compounds and structurally similar toxins [234]. Besides, antibodies are expensive to produce, and their isoelectric point modulates their net charge polarity, ionic composition and pH, whereas some antibody immobilization methods affect their activity and might produce denaturation [21, 148, 231]. On the contrary, aptamers portray advantages related to their less costly chemical synthesis, which yields high purity small size sequences with no batch variability, low immunogenicity, along with greater stability, reproducibility, shelf life, and reversible denaturation features. This in vitro procedure can also be exploited not only for the chemical modification and labelling of aptamers, but for the controlled selection of aptamers under any specific real testing conditions [71, 95, 234, 237, 240].

Nevertheless, the covalent immobilization of FB1 during SELEX might hinder the specificity of the selected aptamers, as binding could be oriented towards the modified version of the target rather than the free molecule [71]. It has been observed that aptamer 3D folding depends on the buffer compounds and parameters (pH, ionic strength, temperature), which should be considered when creating a sensor in different environmental conditions [74]. In this respect, the performance of two aptamers (96 and 40 nt) carried out by our research group through the development of a AuNP-based colorimetric assay unveiled the role of different binding buffers on the final assay specificity [89]. For instance, unlike previous aptasensors [91,223], assays with the 40 nt aptamer under the presence of Tris HCl denoted lack of specificity when OTA was included [89].

Multiplex aptasensors are strongly desired in food safety, where the simultaneous determination of mycotoxins is beneficial for the overall method cost and efficiency [149, 229]. As previously discussed, multiplex aptasensing methods including FB1 analysis have been successfully developed mainly as fluorescent and electrochemical assays, with one bulk colorimetric design.

Furthermore, aptasensors are still debatable regarding their on-site application, especially when considering that many approaches still require expensive platforms and equipment, skilled users, refrigeration, and electrical installations [71]. The commercialization of aptamer-based biosensor has been outshined by the development of chromatographic methods and ELISA-based kits, mainly because of the laborious SELEX process, which have resulted in the selection of a low number of new sequences specific to FB1. Yet, the application of bioinformatics for *in-silico* studies is a good alternative for coping with the disadvantages of SELEX [78]. Nevertheless, cost-effective, and simple biosensing techniques, with miniaturized and portable features are still required for in-field analysis, in which aptamers have shown an excellent potential as recognition elements [231]. Inexpensive and sensitive in-field assays for FB1 could be accomplished with paper-based designs, in which the utilization of stable AuNPs is suitable due to their van der Waals interactions with aptamers, their surface area, biological compatibility, and their simple and low cost synthesis [18, 149, 171]. Apart from colorimetric sensors, fluorescent paper-based designs could integrate AuNP with FRET dyes [156] and fluorescent materials such as UCNPs, due to their wide absorption, photostability, high yield, easy modification, as well as their narrow yet symmetric emission spectra [81, 149]. In summary, despite the excellent specificity and sensitivity indicated by aptamer-based biosensors for the quantification of FB1, there are many improvements to be applied. Computer-based simulations can be used for the investigation of new sequences specific to this mycotoxin, where more approachable and feasible methods are required for on-site analysis, especially in developing areas with limited infrastructure. As observed with other mycotoxins, more food matrices should be analyzed in new biosensing developments, as only cereals (rice, wheat, maize), beer and peanuts have been screened thus far.

## 5 Conclusions

The use of aptamers for the quantification of fumonisin B1 is at the central focus in the field of biosensors with many areas of opportunity, on account of their relatively recent dissemination and the few strands already reported. Even when sensitive, aptasensors featured similar or lower detections limits than well-established immunosensing techniques, LC-MS assays and Raman-based methods, the recent application of MIPS has redirected the attention on the improvement of the LODs from aptamer-based biosensors. Additionally, despite the diversity of approaches performed with the two selected aptamers and their shortened forms, to date around 95% of all the aptasensors have been proposed as bulk experiments. Hence, there is considerable room of opportunity for the exploration of different supports, ideally paper matrices for the refinement of on-site testing. Additionally, reducing the extraction steps is a desirable quality for quick analysis of samples in remote areas.

Thus far, the specificity of the aptamers utilized for FB1 quantification has been confirmed against up to 19 different molecules, and in multiplex detections of up to 4 targets, while their limits of detection confirmed the feasibility of addressing contamination levels under the regulated limits. It is important to understand and uncover the role of the selected support, and binding conditions (binding buffer, temperature, time) on the selectivity and affinity of the resulting biosensor. Despite all

the advances regarding aptamers, more efforts are necessary to obtain shorter strands with high affinity towards FB1 or novel targets, so the final sensing method can be simplified, yet be effective.

**Acknowledgments:** V.A. Miron-Merida acknowledges Mexico's National Council of Science and Technology (CONACyT) for their support in his Postgraduate Studies through and Academic Scholarship.

**Conflicts of Interest:** The authors declare no conflict of interest.

**References**

1 Eskola, M.; Kos, G.; Elliott, C.T.; Hajšlová, J.; Mayar, S.; Krska, R. Worldwide contamination of food-crops with mycotoxins: Validity of the widely cited 'FAO estimate'of 25%. *Critical reviews in food science and nutrition* **2020**., *60*(16), pp.2773-2789.

2 Khaneghah, A.M.; Fakhri, Y.; Gahruie, H.H.; Niakousari, M.; Sant'Ana, A.S. Mycotoxins in cereal-based products during 24 years (1983–2017): A global systematic review. *Trends in Food Science & Technology* **2019**, *91*, pp.95-105.

3 Marin, S.; Ramos, A.J.; Cano-Sancho, G.; Sanchis, V. Mycotoxins: Occurrence, toxicology, and exposure assessment. *Food and Chemical Toxicology*, **2013**, *60*, pp.218-237.

4 Magnoli, A.P.; Poloni, V.L.; Cavaglieri, L. Impact of mycotoxin contamination in the animal feed industry. *Current Opinion in Food Science* **2019**, *29*, pp.99-108.

5 Quintela, S. Mycotoxins in Beverages: Occurrence, Regulation, Economic Impact and Cost-Effectiveness of Preventive and Removal Methods. In *Safety Issues in Beverage Production*: Academic Press, **2020**, pp. 147-186.

6 Kebede, H.; Liu, X.; Jin, J.; Xing, F. Current status of major mycotoxins contamination in food and feed in Africa. *Food Control* **2020**., *110*, p.106975.

7 Karlovsky, P.; Shman, M.; Berthiller, F.; De Meester, J.; Eisenbrand, G.; Perrin, I.; Oswald, I.P.; Speijers, G.; Chiodini, A.; Recker, T.; Dussort, P. Impact of food processing and detoxification treatments on mycotoxin contamination. *Mycotoxin Research* **2016**, *32(4)*, pp.179-205.

8 BIOMIN. 2015. 2014 BIOMIN mycotoxin survey results: Why advanced multiple mycotoxin detection matters. Available online: https://issuu.com/biomin/docs/mag_scisol_special_02_mtx_en_0515 (Accessed on 2 February 2021).

9 Liu, Y.; Galani-Yamdeu, J.H.; Gong, Y.Y.; Orfila, C. A review of postharvest approaches to reduce fungal and mycotoxin contamination of foods. *Comprehensive Reviews in Food Science and Food Safety* **2020**, *19*(4), pp.1521-1560.

10 Bennett, J.W.; Klich, M. Mycotoxins. *Clinical Microbiology Reviews* **2003**, *16(3)*, pp.497-516.

11 Pitt, J.I.; Wild, C.P.; Baan, R.A.; Gelderblom, W.C.; Miller, J.D.; Riley, R.T.; Wu, F. *Improving public health through mycotoxin control*. (Ed.). Lyon, France: International Agency for Research on Cancer, **2012**.

12 European Commission. 2018. RASFF portal. Available online: https://ec.europa.eu/food/safety/rasff_en (Accessed on 07 April 2020)

13 Agriopoulou, S.; Stamatelopoulou, E.; Varzakas, T. Advances in occurrence, importance, and mycotoxin control strategies: prevention and detoxification in foods. *Foods* **2020**, *9(2)*, p.137.

14 Cinar, A.; Onbaşı, E. Mycotoxins: The hidden danger in foods. In *Mycotoxins and food safety*. IntechOpen, **2019**.

15 Food Standards Agency. 2019. Consolidated annual report and accounts 2018/2019. United Kingdom: APS Group. Available online: https://www.food.gov.uk/sites/default/files/media/document/fsa-annual-report-accounts-2018-19-consolidated.pdf (Accessed on 20 December 2020).

16 Lee, S.; Kim, G.; Moon, J. Performance improvement of the one-dot lateral flow immunoassay for Aflatoxin B1 by using a smartphone-based reading system. *Sensors* **2013**, *13(4)*, pp.5109-5116.

17 Lin, X.; Guo, X. Advances in biosensors, chemosensors and assays for the determination of Fusarium mycotoxins. *Toxins* **2016**, *8(6)*, p.161.

18 Majdinasab, M.; Ben Aissa, S.; Marty, J.L. Advances in Colorimetric Strategies for Mycotoxins Detection: Toward Rapid Industrial Monitoring. *Toxins* **2020**,*13(1)*, p.13.

19 Tittlemier, S.A.; Cramer, B.; Dall'Asta, C.; Iha, M.H.; Lattanzio, V.M.T.; Malone, R.J.; Maragos, C.; Solfrizzo, M.; Stranska-Zachariasova, M.; Stroka, J. Developments in mycotoxin analysis: an update for 2017-2018. *World Mycotoxin Journal* **2019**, *12*(1), pp.3-29.

20 Tittlemier, S.A.; Cramer, B.; Dall'Asta, C.; Iha, M.H.; Lattanzio, V.M.; Maragos, C.; Solfrizzo, M.; Stranska, M.; Stroka, J.; Sumarah, M. Developments in mycotoxin analysis: an update for 2018-19. *World Mycotoxin Journal* **2020**, *13(1)*, pp.3-24.

21 Tang, D.; Lin, Y.; Zhou, Q.; Lin, Y.; Li, P.; Niessner, R.; Knopp, D. Low-cost and highly sensitive immunosensing platform for aflatoxins using one-step competitive displacement reaction mode and portable glucometer-based detection. *Analytical Chemistry* **2014**, *86*(22), pp.11451-11458.

22 Castillo, G.; Spinella, K.; Poturnayová, A.; Šnejdárková, M.; Mosiello, L.; Hianik, T. Detection of aflatoxin B1 by aptamer-based biosensor using PAMAM dendrimers as immobilization platform. *Food Control* **2015**, *52*, pp.9-18.

23 Lin, Y.; Zhou, Q.; Lin, Y.; Tang, D.; Niessner, R.; Knopp, D. Enzymatic hydrolysate-induced displacement reaction with multifunctional silica beads doped with horseradish peroxidase–thionine conjugate for ultrasensitive electrochemical immunoassay. *Analytical chemistry* **2015**, *87*(16), pp. 8531-8540.

24 Lin, Y.; Zhou, Q.; Tang, D.; Niessner, R.; Knopp, D. Signal-on photoelectrochemical immunoassay for aflatoxin B1 based on enzymatic product-etching $MnO_2$ nanosheets for dissociation of carbon dots. *Analytical Chemistry* **2017**, *89*(10), 5637-5645.

25 Lin, Y.; Zhou, Q.; Tang, D. Dopamine-loaded liposomes for in-situ amplified photoelectrochemical immunoassay of AFB1 to enhance photocurrent of $Mn^{2+}$-doped $Zn_3(OH)_2V_2O_7$ nanobelts. *Analytical Chemistry* **2017**, *89*(21), pp.11803-11810.

26 Lin, Y.; Zhou, Q.; Zeng, Y.; Tang, D. Liposome-coated mesoporous silica nanoparticles loaded with L-cysteine for photoelectrochemical immunoassay of aflatoxin B 1. *Microchimica Acta* **2018**, *185*(6), pp.1-9.

27 Lin, Y.; Zhou, Q.; Tang, D.; Niessner, R.; Yang, H.; Knopp, D. Silver nanolabels-assisted ion-exchange reaction with CdTe quantum dots mediated exciton trapping for signal-on photoelectrochemical immunoassay of mycotoxins. *Analytical Chemistry* **2016**, *88*(15), pp.7858-7866.

28 Sabet, F. S.; Hosseini, M.; Khabbaz, H.; Dadmehr, M.; Ganjali, M. R. FRET-based aptamer biosensor for selective and sensitive detection of aflatoxin B1 in peanut and rice. *Food Chemistry* **2017**, *220*, pp.527-532.

29 Shim, W. B.; Kim, M. J.; Mun, H.; Kim, M. G. An aptamer-based dipstick assay for the rapid and simple detection of aflatoxin B1. *Biosensors and Bioelectronics* **2014**, *62*, pp.288-294.

30 Tittlemier, S.A.; Brunkhorst, J.; Cramer, B.; DeRosa, M.C.; Lattanzio, V.M.T.; Malone, R.; Maragos, C.; Stranska, M.; Sumarah, M.W. Developments in mycotoxin analysis: an update for 2019-2020. *World Mycotoxin Journal* **2021**, pp.1-24.

31 Moon, J.; Kim, G.; Lee, S. A gold nanoparticle and aflatoxin B1-BSA conjugates based lateral flow assay method for the analysis of aflatoxin B1. *Materials* **2012**, *5*(4), pp.634-643.

32 Kamle, M.; Mahato, D.K.; Devi, S.; Lee, K.E.; Kang, S.G.; Kumar, P. Fumonisins: Impact on agriculture, food, and human health and their management strategies. *Toxins* **2019**, *11*(6), p.328.

33 Knutsen, H.-K.; Alexander, J.; Barregård, L.; Bignami, M.; Brüschweiler, B.; Ceccatelli, S.; Cottrill, B.; Dinovi, M.; Edler, L.; Grasl-Kraupp, B.; Hogstrand, C.; Hoogenboom, L.; Nebbia, C.S.; Petersen, A.; Rose, M.; Roudot, A.-C.; Schwerdtle, T.; Vleminckx, C.; Vollmer, G.; Wallace, H.; Dall'Asta, C.; Eriksen, G.-S.; Taranu, I.; Altieri, A.; Roldán-Torres, R.; Oswald, I.P. Risks for animal health related to the presence of fumonisins, their modified forms and hidden forms in feed. *EFSA Journal* **2018**, *16*(5), p.e05242.

34 Lamprecht, S.C.; Marasas, W.F.O.; Alberts, J.F.; Cawood, M.E.; Gelderblom, W.C.A.; Shephard, G.S.; Thiel, P.G.; Calitz, F.J. Phytotoxicity of fumonisins and TA-toxin to corn and tomato. *Phytopathology* **1994**, *84(4)*, pp.383-391.

35 Rheeder, J.P.; Marasas, W.F.O.; Vismer, H.F. Production of fumonisin analogs by *Fusarium* species. *Applied and environmental microbiology* **2002,** *68(5)*, pp.2101-2105.

36 Gelderblom, W.C.A.; Jaskiewicz, K.; Marasas, W.F.O.; Thiel, P.G.; Horak, R.M.; Vleggar, R.; Kriek, N.P.J. Fumonisins- Novel mycotoxins with cancer-promoting activity produced by *Fusarium moniliforme*. *Applied and Environmental Microbiology* **1988**, *54(7)*, pp.1806-1811.

37 Abbas, H.K.; Vesonder, R.F.; Boyette, C.D.; Hoagland, R.E.; Krick, T. Production of fumonisins by *Fusarium moniliforme* cultures isolated from jimsonweed in Mississippi. *Journal of Phytopathology* **1992**, *136(3)*, pp.199-203.

38 Bezuidenhout, S.C.; Gelderblom, W.C.A.; Gorst-Allman, C.P.; Horak, R.M.; Marasas, W.F.O.; Spiteller, G.; Vleggaar, R. Structure elucidation of the fumonisins, mycotoxins from *Fusarium moniliforme*. *Journal of the Chemical Society, Chemical Communications* **1988**, *0(11)*, pp.743-745.

39 Branham, B.E.; Plattner, R.D. Isolation and characterization of a new fumonisin from liquid cultures of *Fusarium moniliforme*. *Journal of Natural Products* **1993**, *56(9)*, pp.1630-1633.

40 Abbas, H.K.; Riley, R.T. The presence and phytotoxicity of fumonisins and AAL-toxin in Alternaria alternate. *Toxicon* **1995**, *34(1)*, pp.133-136.

41 Frisvad, J.C.; Smedsgaard, J.; Samson, R.A.; Larsen, T.O.; Thrane, U. Fumonisin $B_2$ production by *Aspergillus niger*. *Journal of Agricultural and Food Chemistry* **2007**, *55(23)*, pp.9727-9732.

42 Månsson, M.; Klejnstrup, M.L.; Phipps, R.K.; Nielsen, K.F.; Frisvad, J.C.; Gotfredsen, C.H.; Larsen, T.O. Isolation and NMR characterization of Fumonisin $B_2$ and a new fumonisin $B_6$ from *Aspergillus niger*. *Journal of Agricultural and Food Chemistry* **2010**, *58(2)*, pp.949-953.

43 Mogensen, J.M.; Møller, K.A.; Freiesleben, P.; Labuda, R.; Varga, E.; Sulyok, M.; Kubatova, A.; Thrane, U.; Andersen, B.; Nielsen, K.F. Production of fumonisins $B_2$ and $B_4$ in *Tolypocladium* species. *Journal of Industrial Microbiology & Biotechnology* **2011**, *38(9)*, pp.1329-1335.

44 Ostry, V.; Malir, F.; Toman, J.; Grosse, Y. Mycotoxins as human carcinogens-the *IARC Monographs* classification. *Mycotoxin Research* ***2017***, *33(1)*, pp.65-73.

45 Gutleb, A.C.; Morrison, E.; Murk, A.J. Cytotoxicity assays for mycotoxins produced by *Fusarium* strains: a review. *Environmental Toxicology and Pharmacology* **2002**, *11(3-4)*, pp.309-320.

46 Riley, R.T.; Merrill, A.H. Ceramide synthase inhibition by fumonisins: a perfect storm of perturbed sphingolipid metabolism, signaling, and disease. *Journal of Lipid Research* **2019**, *60(7)*, pp.1183-1189.

47 Régnier, M.; Polizzi, A.; Lukowicz, C.; Smati, S.; Lasserre, F.; Lippi, Y.; Naylies, C.; Laffitte. J.; Bétoulières, C.; Montagner, A.; Ducheix, S.; Gourbeyre, P.; Ellero-Simatos, S.; Menard, S.; Bertrand-Michel, J.; Al Saati, T.; Lobaccaro, J.M.; Burger, H.M.; Gelderblom, W.C.; Guillou, H.; Oswald, I.P.; Loiseau, N. The protective role of liver X receptor (LXR) during fumonisin B1-induced hepatotoxicity. *Archives of Toxicology* **2019**, *93*, pp.505-517.

48 Liu, X.; Fan, L.; Yin, S.; Chen, H.; Hu, H. Molecular mechanisms of fumonisin B1-induced toxicities and its applications in the mechanism-based interventions. *Toxicon* **2019**, *167*, pp.1-5.

49 Yuan, Q.; Jiang, Y.; Fan, Y.; Ma, Y.; Lei, H.; Su, J. Fumonisin B1 induces oxidative stress and breaks barrier functions in pig iliac endothelium cells. *Toxins* **2019**, *11*, p.387.

50 Sharma, S.K.; Sharma, S.P.; Miller, D.; Parel. J.M.A.; Leblanc, R.M. Interfacial behavior of fumonisin B1 toxin and its degradation on the membrane. *Langmuir* **2019**, *35(7)*, pp.2814-2820.

51 Marasas, W.F.O.; Jaskiewicz, K.; Venter, F.S.; Van Schalkwyk, D.J. *Fusarium moniliforme* contamination of maize in oesophageal cancer areas in Transkei. *South African Medical Journal* **1988**, *74(3)*, pp.110-114.

52 Yoshizawa, T.; Yamashita, A.; Luo, Y. Fumonisin occurrence in corn from high- and low-risk areas for human esophageal cancer in China. *Applied and Environmental Microbiology* **1994**, *60(5)*, pp.1626-1629.

53 Missmer, S.A.; Suarez, L.; Felkner, M.; Wang, E.; Merrll Jr, A. H.; Rothman, K.J.; Hendricks, K.A. Exposure to fumonisins and the occurrence of neural tube defects along the Texas-Mexico border. *Environmental Health Perspectives* **2006**, *114(2)*, pp. 237-241.

54 Magoha, H.; De Meulenaer, B.; Kimanya, M.; Hipolite, C.L.; Kolsteren, P. Fumonisin B1 contamination in breast milk and its exposure in infants under 6 months of age in Rombo, Nothern Tanzania. *Food and Chemical Toxicology* **2014**, *74*, pp.112-116.

55 Riley, R.T.; Torres, O.; Matute. J.; Gregory, S.G.; Ashley-Koch, A.E.; Showker, J.L.; Mitchell, T.; Voss, K.A.; Maddox, J.R.; Gelineau-van Waes, J.B. Evidence for fumonisin inhibition of ceramide synthase in humans consuming maize-based foods and living in high exposure communities in Guatemala. *Molecular Nutrition & Food Research* **2015**, *59(11)*, pp.2209-2224.

56 Torres, O.; Matute, J.; Gelineau-van Waes, J.; Maddox, J.R.; Gregory, S.G.; Ashley-Koch, A.; Showker, J.l.; Zitomer, N.C.; Voss, K.A.; Riley, R.T. Urinary fumonisin B1 and estimated fumonisin intake in women from high- and low- exposure communities in Guatemala. *Molecular Nutrition & Food Research* **2014**, *58(5)*, pp.973-983.

57 Chen, C.; Mitchell, N.J.; Gratz, J.; Houpt, E.R.; Gong, Y.; Egner, P.A.; Groopman, J.D.; Riley, R.T.; Showker, J.L.; Svensen, E.; Mduma, E.R.; Patil, C.L.; Wu, F. Exposure to aflatoxin and fumonisin in children at risk for growth impairment in rural Tanzania. *Environment International* **2018**, *115*, pp.29-37.

58 Food and Agriculture Organization of the United Nations. 2004. *Worldwide regulations for mycotoxins in food and feed in 2003* (31 December 2003). Available online: http://www.fao.org/docrep/007/y5499e/y5499e00.htm (Accessed on 31 October 2017)

59 Udomkun, P.; Wiredu, A.N.; Nagle, M.; Bandyopadhyay, R.; Müller, J.; Vanlauwe, B. Mycotoxins in Sub-Saharan Africa: Present situation, socio-economic impact, awareness, and outlook. *Food Control* **2017**, *72(A)*, pp.110-122.

60 Bartók, T.; Szécsi, A.; Szekeres, A.; Mesterházy, A.; Bartók, M. Detection of new fumonisin mycotoxins and fumonisin-like compounds by reversed-phase high-performance liquid chromatography/electrospray ionization ion trap mass spectrometry. *Rapid Communications in Mass Spectrometry* **2006**, *20(16)*, pp.2447-2462.

61 Savi, G.D.; Piacentini, K.C.; Marchi, D.; Scussel, V.M. Fumonisins $B_1$ and $B_2$ in the corn-milling process and corn-based products, and evaluation of estimated daily intake. *Food Additives & Contaminants: Part A* **2016**, *33(2)*, pp.339-345.

62 Yamagishi, D.; Akamatsu, H.; Otani, H.; Kodama, M. Pathological evaluation of host-specific AAL-toxins and fumonisin mycotoxins produced by *Alternaria* and *Fusarium* species. *Journal of General Plant Pathology* **2006**, *72(5)*, pp.323-327.

63 Noonim, P.; Mahakarnchanakul, W.; Nielsen, K.F.; Frisvad, J.C.; Samson, R.A. Fumonisin $B_2$ production by *Aspergillus niger* in Thai coffee beans. *Food Additives & Contaminants: Part A* **2009**, *26(1)*, pp.94-100.

64 Varga, J.; Kocsubé, S.; Suri, K.; Szigeti, G.; Szekeres, A.; Varga, M.; Tóth, B.; Bartók, T. Fumonisin contamination and fumonisin producing black Aspergilli in dried vine fruits of different origin. *International Journal of Food Microbiology* **2010**, *143(3)*, pp.143-149.

65 Yüce, M.; Ullah, N.; Budak, H. Trends in aptamer selection methods and applications. *Analyst* **2015**, *140(16)*, pp.5379-99.

66 Nguyen, V.T.; Kwon, Y.S.; Gu, M.B. Aptamer-based environmental biosensors for small molecule contaminants. *Current Opinion in Biotechnology* **2017**, *45*, pp.15-23.

*67* Song, S.H.; Gao, Z.F.; Guo, X.; Chen, G.H. Aptamer-based detection methodology studies in food safety. *Food Analytical Methods* **2019**, *12(4)*, pp. 966-990.

68 Schmitz F.R.; Valério, A.; de Oliveira, D.; Hotza, D. An overview and future prospects on aptamers for food safety. *Applied Microbiology and Biotechnology* **2020**, *104,* pp.6929-6939.

69 McKeague, M.; Bradley, C.R.; De Girolamo, A.; Visconti, A.; Miller, J.D.; DeRosa, M.C. Screening and initial binding assessment of fumonisin B1 aptamers. *International Journal of Molecular Sciences* **2010**, *11(12)*, pp.4864-4881.

70 Chen, X.; Huang, Y.; Duan, N.; Wu, S.; Xia, Y.; Ma, X.; Zhu, C.; Jiang, Y.; Ding, Z.; Wang, Z. Selection and characterization of single stranded DNA aptamers recognizing fumonisin B1. *Microchimica Acta* **2014**, *181*, pp.1317-1324.

71 Ruscito, A.; Smith, M.; Goudreau, D.N.; DeRosa, M.C. Current status and future prospects for aptamer-based mycotoxin detection. *Journal of AOAC International* **2016**, *99(4)*, pp.865-877.

72 Pfeiffer, F.; Mayer, G. Selection and biosensor application of aptamers for small molecules. *Frontiers in Chemistry* **2016**, *4*, p.25.

73 Berthiller, F.; Cramer, B.; Iha, M.H.; Krska, R.; Lattanzio, V.M.; MacDonald, S.; Malone, R.J.; Maragos, C.; Solfrizzo, M.; Stranska-Zachariasova, M.; Stroka, J. Developments in mycotoxin analysis: an update for 2016-2017. *World Mycotoxin Journal* **2018**, *11(1)*, pp.5-32.

74 Evtugyn, G.; Hianik T. Aptamer-based biosensors for mycotoxin detection. In *Nanomycotoxicology* **2020**, pp. 35-70. Academic Press.

75 Zhang, K.; Li, H.; Wang, W.; Cao, J.; Gan, N.; Han, H. Application of multiplexed aptasensors in food contaminants detection. *ACS sensors* **2020**, *5(12)*, pp.3721-3738.

76 Goud. K.Y.; Reddy, K.K.; Satyanarayana, M.; Kummari, S.; Gobi, K.V. A review on recent developments in optical and electrochemical aptamer-based assays for mycotoxins using advanced nanomaterials. *Microchimica Acta* **2020**, *187(1)*, p.29.

77 Zhou, Q.; Tang, D. Recent advances in photoelectrochemical biosensors for analysis of mycotoxins in food. *TrAC Trends in Analytical Chemistry* **2020**, *124*, p.115814.

78 Yoo, H.; Jo, H.; Oh, S. S. Detection and beyond: challenges and advances in aptamer-based biosensors. *Materials Advances* **2020**, *1*(8), pp.2663-2687.

79 Kadir, M.K.; Tothill, I.E. Development of an electrochemical immunosensor for fumonisins detection in foods. *Toxins* **2010**, *2(4)*, pp.382-398.

80 Liu, R.; Li, W.; Cai, T.; Deng, Y.; Ding, Z.; Liu, Y.; Zhu, X.; Wang, X.; Liu, J.; Liang, B.; Zheng, T.; LI, J. $TiO_2$ nanolayer-enhanced fluorescence for simultaneous multiplex mycotoxin detection by aptamer microarrays on a porous silicon surface. *Applied Materials and Interfaces* **2018**, *10*, pp.14447-14453.

81 Wu, S.; Duan, N.; Ma, X.; Xia, Y.; Wang, H.; Wang, Z.; Zhang, Q. Multiplexed fluorescence resonance energy transfer aptasensor between upconversion nanoparticles and graphene oxide for the simultaneous determination of mycotoxins. *Analytical Chemistry* **2012**, *84(14)*, pp.6263-6270.

82 Ghali, R.; Ghorbel, H.; Hedilli, A. Fumonisin determination in Tunisian foods and feeds. ELISA and HPLC methods comparison. *Journal of Agricultural and Food Chemistry* **2009**, *57(9)*, pp.3955-3960.

83 Hossain, S.M.; Luckham, R.E.; Smith, A.M.; Lebert, J.M.; Davies, L.M.; Pelton, R.H.; Filipe, C.; Brennan, J.D. Development of a bioactive paper sensor for detection of neurotoxins using piezoelectric inkjet printing of sol-gel-derived bioinks. *Analytical Chemistry* **2009**, *81(13)*, pp.5474–5483.

84 Ren, W.; Huang, Z.; Xu, Y.; Li, Y.; Ji, Y.; Su, B. Urchin-like gold nanoparticle-based immunochromatographic strip test for rapid detection of fumonisin $B_1$ in grains. *Analytical and Bioanalytical Chemistry* **2015**, *407(24)*, pp.7341-7348.

85 Huang, X.; Huang, T.; Li, X.; Huang, Z. Flower-like gold nanoparticles-based immunochromatographic test strip for rapid simultaneous detection of fumonisin B1 and deoxynivalenol in Chinese traditional medicine. *Journal of Pharmaceutical and Biomedical Analysis* **2020**, *177*, p. 112895.

86 Munawar, H.; Garcia-Cruz, A.; Majewska, M.; Karim, K.; Kutner, W.; Piletsky, S.A., Electrochemical determination of fumonisin B1 using a chemosensor with a recognition unit comprising molecularly imprinted polymer nanoparticles. *Sensors and Actuators B: Chemical* **2020**, *321*, p.128552.

87 He, D.; Wu, Z.; Cui, B.; Xu, E. Aptamer and gold nanorod–based fumonisin B1 assay using both fluorometry and SERS. *Microchimica Acta* **2020**, *187(4)*, pp.1-8.

88 Wu, Z.; He, D.; Cui, B.; Jin, Z.; Xu, E.; Yuan, C.; Liu, P.; Fang, Y.; Chai, Q. Trimer-based aptasensor for simultaneous determination of multiple mycotoxins using SERS and fluorimetry. *Microchimica Acta* **2020**, *187(9)*, pp.1-7.

89 Mirón-Mérida, V.A.; González-Espinosa, Y.; Collado-González, M.; Gong, Y.Y.; Guo, Y.; Goycoolea, F. M. Aptamer–target–gold nanoparticle conjugates for the quantification of fumonisin B1. *Biosensors* **2021**, *11*(1), p.18.

90 Gui, H.; Jin, Q.; Zhang, Y.; Wang, X.; Yang, Y.; Shao, C.; Cheng, C.; Wei, F.; Yang, Y.; Yang, M.; Song, H. Development of an aptamer/ fluorescence dye PicoGreen-based method for detection of fumonisin B1. *Sheng Wu Gong Cheng Xue Bao* **2015**, *31(9)*, pp.1393–1400.

91 Cheng, Z.; Bonanni, A. All-in-One: Electroactive nanocarbon as simultaneous platform and label for single-step biosensing. *Nanomaterials* **2018**, *24*, pp.6380-6385.

92 Souto, P.C.M.C.; Jager, A.V.; Tonin, F.G.; Petta, T.; Di Gregório, M.C.; Cossalter, A-M.; Pinton, P.; Oswald, I.P.; Rottinghaus, G.E.; Oliveira, A.A.F. Determination of fumonisin B1 levels in body fluids and hair from piglets fed fumonisin B1-contaminates diets. *Food and Chemical Toxicology* **2017**, *108(A)*, pp.1-9.

93 Da Silva, L.P.; Madureira, F.; De Azevedo, E.; Ferreira, A.; Augusti, R. Development and validation of a multianalyte method for quantification of mycotoxins and pesticides in rice using a simple dilute and shoot procedure and UHPLC-MS/MS. *Food Chemistry* **2019**, *270*, pp.420-427.

94 Lee, K.M.; Herrman, T. Determination and prediction of fumonisin contamination in Maize by surface-enhanced Raman spectroscopy (SERS). *Food Bioprocess Technology* **2016**, *9(4)*, pp.588-603.

95 Niazi, S.; Khan, I.M.; Yan, L.; Khan, M.I.; Mohsin, A.; Duan, N.; Wu, S.; Wang, Z. Simultaneous detection of fumonisin B1 and ochratoxin A using dual-color, time-resolved luminescent nanoparticles ($NaYF_4$: Ce, Tb and $NH_2$-Eu/DPA@$SiO_2$) as labels. *Analytical and Bioanalytical Chemistry* **2019**; *411*, pp.1453-1465.

96 He, D.; Wu, Z.; Cui, B.; Jin, Z.; Xu, E. A fluorometric method for aptamer-based simultaneous determination of two kinds of the fusarium mycotoxins zearalenone and fumonisin B1 making use of gold nanorods and upconversion nanoparticles. *Microchimica Acta* **2020**, 187, p.254.

97 Masikini, M.; Mailu, S.N.; Tsegaye, A.; Njomo, N.; Molapo, K.M.; Ikpo, C.O.; Sunday, C.E.; Rassie, C.; Wilson, L.; Baker, P.G.L.; Iwuoha, E.I. A fumonisin immunosensor based on polyanilino-carbon nanotubes doped with palladium telluride quantum dots. *Sensors* **2015**, *15(1)*, pp.529-546.

98 Masikini, M.; Williams, A.R.; Sunday, C.E.; Waryo, T.T.; Nxusani, E.; Wilson, L.; Qakala, S. Bilibana, M.; Douman, S.; Jonnas, A.; Baker, P.G.L.; Iwuoha, E.I. Label free poly(2,5-dimethoxyaniline)-multi-walled carbon nanotubes impedimetric immunosensor for fumonisin B1 detection. *Materials* **2016**, *9(4)*, pp.273-286.

99 Venkataramana, M.; Navya, K.; Chandranyaka, S.; Privanka, S.R.; Murali, H.S.; Batra, H.V. Development and validation of an immunochromatographic assay for rapid detection of fumonisin B1 from cereal samples. *Journal of Food Science and Technology* **2014**, *51(9)*, pp.1920-1928.

100 Li, L.; Chen, W.; Li, H.; Iqbal, J.; Zhu, Y.; Wu, T.; Du, Y. Rapid determination of fumonisin (FB1) by syringe SPE coupled with solid-phase fluorescence spectrometry. *Spectrochimica Acta Part A: Molecular and Biomolecular Spectroscopy* **2020**, *226*, p.117549.

101 Gong, Y.Y.; Torres-Sanchez, L.; Lopez-Carrillo, L.; He Peng, J.; Sutcliffe, A.E.; White, K.L.; Humpf, H-U.; Turner, P.C.; Wild, C.P. Association between tortilla consumption and human urinary fumonisin B1 levels in a 33omencl population. *Cancer Epidemiology, Biomarkers & Prevention,* **2008**, *17(3)*, pp.688-694.

102 Silva, L.J.G.; Pena, A.; Lino, C.M.; Fernández, M.F.; Mañes, J. Fumonisin determination in urine by LC-MS-MS. *Analytical and Bioanalytical Chemistry* **2010**, *396(2)*, pp.809-816.

103 Siler, D.J.; Gilchrist, D.G. Determination of host-selective phytotoxins from *Alternaria alternata* f.sp. *lycopersici* as their maleyl derivatives by high-performance liquid chromatography. *Journal of Chromatography* **1982***, 238*, pp.167-173.

104 Sydenham, E.W.; Gelderblom, W.C.A.; Thiel, P.G.; Marasas, W.F.O. Evidence for the natural occurrence of fumonisin B1, a mycotoxin produced by *Fusarium moniliforme,* in corn. *Journal of Agricultural and Food Chemistry* **1990**, *38(1)*, pp.285-290.

105 Campa, R.; Miller, D.; Hendricks, K. Fumonisin in tortillas produced in small-scale facilities and effect of traditional masa production methods on this mycotoxin. *Journal of Agricultural and Food Chemistry* **2004**, *52*, pp.4432-4437.

106 Petrarca, M.H.; Rodrigues, M.I.; Rossi, E.A.; De Sylos, C.M. Optimisation of a simple preparation method for the determinations of fumonisin B1 in rice. *Food Chemistry* **2014**, *158*, pp.270-277.

107 Shepard, G.S.; Sydenham, E.W.; Thiel, P.G.; Gelderblom, C.A. Quantitative determination of fumonisins B1 and B2 by high-performance liquid chromatography with fluorescence detection. *Journal of Liquid Chromatography* **1990***, 13(10)*, pp.2077-2087.

108 Bordin, K.; Rosim, R.E.; Neeff, D.V.; Rottinghaus, G.E.; Oliveira, C.A.F. Assessment of dietary intake of fumonisin B1 in São Paulo, Brazil. *Food Chemistry* **2014**, *155*, pp.174-178.

109 Dall'Asta, C.; Mangia, M.; Berthiller, F.; Molinelli, A.; Sulyok, M.; Schuhmacher, R.; Krska, R.; Galaverna, G.; Dossena, A.; Marchello, R. Difficulties in fumonisin determination: the issue of hidden fumonisins. *Analytical and Bioanalytical Chemistry* **2009**, *395(5)*, pp.1335-1345.

110 Holcomb, M.; Thompson, H.C.; Hankins, L.J. Analysis of fumonisin B1 in rodent feed by gradient elution HPLC using precolumn derivatization with FMOC and fluorescence detection. *Journal of Agricultural and Food Chemistry* **1993**, *41(5)*, pp.764-767.

111 Smith, L.L.; Francis, K.A.; Johnson, J.T.; Gaskill, C.L. Quantification of fumonisin B1 and B2 in feed using FMOC pre-column derivatization with HPLC and fluorescence detection. *Food Chemistry* **2017**, *234*, pp.174-179.

112 Ueno, Y.; Iijima, K.; Wang, S.-D.; Sugiura, Y.; Sekijima, M.; Tanaka, T.; Chen, C.; Yu, S.-Z. Fumonisins as a possible contributory risk factor for primary liver cancer: a 3-year study of corn harvested in Haimen, China, by HPLC and ELISA. *Food and Chemical Toxicology* **1997**, *35(12)*, pp.1143-1150.

113 Bordin, K.; Rottinghaus, G.E.; Landers, B.R.; Ledoux, D.R.; Kobashigawa, E.; Corassin, C.H.; Oliveira, C.A.F. Evaluation of fumonisin exposure by determination of fumonisin B1 in human hair and in Brazilian corn products. *Food Control* **2015**, *53*, pp.67-71.

114 Liu, H.; Luo, J.; Kong, W.; Liu, Q.; Hu, Y.; Yang, M. UFLC-ESI-MS/MS analysis of multiple mycotoxins in medicinal and edible *Areca catechu*. *Chemosphere* **2016**, *150*, pp.176-183.

115 Li, M.; Kong, W.; Li, Y.; Liu, H.; Liu, Q.; Dou, X.; Ou-yang, Z.; Yang, M. High-throughput determination of multi-mycotoxins in Chinese yam and related products by ultra fast liquid chromatography coupled with tandem mass spectrometry after one-step extraction. *Journal of Chromatography B* **2016**, *1022*, pp. 118-125.

116 Xing, Y.; Meng, W.; Sun, W.; Li, D.; Yu, Z.; Tong, L.; Zhao, Y. Simultaneous qualitative and quantitative analysis of 21 mycotoxins in *Radix Paeoniae Alba* by ultra-high performance liquid chromatography quadrupole linear ion trap mass spectrometry and QuEChERS for sample preparation. *Journal of Chromatography B* **2016**, *1031*, pp.202-213.

117 Dagnac, T.; Latorre, A.; Fernández, B.; Maria, M. Validation and application of a liquid chromatography-tandem mass spectrometry based method for the assessment of the cooccurrence of mycotoxins in maize silages from dairy farms in NW Spain. *Food Additives & Contaminants: Part A* **2016**, *33(12)*, pp.1850-1863.

118 Sun, J.; Li, W.; Zhang, Y.; Hu, X.; Wu, L.; Wang, B. QuEChERS purification combined with ultrahigh-performance liquid chromatography tandem mass spectrometry for simultaneous quantification of 25 mycotoxins in cereals. *Toxins* **2016**, *8*, pp.375-392

119 Osteresch, B.; Viegas, S.; Cramer, B.; Humpf, H-U. Multi-mycotoxin analysis using dried blood spots and dried serum spots. *Analytical and Bioanalytical Chemistry* **2017**, *409*, pp.3369-3382.

120 Flores-Flores, M.E.; González-Peñas, E. An LC-MS/MS method for multi-mycotoxin quantification in cow milk. *Food Chemistry* **2017**, *218*, pp.378-385.

121 Zhao, Y.; Wan, L.; Bai, X.; Liu, Y.; Zhang, F.; Liu, Y.; Liao, X. Quantification of mycotoxins in vegetable oil by UPLC-MS/MS after magnetic solid-phase extraction. *Food Additives & Contaminants: Part A* **2017**, *34(7)*, pp.1201-1210.

122 Annunziata, L.; Stramenga, A.; Visciano, P.; Schirone, M.; De Colli, L.; Novella, M.; Campana, G.; Scortichini, G. Simultaneous determination of aflatoxins, T-2 and HT-2 toxins, and fumonisins in cereal-derived products by QuEChERS extraction coupled with LC-MS/MS. *Analytical and Bioanalytical Chemistry* **2017**, *409*, pp.5143-5155.

123 Miró-Abella, E.; Herrero, P.; Canela, N.; Arola, L.; Borrull, F.; Ras, R.; Fontanals, N. Determination of mycotoxins in plant-based beverages using QuEChERS and liquid chromatography-tandem mass spectrometry. *Food Chemistry* **2017**, *229*, pp.366-372.

124 Zhao, X.S.; Kong, W.J.; Wang, S.; Wei, J.H.; Yang, M.H. Simultaneous analysis of multiple mycotoxins in *Alpinia oxyphylla* by UPLC-MS/MS. *World Mycotoxin Journal* **2017**, *10(1), pp.41-51.*

125 Du, L.-J.; Chu, C.; Warner, E.; Wang, Q.-Y.; Hu, Y.-H.; Chai, K.-J.; Cao, J.; Peng, L.-Q.; Chen, Y.-B.; Yang, J.; Zhang, Q.-D. Rapid microwave-assisted dispersive micro-solid phase extraction of mycotoxins in food using zirconia nanoparticles. *Journal of Chromatography A* **2018**,*1561*, pp.1-12.

126 Huang, P.; Kong, W.; Wang, S.; Wang, R.; Lu, J.; Yang, M. Multiclass mycotoxins in lotus seeds analysed by an isotope-labelled internal standard-based UPLC-MS/MS. *Journal of Pharmacy and Pharmacology* **2018**, *70*, pp.1378-1388.

127 Zhang, B.; Chen, X.; Han, S.-Y.; Li, M.; Ma, T.-Z.; Sheng, W.-J.; Zhu, X. Simultaneous analysis of 20 mycotoxins in grapes and wines from Hexi corridor region (China): based on a QuEChERS–UHPLC–MS/MS method. *Molecules* **2018**, *23(8)*, p.1926.

128 Carballo, C.; Font, G.; Ferrer, E.; Berrada, H. Evaluation of mycotoxin residues on ready-to-eat food by chromatographic methods coupled to mass spectrometry in tandem. *Toxin* **2018**, *10(10)*, p.243.

129 Park, J.; Kim, D.-H.; Moon, J.-Y.; An, J.-A.; Kim, Y.-W.; Chung, S.-H.; Lee, C. Distribution analysis of twelve mycotoxins in corn and corn-derived products by LC-MS/MS to evaluate the carry-over ratio during wet-milling. *Toxins* **2018**, *10(8)*, p.319.

130 Šarkanj, B.; Ezekiel, C.N.; Turner, P.C.; Abia, W.A.; Rychlik, M.; Krska, R.; Sulyok, M.; Warth, B. Ultra-sensitive, stable isotope assisted quantification of multiple urinary mycotoxin exposure biomarkers. *Analytica Chimica Acta* **2018**, *1019*, pp.84-92.

131 González-Jartín, J.M.; Alfonso, A.; Rodríguez, I.; Sainz, M.J.; Vieytes, M.R.; Botana, L.M.A. QuEChERS based extraction procedure coupled to UPLC-MS/MS detection for mycotoxins analysis in beer. *Food Chemistry* **2019**, *275*, pp.703-710.

132 Jedziniak, P.; Panasiuk, L.; Pietruszka, K.; Posyniak, A. Multiple mycotoxins analysis in animal feed with LC-MS/MS: Comparison of extract dilution and immune affinity clean-up. *Journal of Separation Science* **2019**, *42*, pp.1240-1247.

133 Abdallah, M.F.; Audenaert, K.; Lust, L.; Landschoot, S.; Bekaert, B.; Haesaert, G.; De Boevre, M.; De Saeger, S. Risk characterization and quantification of mycotoxins and their producing fungi in

sugarcane juice: A neglected problem in a widely-consumed traditional beverage. *Food Control* **2020**, *108*, p.106811.

134 Hort, V.; Nicolas, M.; Travel, A.; Jondreville, C.; Maleix, C.; Baéza, E.; Engel, E.; Guérin, T. Carry-over assessment of fumonisins and zearalenone to poultry tissues after exposure of chickens to a contaminated diet–A study implementing stable-isotope dilution assay and UHPLC-MS/MS. *Food Control* **2020**, *107*, p.106789.

135 Sulyok, M.; Krska, R.; Senyuva, H. Profiles of fungal metabolites including regulated mycotoxins in individual dried Turkish figs by LC-MS/MS. *Mycotoxin Research* **2020**, *36(4)*, pp.381-387.

136 Danezis, G.P.; Anagnostopoulos, C.J.; Liapis, K.; Koupparis, M.A. Multi-residue analysis of pesticides, plant hormones, veterinary drugs and mycotoxins using HILIC chromatography e MS/MS in various food matrices. *Analytica Chimica Acta* **2016**, *942*, pp. 121-138.

137 Cladière, M.; Delaporte, G.; Le Roux, E.; Came, V. Multi-class analysis for simultaneous determination of pesticides, mycotoxins, process-induced toxicants and packaging contaminants in tea. *Food Chemistry* **2018**, *242*, pp.113-121.

138 Hamed, A.M.; Arroyo-Manzanares, N.; García-Campaña, A.M.; Gámiz-Gracia, L. Determination of Fusarium toxins in functional vegetable milks applying salting-out-assisted liquid-liquid extraction combined with ultra-high performance liquid chromatography tandem mass spectrometry. *Food Additives & Contaminants: Part A* **2017**, *34(11)*, pp.2033-2041.

139 Abdallah, M.F.; Krska, R.; Sulyok, M. Occurrence of ochratoxins, fumonisin B2, aflatoxins(B1 and B2), and other secondary fungal metabolites in dried date palm fruits from Egypt: A mini-survey. *Journal of Food Science* **2018**, *83(2)*, pp.559-564.

140 Abia, W.A.; Warth, B.; Ezekiel, C.N.; Sarkanj, B.; Turner, P.C.; Marko, D.; Krska, R.; Sulyok, M. Uncommon toxic microbial metabolite patterns in traditionally home-processed maize dish (fufu) consumed in rural Cameroon. *Food and Chemical Toxicology* **2017**, *107*, pp.10-19.

141 Nafuka, S. N.; Misihairabgwi, J. M.; Bock, R.; Ishola, A.; Sulyok, M.; Krska, R. Variation of fungal metabolites in sorghum malts used to prepare Namibian traditional fermented beverages Omalodu and Otombo. *Toxins* **2019**, *11(3)*, p.165.

142 Gazzotti, T.; Lugoboni, B.; Zironi, E.; Barbarossa, A.; Serraino, A.; Pagliuca, G. Determination of fumonisin B1 in bovine milk by LC-MS/MS. *Food Control* **2009**, *20(12)*, pp.1171-1174.

143 Zhang, S.; Lu, J.; Wang, S.; Mao, D.; Miao, S.; Ji, S. Multy-mycotoxins analysis in *Pheretima* using ultra-high-performance liquid chromatography tandem mass spectrometry based on a modified QuEChERS method. *Journal of Chromatography B* **2016**, *1035*, pp.31-41.

144 Gilbert-Sandoval, I.; Wesseling, S.; Rietjens, I.M. Occurrence and probabilistic risk assessment of fumonisin B1, fumonisin B2 and deoxynivalenol in nixtamalized maize in Mexico City. *Toxins* **2020**, *12(10)*, p.644.

145 Yapo, A.E.; Strub, C.; Durand, N.; Ahoua, A.R.C.; Schorr-Galindo, S.; Bonfoh, B.; Fontana, A.; Koussémon, M. Mass spectrometry-based detection and risk assessment of mycotoxin contamination of 'kankankan'used for roasted meat consumption in Abidjan, Côte d'Ivoire. *Food Additives & Contaminants: Part A* **2020**, *37(9)*, pp.1564-1578.

146 Tansakul, N.; Jala, P.; Laopiem, S.; Tangmunkhong, P.; Limsuwan, S. Co-occurrence of five Fusarium toxins in corn-dried distiller´s grains with solubles in Thailand and comparison of ELISA and LC-MS/MS for fumonisin analysis. *Mycotoxin Research* **2013**, *29(4)*, pp.255.260.

147 De Baere, S.; Croubels, S.; Novak, B.; Bichl, G.; Antonissen, G. Development and validation of a UPLC-MS/MS and UPLC-HR-MS method for the determination of fumonisin B1 and its hydrolysed metabolites and fumonisin B2 in broiler chicken plasma. *Toxins* **2018**, *10(2), p.62.*

148 Chen, X.; Bai, X.; Li, H.; Zhang, B. Aptamer-based microcantilever array biosensor for detection of fumonisin $B_1$. *RSC Advances* **2015**, *5*, pp.35448-35452.

149 Jiang, D.; Huang, C.; Shao, L.; Wang, X.; Jiao, Y.; Li, W.; Chen, J.; Xu, X. Magneto-controlled aptasensor for simultaneous detection of ochratoxin A and fumonisin B1 using inductively coupled plasma mass spectrometry with multiple metal nanoparticles as element labels. *Analytica Chimica Acta* **2020**, *1127*, pp.182-189.

150 Bessaire, T.; Perrin, I.; Tarres, A.; Bebius, A.; Reding, F.; Theurillat, V. Mycotoxins in green coffee: Occurrence and risk assessment. *Food Control* **2019**, *96*, pp.59-67.

151 Ligler, F.S.; Taitt, C.R.; Shriver-Lake, L.C.; Sapsford, K.E.; Shubin, Y.; Golden, J.P. Array biosensor for detection of toxins. *Analytical and Bioanalytical Chemistry* **2003**, *377(3)*, pp.469-477.

152 Quan, Y.; Zhang, Y.; Wang, S.; Lee, N.; Kennedy, I.R. A rapid and sensitive chemiluminescence enzyme-linked immunosorbent assay for the determinations of fumonisins B1 in food samples. *Analytica Chimica Acta* **2006**, *580(1)*, pp.1-8.

153 Yang, H.; Zhang, Q.; Liu, X.; Yang, Y.; Yang, Y.; Liu, M.; Li, P.; Zhou, Y. Antibody-biotin-streptavidin-horseradish peroxidase (HRP) sensor for rapid and ultra-sensitive detection of fumonisins. *Food Chemistry* **2020**, *316*, p.126356.

154 Zhan, S.; Zheng, L.; Zhou, Y.; Wu, K.; Duan, H.; Huang, X.; Xiong, Y. A Gold Growth-Based Plasmonic ELISA for the Sensitive Detection of Fumonisin B1 in Maize. Toxins **2019**, *11(6)*, p.323.

155 Ren, W.; Xu, Y.; Huang, Z.; Li, Y.; Tu, Z.; Zou, L.; He, Q.; Fu, J.; Liu, S.; Hammock, B. D. Single-chain variable fragment antibody-based immunochromatographic strip for rapid detection of fumonisin B1 in maize samples. *Food Chemistry* **2020**, p. 126546.

156 Zhang, L.; Sun, Y.; Liang, X.; Yang, Y.; Meng, X.; Zhang, Q.; Li, P.; Zhou, Y. Cysteamine triggered “turn-on” fluorescence sensor for total detection of fumonisin B1, B2 and B3. *Food Chemistry* **2020**, *327*, p.127058.

157 Shu, M.; Xu, Y.; Dong, J.; Zhong, C.; Hammock, B.D.; Wang, W.; Wu, G. Development of a noncompetitive idiometric nanobodies phage immumoassay for the determination of fumonisin B1. *Food and Agricultural Immunology* **2019**, *30(1)*, pp.510-521.

158 Qu, J.; Xie, H.; Zhang, S.; Luo, P.; Guo, P.; Chen, X.; Ke, Y.; Zhuang, J.; Zhou, F.; Jiang, W. Multiplex flow cytometric immunoassays for high-throughput screening of multiple mycotoxin residues in milk. *Food Analytical Methods* **2019**, *12*, pp. 877-886.

159 Munawar, H.; Smolinska-Kempisty, K.; Cruz, A.G.; Canfarotta, F.; Piletska, E.; Karim, K.; Piletsky, S.A. Molecular imprinted polymer nanoparticle-based assay (MINA): application for fumonisin B1 determination. *Analyst* **2018**,*143*, pp.3481-3488.

160 Yang, X.; Zhou, X.; Zhang, X.; Qing, Y.; Luo, M.; Liu, X.; Li, C.; Li, Y.; Xia, H.; Qiu, J. A highly sensitive electrochemical immunosensor for fumonisin B1 detection in corn using single-walled carbon nanotubes/chitosan. *Electroanalysis* **2015**, *27(11)*, pp.2679-2687.

161 Wang, X.; Park, S.-G.; Ko, J.; Xiao, X.; Giannini, V.; Maier, S.A.; Kim, D.-H.; Choo, J. Sensitive and reproducible immunoassay of multiple mycotoxins using surface-enhanced Raman scattering mapping on 3D plasmonic nanopillar arrays. *Small* **2018**, *14*, p.1801623.

162 Molinelli, A.; Grossalber, K.; Krska, R. A rapid lateral flow test for the determination of total type B fumonisins in maize. *Analytical and Bioanalytical Chemistry* **2009**, *395*, pp.1309-1316.

163 Anfossi, L.; Calderara, M.; Baggiani, C.; Giovannoli, C.; Arletti, E.; Giraudi, G. Development and application of a quantitative lateral flow immunoassay for fumonisins in maize. *Analytica Chimica Acta* **2010**, *682*(1-2), pp.104-109.

164 Li, Y.-S.; Zhou, Y.; Lu, S.-Y.; Guo, D.-J.; Ren, H.-L.; Meng, X.-M.; Zhi, B.-H.; Lin, C.; Wang, Z.; Li, X.-B.; Liu, Z.-S. Development of a one-step strip for rapid screening of fumonisins $B_1$, $B_2$ and $B_3$ in maize. *Food Control* **2012**, *24(1-2)*, pp.72-77.

165 Lattanzio, V.M.T.; Nirvarlet, N.; Lippolis, V.; Gatta, S.D.; Huet, A.-C.; Delahaut, P.; Granier, B.; Visconti, A. Multiplex dipstick immunoassay for semi-quantitative determination of *Fusarium* mycotoxins in cereals. *Analytica Chimica Acta* **2012**, *718*, pp.99-108.

166 Wang, Y-K.; Yan, Y-X.; Ji, W-H.; Wang, H.; Li, S-Q.; Zou, Q.; Sun, J-H. Rapid simultaneous quantification of zearalenone and fumonisin $B_1$ in corn and wheat by lateral flow dual immunoassay. *Journal of Agricultural and Food Chemistry* **2013**, *61(21)*, pp.5031-5036.

167 Zangheri, M.; Nardo, F.; Anfossi, L.; Giovannoli, C.; Baggiani, C.; Roda, A.; Mirasoli, M. A multiplex chemiluminescent biosensor for type B-fumonisins and aflatoxin B1 quantitative detection in maize flour. *Analyst* **2015**, *140*, pp.358-365.

168 Tang, X.; Li, P.; Zhang, Z.; Zhang, Q.; Guo, J.; Zhang, W. An ultrasensitive gray-imaging- based quantitative immunochromatographic detection method for fumonisin B1 in agricultural products. *Food control* **2017**, *80*, pp.333-340.

169 Anfossi, L.; Di Nardo, F.; Cavalera, S.; Giovannoli, C.; Spano, G.; Speranskaya, E.S.; Goryacheva, I.Y.; Baggiani, C. A lateral flow immunoassay for straightforward determination of fumonisin mycotoxins based on the quenching of the fluorescence of CdSe/ZnS quantum dots by gold and silver nanoparticles. *Microchimica Acta* **2018**, *185(2)*, p.94.

170 Yu, S.; He, L.; Yu, F.; Liu, L.; Qu, C.; Qu, L.; Liu, J.; Wu, Y.; Wu, Y. A lateral flow assay for simultaneous detection of Deoxynivalenol, Fumonisin B1 and Aflatoxin B1. *Toxicon* **2018**, *156*, pp.23-27.

171 Hou, S.; Ma, J.; Cheng, Y.; Wang, H.; Sun, J.; Yan, Y. One-stop rapid detection of fumonisin B1, dexyonivalenol and zearalenone in grains. *Food Control* **2020**, pp.107107._

172 Mirasoli, M.; Buragina, A.; Dolci, L.S.; Simoni, P.; Anfossi, L.; Giraudi, G.; Roda, A. Chemiluminescence-based biosensor for fumonisins quantitative detection in maize samples. *Biosensors and Bioelectronics* **2012**, *32(1)*, pp.283-287.

173 Zhang, X.; Wang, Z.; Fang, Y.; Sun, R.; Cao, T.; Paudyal, N.; Fang, W.; Song, H. Antibody microarray immunoassay for simultaneous quantification of multiple mycotoxins in corn samples. *Toxins* **2018**, *10(10)*, pp.415.

174 Shao, Y.; Duan, H.; Zhou, S.; Ma, T.; Guo, L.; Huang, X.; Xiong, Y. Biotin–streptavidin system-mediated ratiometric multiplex immunochromatographic assay for simultaneous and accurate quantification of three mycotoxins. *Journal of Agricultural and Food Chemistry* **2019**, *67(32)*, pp. 9022-9031.

175 Hou, S.; Ma, J.; Cheng, Y.; Wang, H.; Sun, J.; Yan, Y. Quantum dot nanobead-based fluorescent immunochromatographic assay for simultaneous quantitative detection of fumonisin B1, dexyonivalenol, and zearalenone in grains. *Food Control* **2020**, *117*, p.107331.

176 Guo, L.; Wang, Z.; Xu, X.; Xu, L.; Kuang, H.; Xiao, J.; Xu, C. Europium nanosphere-based fluorescence strip sensor for ultrasensitive and quantitative determination of fumonisin B 1. *Analytical Methods* **2020**, *12*, pp.5229-5235.

177 Liu, Z.; Hua, Q.; Wang, J.; Liang, Z.; Li, J.; Wu, J.; Shen, X.; Lei, H.; Li, X. A smartphone-based dual detection mode device integrated with two lateral flow immunoassays for multiplex mycotoxins in cereals. *Biosensors and Bioelectronics* **2020,** pp.112178.

178 Di Nardo, F.; Baggiani, C.; Giovannoli, C.; Spano, G.; and Anfossi, L. Multicolor immunochromatographic strip test based on gold nanoparticles for the determination of aflatoxin B1 and fumonisins. *Microchimica Acta* **2017**, *184(5)*, pp.1295-1304.

179 Hao, K.; Suryoprabowo, S.; Hong, T.; Song, S.; Liu, L.; Zheng, Q.; Kuan, H. Immunochromatographic strip for ultrasensitive detection of fumonisin B1. *Food and Agricultural Immunology* **2018**, *29(1)*, pp.699-710.

180 Sheng, W.; Wu, H.; Ji, W.; Li, Z.; Chu, F.; Wang, S. Visual non-instrumental on-site detection of fumonisin B1, B2, and B3 in cereal samples using a clean-up combined with gel-based immunoaffinity test column assay. *Toxins* **2018**, *10(4)*, pp.165-179.

181 Duan, H.; Li, Y.; Shao, Y.; Huang, X.; Xiong, Y. Multicolor quantum dot nanobeads for simultaneous multiplex immunochromatographic detection of mycotoxins in maize. *Sensors & Actuators: B. Chemical* **2019**, *291, pp. 411-417.*

182 Jodra, A.; López, M.A.; Escarpa, A. Disposable and reliable electrochemical magnetoimmunosensor for fumonisins simplified determinations in maize-based foodstuffs. *Biosensors and Bioelectronics* **2015**, *64*, pp.633-638.

183 Peters, J.; Thomas, D.; Boers, E.; Rijk, T.; Berthiller, F.; Hasnoot, W.; Nielen, M.W.F. Colour-encoded paramagnetic microbead-based direct inhibition triplex flow cytometric immunoassay for ochratoxin A, fumonisins and zearalenone in cereals and cereal-based feed. *Analytical and Bioanalytical Chemistry* **2013**, *405(24)*, pp.7783-7794.

184 Li, C.; Mi, T.; Conti, G.O.; Yu, Q.; Wen, K.; Shen, J.; Ferrante, M.; Wang, Z. Development of screening fluorescence polarization immunoassay for the simultaneous detections of fumonisins B1 and B2 in maize. *Journal of Agricultural and Food Chemistry* **2015**, *63(20)*, pp.4940-4946.

185 Bánati, H.; Darvas, B.; Fehér-Tóth, S.; Czéh, A.; Székacs, A. Determination of mycotoxin production of Fusarium species in genetically modified maize varieties by quantitative flow immunocytometry. *Toxins* **2017**, *9(2)*, pp.70-81.

186 Pagkali, V.; Petrou, P.S.; Makarona, E.; Peters, J.; Haasnoot, W.; Jobst, G.; Moser, I.; Gajos, K.; Budkowski, A.; Economou, A.; Misiakos, K.; Raptis, I.; Kakabakos, S.E. Simultaneous determination of aflatoxin B1, fumonisin B1 and deoxynivalenol in beer samples with a label-free monolithically integrated optoelectronic biosensor. *Journal of Hazardous Materials* **2018**, *359*, pp.445-453.

187 Peltomaa, R.; Amaro-Torres, F.; Carrasco, S.; Orellana, G.; Benito-Peña, E.; Moreno-Bondi, M.C. Homogeneous quenching immunoassay for fumonisin B1 based on gold nanoparticles and an epitope-mimicking yellow fluorescent protein. *ACS Nano* **2018**,*12*, pp.11333-11342.

188 Zhou, Y.; Huang. X.; Zhang, W.; Ji, Y.; Chen, R.; Xiong, Y. Multi-branched gold nanoflower-embedded iron porphyrin for colorimetric immunosensor. *Biosensors and Bioelectronics* **2018**, *102*, pp.9-16.

189 Ezquerra, A.; Vidal, J.C.; Bonel, L.; Castillo, J.R. A validated multi-channel electrochemical immunoassay for rapid fumonisin B1 determination in cereal samples. *Analytical Methods* **2015**, *7*, pp.3742-3749.

190 Thompson, V.S.; Maragos, C.M. Fiber-optic immunosensor for the detection of fumonisin B1. *Journal of Agricultural and Food Chemistry* **1996**, *44(4)*, pp.1041-1046.

191 Mullett, W.; Lai, E.P.C.; Yeung, J.M. Immunoassay of fumonisins by a surface plasmon resonance biosensor. *Analytical Biochemistry* **1998**, *258(2)*, pp.161-167.

192 Ho, J.A.; Durst, R.A. Development of a flow-injection liposome immunoanalysis system for fumonisin B1. *Analytica Chimica Acta* **2000**, *414(1-2)*, pp.61-69.

193 Maragos, C.M.; Jolley, M.E.; Plattner, R.D.; Nasir, M.S. Fluorescence polarization as means for determination of fumonisin in maize. *Journal of Agricultural and Food Chemistry* **2011**, *49(2)*, pp.596-602.

194 Lamberti, I.; Tanzarella, C.; Solinas, I.; Padula, C.; Mosiello, L. An antibody-based microarray assay for the simultaneous detection of aflatoxin B1 and fumonisin B1. *Mycotoxin Research* **2009**, *25*, pp.193-200.

195 Anderson, G.P.; Kowtha, V.A.; Taitt, T.C. Detection of fumonisin B1 and Ochratoxin A in grain products using microsphere- based fluid array immunoassays. *Toxins* **2010**, *2(2)*, pp.297-309.

196 Wang, X.; Zhang, H.; Liu, H.; He, C.; Zhang, A.; Ma, J.; Ma, Y.; Wu, W. and Zheng, H. An immunoarray for the simultaneous detection of two mycotoxins, ochratoxin A and fumonisin B1. *Journal of Food Safety* **2011**, *31(3)*, pp.408-416.

197 Zou, L.; Xu, Y.; Li, Y.; He, Q.; Chen, B.; Wang, D. Development of a single-chain variable fragment antibody-based enzyme-linked immunosorbent assay for determination of fumonisin B1 in corn samples. *Journal of the Science of Food and Agriculture* **2013**, *94(9)*, pp.1865-1871.

198 Shu, M.; Xu, Y.; Wang, D.; Liu, X.; Li, Y.; He, Q.; Tu, Z.; Qiu, Y.; Ji, Y.; Wang, X. Anti-idiotypic nanobody: A strategy for development of sensitive and green immunoassay for fumonisin B1. *Talanta* **2015**, *143*, pp.388-393.

199 Lu, L.; Seenivasan, R.; Wang, Y.-C.; Yu, J.-H.; Gunasekaran, S. An electrochemical immunosensor for rapid sensitive detection of mycotoxins fumonisin B1 and deoxynivalenol. *Electrochimia Acta* **2016**, *213*, pp.89-97.

200 Urusov, A.E.; Petrakova, A.V.; Gubaydullina, M.K.; Zherdev, A. V.; Eremin, S. A.; Kong, D.; Liu, L.; Xu, C.; Dzantiev, B.B. High- sensitivity immunochromatographic assay for fumonisin B1 based on indirect antibody labelling. *Biotechnology Letters* **2017**, *39(5)*, pp.751-758.

201 Peltomaa, R.; Benito-Peña, E.; Barderas, R.; Sauer, U.; González, M.; Moreno-Bondi, M.C. Microarray-based immunoassay with synthetic mimotopes for the detection of fumonisin B1. *Analytical Chemistry* **2017**, *89*, pp.6216-6223.

202 Lu, T.; Zhan, S.; Zhou, Y.; Chen, X.; Huang, X.; Leng, Y.; Xiong, Y.; Xu, Y. Fluorescence ELISA based on CAT-regulated fluorescence quenching of CdTe QDs for sensitive detection of FB1. *Analytical Methods* **2018**, *10***,** pp.5797-5802.

203 Jie, M.; Yu, S.; Yu, F.; Liu, L.; He, L.; Li, Y.; Zhang, H.; Ou, L.; Harrington, P.; Wu, Y. An ultrasensitive chemiluminescence immunoassay for fumonisin B1 detections in cereals based on gold-coated magnetic nanoparticles. *Journal of the Science of Food and Agriculture* **2018**, *98(9)*, pp.3384-3390.

204 Li, Z.; Sheng, W.; Li, S.; Shi, Y.; Zhang, Y.; Wang, S. Development of a gold nanoparticle enhanced enzyme linked immunosorbent assay based on monoclonal antibodies for the detections of fumonisin B1, B2 and B3 in maize. *Analytical Methods* **2018**, *10*, pp.3506-3513.

205 Chen, X.; Liang, Y.; Zhang, W.; Leng, Y.; Xiong, Y. A colorimetric immunoassay based on glucose oxidase-induced AuNP aggregation for the detection of fumonisin B1. *Talanta* **2018**, *186*, pp.29-35.

206 Lu, L.; Gunasekaran, S. Dual-channel ITO-microfluidic electrochemical immunosensor for simultaneous detection of two mycotoxins. *Talanta* **2019**, *194*, pp.709-716.

207 Cheng, Z.X.; Ang, W.L.; Bonanni, A. Electroactive nanocarbon can simultaneously work as platform and signal generator for label-free immunosensing*. ChemElectroChem* **2019***, 6(14)*, pp. 3615-3620.

208 Smolinska-Kempisty, K.; Guerreiro, A.; Canfarotta, F.; Cáceres, C.; Whitcombe, M.J.; Piletsky, S. A comparison of the performance of molecularly imprinted polymer nanoparticles for small molecule targets and antibodies in the ELISA format. *Scientific Reports* **2016**, *6*, pp. 37638.

209 Munawar, H.; Safaryan, A. H.; De Girolamo, A.; Garcia-Cruz, A.; Marote, P.; Karim, K.; Lippolis, V.; Pascale, M.; Piletsky, S. A. Determination of Fumonisin B1 in maize using molecularly imprinted polymer nanoparticles-based assay. *Food chemistry* **2019**, *298*, p.125044.

210 Chotchuang, T.; Cheewasedtham, W.; Jayeoye, T. J.; Rujiralai, T. Colorimetric determination of fumonisin B1 based on the aggregation of cysteamine-functionalized gold nanoparticles induced by a product of its hydrolysis. *Microchimica Acta* **2019**, *186(9)*, p.655.

211 Zhang, W.; Xiong, H.; Chen, M.; Zhang, X.; Wang, S. Surface-enhanced molecularly imprinted electrochemiluminescence sensor based on Ru@SiO2 for ultrasensitive detection of fumonisin B1. *Biosensors and Bioelectronics* **2017**, *96*, pp. 55-61.

212 Mao. L.; Ji, K.; Yao, L.; Xue, X.; Wen, W.; Zhang, X.; Wang, S. Molecularly imprinted photoelectrochemical sensor for fumonisin B1 based on GO-CdS heterojunction. *Biosensors and Bioelectronics* **2019**, *127*, pp. 57-63.

213 Hines, H.B.; Brueggemann, E.E.; Holcomb, M.; Holder, C.L. Fumonisin B1 analysis with capillary electrophoresis–electrospray ionization mass spectrometry. *Rapid Communications in Mass Spectrometry* **1995**, *9(6)*, pp.519-524.

214 Holcomb, M.; Thompson Jr, H.C. Analysis of fumonisin B1 in corn by capillary electrophoresis with fluorescence detection of the FMOC derivative. *Journal of Microcolumn Separations* **1995**, *7(5)*, pp.451-454.

215 Maragos, C.M. Capillary zone electrophoresis and HPLC for the analysis of fluorescein isothiocyanate-labeled fumonisin B1. *Journal of Agricultural and Food Chemistry* **1995**, *43(2)*, pp.390-394.

216 Maragos, C.M. Detection of the mycotoxin fumonisin B1 by a combination of immunofluorescence and capillary electrophoresis. *Food and Agricultural Immunology* **1997**, *9(3)*, pp.147-157.

217 Kecskeméti, Á.; Nagy, C.; Biró, P.; Szabó, Z.; Pócsi, I.; Bartók, T.; Gáspár, A. Analysis of fumonisin mycotoxins with capillary electrophoresis–mass spectrometry. *Food Additives & Contaminants: Part A* **2020**, *37(9)*, pp.1553-1563.

218 Ciriaco, F.; De Leo, V.; Catucci, L.; Pascale, M.; Logrieco, A.F.; DeRosa, M.C.; De Girolamo, A. An *In-Silico* pipeline for rapid screening of DNA aptamers against mycotoxins: The case-study of fumonisin B1, aflatoxin B1 and ochratoxin A. *Polymers* **2020**, *12(12)*, p. 2983.

219 Wang, Z.J.; Chen, E.N.; Yang, G.; Zhao, X.Y.; Qu, F. Research advances of aptamers selection for small molecule targets. *Chinese Journal of Analytical Chemistry* **2020**, 48(5), pp.573-582.

220 Zuker, M. Mfold web server for nucleic acid folding and hybridization prediction. *Nucleic Acids Research* **2003**, *31*(13), pp.3406-3415.

221 Frost, N.R.; McKeague, M.; Falcioni, D.; DeRosa, M.C. An in solution assay for interrogation of affinity and rational minimer design for small molecules binding aptamers. *Analyst* **2015**, *140*, pp.6643-6651.

222 Chen, X.; Huang, Y.; Ma, X.; Jia, F.; Guo, X.; Wang, Z. Impedimetric aptamer-based determination of the mold toxin fumonisin $B_1$. *Microchimica Acta* **2015**, *182(9-10)*, pp.1709-1714.

223 Tian, H.; Sofer, Z.; Pumera, M.; Bonanni, A. Investigation on the ability of heteroatom-doped graphene for biorecognition. *Nanoscale* **2017**, *9*, pp.3530-3536.

224 吴淑庆; 杨在明; 张良. Fumonisins B1 aptamer and applications thereof. Patent No. CN 102517291 A, 27 June 2012.

225 Wang, Z.; Wu, S. Oligonucleotides aptamer special for distinguishing fumonisin B1. Patent No. CN 103013999 B, 10 September 2014.

226 Zheng, Y.T.; Zhao, B.S.; Zhang, H.B.; Jia, H.; Wu, M. Colorimetric aptasensor for fumonisin B1 detection by regulating the amount of bubbles in closed bipolar platform. *Journal of Electroanalytical Chemistry* **2020**, *877*, p.114584.

227 Wei, M.; Zhao, F.; Feng, S.; Jin, H. A novel electrochemical aptasensor for fumonisin B 1 determination using DNA and exonuclease-I as signal amplification strategy. *BMC Chemistry* **2019**, *13(1)*, pp.1-6.

228 Han, Z.; Tang, Z.; Jiang, K.; Huang, Q.; Meng, J.; Nie, D.; Zhao, Z. Dual-target electrochemical aptasensor based on co-reduced molybdenum disulfide and Au NPs ($rMoS_2$-Au) for multiplex detection of mycotoxins. *Biosensors and Bioelectronics* **2020**, *150*, p.11894.

229 Wei, M.; Xin, L.; Feng, S.; Liu, Y. Simultaneous electrochemical determination of ochratoxin A and fumonisin B1 with an aptasensor based on the use of a Y-shaped DNA structure on gold nanorods. *Microchimica Acta* **2020**, *187(2)*, pp.1-7.

230 Zhao, Y.; Luo, Y.; Li, T.; Song, Q. AuNPs driven electrochemiluminescence aptasensors for sensitive detection of fumonisin B1. *RSC Advances* **2014**, *4*, pp.57709-57714.

231 Ren, C.; Li, H.; Lu, X.; Quian, J.; Zhu, M.; Chen, W.; Liu, Q.; Hao, N; Li, H.; Wang, K. A disposable aptasensing device for label-free detection of fumonisin B1 by integrating PDMS film-based micro-cell and screen-printed carbon electrode. *Sensors and Actuators B: Chemical* **2017**, *251*, pp.192-199.

232 Wu, S.; Duan, N.; Li X.; Tan, G.; Ma, X.; Xia, Y.; Wang, Z.; Wang, H. Homogenous detection of fumonisin $B_1$ with a molecular beacon based on fluorescence energy transfer between $NaYF_4$:YB, Ho upconversion nanoparticles and gold nanoparticles. *Talanta* **2013**, *116(15)*, pp.611-618.

233 Tao, Z.; Zhou, Y.; Li, X.; Wang, Z. Competitive HRP-linked colorimetric aptasensor for the detection of fumonisin B1 in food based on dual biotin-streptavidin interaction. *Biosensors* **2020**, *10(4)*, p.31.

234 Yue, S.; Jie, X.; Wei, L.; Bin, C.; Dou, W.D.; Yi, Y.; QingXia, L.; JianLin, L.; TieSong, Z. Simultaneous detection of ochratoxin A and fumonisin B1 in cereal samples using an aptamer-photonic crystal encoded suspension array. *Analytical Chemistry* **2014**, *86(23)*, pp.11797-11802.

235 Yang, Y.; Li, W.; Shen, P.; Liu, R.; Li, Y.; Xu, J.; Zheng, Q.; Zhang, Y.; Li, J.; Zheng. T. Aptamer fluorescence signal recovery screening for multiplex mycotoxins in cereal samples based on photonic crystal microsphere suspension array. *Sensors and Actuators B: Chemical* **2017**, *248*, pp.351-358.

236 Wang, C.; Qian, J.; An, K.; Huang, X.; Zhao, L.; Liu, Q.; Hao, N.; Wang, K. Magneto-controlled aptasensor for simultaneous electrochemical detection of dual mycotoxins in maize using metal sulfide quantum dots coated silica as labels. *Biosensors and Bioelectronics* **2017**, *89*, pp.802-809.

237 Molinero-Fernández, A.; Moreno-Guzmán, M.; Ángel López, M.; Escarpa, A. Biosensing strategy for simultaneous and accurate quantitative analysis of mycotoxins in food samples using unmodified graphene micromotors. *Analytical Chemistry* **2017**, *89*, pp.10850-10857.

238 Molinero-Fernández, A.; Jodra, A.; Moreno-Guzmán, M.; López, M.A.; Escarpa, A. Magnetic reduced graphene oxide/nickel/platinum nanoparticles micromotors for mycotoxin analysis. *Chemistry A European Journal* **2018**, *24*, pp.7172-7176.

239 Wang, C.; Huang, X.; Tian, X.; Zhang, X.; Yu, S.; Chang, X.; Ren, Y.; Qian, J. A multiplexed FRET aptasensor for the simultaneous detection of mycotoxins with magnetically controlled graphene oxide/Fe3O4 as a single energy acceptor. *Analyst* **2019**, *144(20)*, pp.6004-6010.

240 Shi, Z.-Y.; Zheng Y.-T.; Zhang, H.-B.; He, C.-H.; Wu, W.-D.; Zhang, H.-B. DNA electrochemical aptasensor for detecting fumonisin B1 based on graphene and thionine nanocomposite. *Electroanalysis* **2015**, *27(5)*, pp.1097-1103.

241 Wang, W.F.; Wu, S.; Ma, X.Y.; Xia, Y.; Wang, Z.P. Novel methods for fumonisin B1 detection based on AuNPs labelling and aptamer recognition. *Journal of Food Science and Biotechnology* **2013**, *32(5)*, pp.501-508.

242 Hao, N.; Lu, J.; Zhou, Z.; Hua, R.; Wang, K. A pH-resolved colorimetric biosensor for simultaneous multiple target detection. *ACS Sensors* **2018**, *3*, pp.2159-2165.

243 王红旗, 王俊艳, 洪慧杰, 尹海燕, Maragos, C., 张 玲, 刘继红.伏马毒素 B1 核酸适配体链置换探针的筛选及应用. *农产品质量与安全* **2017**,*1*, pp.44-48.

244 Zheng, Y.; Shi, Z.; Wu, W.; He, C.; Zhang, H. Label-Free DNA Electrochemical Aptasensor for Fumonisin B 1 Detection in Maize Based on Graphene and Gold Nanocomposite. *Journal of Analytical Chemistry* **2021**, *76*(2), pp. 252-257.

245 Kesici, E.; Erdem, A. Impedimetric detection of Fumonisin B1 and its biointeraction with fsDNA. *International Journal of Biological Macromolecules* **2019**, *139*, pp. 1117-1122.

246 Food Standards Agency. 2019. Incidents annual reports 2006-2017. Available online: https://www.food.gov.uk/about-us/reports-and-accounts (Accessed on 10 April 2020).

**Table 1.** Maximum permitted levels (µg/kg) of fumonisins in food and feed set by different organizations[1]

| Commodity | Maximum Level (µg/kg) | Type | Authority | Regulatory Framework | Country |
|---|---|---|---|---|---|
| Raw maize grain | 4 000 | B1, B2 | FAO, WHO | CODEX STAN 193-1995 | International trade |
| Maize flour and maize meal | 2 000 | B1, B2 | FAO, WHO | CODEX STAN 193-1995 | International trade |
| Unprocessed maize (not for milling) | 4 000 | B1, B2 | CEC | (EC) No 1126/2007 | EU |
| Maize, maize-based foods for direct human consumption | 1 000 | B1, B2 | CEC | (EC) No 1126/2007 | EU |
| Maize-based breakfast cereals and snacks | 800 | B1, B2 | CEC | (EC) No 1126/2007 | EU |
| Processed maize-based foods and baby foods (Infants and young children) | 200 | B1, B2 | CEC | (EC) No 1126/2007 | EU |
| Milling fractions according to size (500 micron) and CN code 19041010 | 1 400 – 2 000 | B1, B2 | CEC | (EC) No 1126/2007 | EU |
| Maize and processed products | 1 000 | B1, B2 | MH | BG1 | Bulgaria |
| Maize, rice | 1 000 | B1 | MPH/INHA | CU1 | Cuba |
| Cereals & cereal products | 1 000 | B1 | DGCCRF | FR1 | France |
| Maize | 1 000 | B1, B2 | ISIRI, MOH | IR1 | Iran |
| Corn & corn products | Not given | B1 | SG1 | AVA | Singapore |
| Maize | 1 000 | B1, B2 | CH1 | OFCACS | Switzerland |
| Maize products | According to the result of risk assessment | B1 | - | - | Taiwan |
| Degermed dry milled corn products (e.g. flaking grits, corn grits, corn meal, corn flour with fat content of <2.25%, dry weight basis) | 2 000 | B1, B2, B3 | US4, US5 | FDA | USA |
| Cleaned corn intended for popcorn | 3 000 | B1, B2, B3 | US4, US5 | FDA | USA |
| Whole of partially degermed dry milled corn products (e.g. flaking grits, corn grits, corn meal, corn flour with fat content of ≥2.25%, dry weight basis); dry milled corn bran; cleaned corn intended for masa production | 4 000 | B1, B2, B3 | US4, US5 | FDA | USA |
| Corn and corn by-products intended for equids and rabbits | 5 000 | B1, B2, B3 | US4, US5 | FDA | USA |
| Corn and corn by-products intended for swine and catfish | 20 000 | B1, B2, B3 | US4, US5 | FDA | USA |
| Corn and corn by-products intended for breeding ruminants, breeding poultry and breeding mink (includes lactating dairy cattle and hens laying eggs for human consumption) | 30 000 | B1, B2, B3 | US4, US5 | FDA | USA |
| Ruminants ≥ 3 months old being raised for slaughter and mink being raised for pelt production | 60 000 | B1, B2, B3 | US4, US5 | FDA | USA |
| Poultry being raised for slaughter | 100 000 | B1, B2, B3 | US4, US5 | FDA | USA |
| All other species or classes of livestock and pet animals | 10 000 | B1, B2, B3 | US4, US5 | FDA | USA |
| Maize grains/ Millet flour | 2 000 | Fumonisin | EAC | EAS | Burundi, Kenya, Rwanda, South Sudan, Tanzania, Uganda. |

[1] Abbreviations: **AVA:** Agri-Food and Veterinary Authority; **BG1:** Ministry of Health in coordination with the Ministry of Agriculture and Forestry, the Ministry of Industry and the State Standardization Agency (2000). Regulation No.11/2000 of 11 July 2000 laying down the maximum levels of mycotoxins in foodstuffs. Official Newspaper of the Republic of Bulgaria No. 58: 18-24.; **CEC:** Commission of the European Communities; **CH1:** Verordnuung uber Fremd-und Inhaltsstoffe in Lebensmitteln. SR817.021.23; **CN:** Combined 45omenclatura; **CU1:** Ministerio de Salud Pública (1999). Manual de indicadores empleados en la evaluación sanitaria de alimentos. Instituto de Nutrición e Higiene de los Alimentos (INHA), Diciembre de 1999; **DGCCRF:** Direction Generale de la Concurrence, de la Consommation de la Repression des Fraudes, Ministere de l'Economie, des Finances et de l'Industrie; **EAC:** East African Community, **EAS:** East African Standard 89: 2011, ICS 67.060; **EC:** Commission Regulations**; FAO:** Food and Agriculture Organization of the United Nations; **FDA:** Food and Drug Administration; **FR1:** Avis du Conseil Superieur d'Hygiene Publique de France du 8/12/1998; **IR1:** National standard of Institute of Standard and Industrial Research of the Islamic Republic of Iran (ISIRI) [2002]. Maximum tolerated levels of mycotoxins in food and feeds. No.5925; **ISIRI:** Institute of Standard and Industrial Research of the Islamic Republic of Iran; **MH:** Ministry of health; **MOH:** Ministry of Health and Medical Education; **MPH/INHA:** Ministry of Public Health/Instituto de Nutrición e Higiene de los Alimentos; **OFCACS:** Official Food Control Authorities of the Cantons of Switzerland; **SG1:** Regulation 34 of the Singapore Food Regulations; **US4:** FDA (2001). Guidance for industry: Fumonisin Levels in Human Foods and Animal Feeds, November 9, 200; **US5:** FDA; **WHO:** World Health Organization

**Table 2.** Chromatographic determination of FB1[1]

| Support | Method | Eluent | Measurement | Assay Time (min) | Limit of Detection | Sample | Fumonisin Type | Ref |
|---|---|---|---|---|---|---|---|---|
| Wakosil 5C18 column | HPLC | Acidified methanol and disodium phosphate (80:20 pH 3.3) | Fluorescence | 24 | 50 &100 µg/kg | Corn | FB1, FB2, FB3 | [112] |
| Synergi Max-RP (80 Å, 5 µm, 250 × 4.60 mm) HPLC column | HPLC | Methanol/0.1 M phosphate buffer (77:23, v/v) adjusted to pH 3.35 with concentrated orthophosphoric acid. | Fluorescence | - | 25 µg/kg | Corn kernels, tortillas and masa | FB1 | [105] |
| Luna C18 column (50 × 4.6 mm ID, 5 µm Phenomenex) | LC-MS | Water/acetonitrile/formic acid at | MS detection | 11 | 0.02 µg/L | Urine (Tortilla consumption) | FB1 | [101] |
| Column C18 Xterra Waters narrow bore with a C18 precolumn cartridge; | LC | Acidified water & methanol | MS/MS analysis | 50 | 5 µg/kg | Corn | FBs,HFBs | [109] |
| Column, C18 Hypersil | LC | Acidified water & acetonitrile | MS/MS analysis | 13 | 16 µg/kg | Corn | HFBs | [109] |
| Gemini® C18 column | HPLC | Methanol/water/acetic acid with ammonium acetate | MS/MS analysis | 21 | 8 µg/kg | Corn | HFBs | [109] |
| Column Brownlee C18 | HPLC | Water–acetonitrile–acetic acid | Fluorescence | - | 100 µg/kg | Corn | FBs | [109] |
| Symmetry Spherisorb ODS2 C18 Column | HPLC | Methanol& sodium dihydrogen phosphate | Fluorescence | 11.20 | 50 µg/kg, 70 µg/kg | Tunisian foods and feed | FB1, FB2 | [82] |
| Xterra MS C18 column | LC-MS-MS | Acidified water:acetonitrile & acetonitrile | MS-MS detection | <4 min (LC-ESI-MS/MS signal) | 0.003 µg/kg | Bovine Milk | FB1 | [142]. |
| Luna C18 column | LC-MS-MS | Acidified water & methanol | MS-MS detection | 25 | 5 µg/L | Urine | FB1,FB2 | [102] |
| Agilent Zorbax Eclipse XDB C- 18 column | LC-MS/MS | Acidified water & methanol | MS | 15 | 9, 6 µg/kg | Maize | FB1,FB2 | [146] |
| Hypersil™ ODS C18 Columns | HPLC | Acetonitrile & sodium phosphate buffer | Fluorescence | ~13.5 (retention time) | 50 µg/kg | Rice | FB1 | [106] |
| Shimadzu C18 column | HPLC | Water/acetonitrile/acetic acid | Fluorescence | - | 30 µg /kg | Corn | FB1 | [113] |
| Thermo Hypersil GOLD column | LC-MS | Acidified water & acetonitrile | MS detection | 6 | 3.3 µg /kg | Human hair | FB1 | [113] |
| SHISEIDO Capcell core C18 column | UFLC | Acetonitrile -water (0.1% formic acid) | MS/MS | 12 | 0.15 µg/kg | *Areca catechu* | FB1, FB2 | [114] |
| SHISEIO Capcell coreC18 column | UFLC | 0.1% formic acid in acetonitrile and water | MS/MS | 12 | 0.05 µg/L 0.15 µg/L | Yam | FB1, FB2 | [115] |
| ACQUITY UPLC BEH C18 column | UHPLC | Water containing 0.1% formic acid (ESI+) or 0.1% ammonia (ESI-) and acetonitrile | MS | 12 | 0.32 µg/kg, 0.08 µg/kg | Radix Paeoniae Alba | FB1, FB2 | [116] |
| ZIC-pHILIC (SeQuant) | LC | Aqueous ammonium formate | MS | 23 | 0.3, 1.3, 1.3, 0.8, 0.9, 2.6 µg/kg | Apples, apricots, lettuce, onion, wheat flour, chickpeas | FB1 | [136] |
| Poroshell 120 PFP column | UHPLC | Ammonium formate and formic acid in Milli-Q water and methanol (ESI+), and Milli-Q water and acetonitrile (ESI−). | MS/MS | 17 | 1, 1, 3 µg/kg | *Pheretima* | FB1, FB2, FB3 | [143] |
| Kinetex C18 column | LC | Water-methanol with ammonium formate and formic acid | MS/MS | 33 | 1.7, 3.9 µg/L | Maize | FB1, FB2 | [117] |
| CORTECS C18 column | UPLC | Methanol-water with 0.5% (v/v) formic acid | MS/MS | 30.3 | 15 µg/kg | Cereals (Wheat, corn, and rice) | FB1,FB2,FB3 | [118] |
| Acclaim 120 C18 analytical column | HPLC | Acidified acetonitrile | Fluorescence | 30 | 30 µg/kg 2.5 µg/L | Corn based feed | $FB_1$,$FB_2$ | [111] |
| BEH C18 column | LC-MS-MS | Acidified water & acetonitrile | MS-MS detection | 2, 4 (only hair) | 0.014, 0.040, 0.012, ND µg/L | Pig plasma, urine, feces, hair | $FB_1$ | [92] |
| Nucleodur C18 Gravity SB column | LC | Acetonitrile (2% acetic acid)- water (0.1% acetic acid) | MS | 11.5 | 0.521 µg/L | Human blood | FB1 | [119] |
| Ascentis Express C18 | LC | Aqueous ammonium formate (0.1% formic acid)-aqueous methanol solution (ammonium formate, + formic acid, 0.1%) | MS/MS | 30.1 | 10.14, 2.5, 0.625 µg/L | Milk | FB1, FB2, FB3 | [120] |
| MNPs + Acquity UPLC®BEH C18 column | UPLC | MeOH/$H_2O$ (60:40) with ammonium acetate and formic acid | MS/MS | 10 | 0.210 µg/kg | Vegetable oil | FB1 | [121] |
| Kinetex XB-C18 100 Å column | HPLC | Methanol- water ( with ammonium formiate+ formic acid) | MS/MS | 30 | 100 µg/kg | Cereal-derived products | FB1, FB2 | [122] |
| Cortecs UHPLC C18 column | LC | Water-MeOH (with $NH_4HCOO$+ HCOOH) | MS/MS | 14.5 | 0.04 µg/L | Soy, oat and rice beverages | FB1,FB2 | [123] |
| Gemini® C18 column | LC | Methanol/water/acetic acid 10:89:1 (v/v/v) -97:2:1 (with ammonium acetate) | MS/MS | 20.5 | 3.2 (FB1), 2.4 µg/kg | Maize-*fufu* | FB1,FB2, FB3, FB4, FA1 | [140] |
| C18 column | UHPLC | Water- MeOH with formic acid and ammonium formate | MS/MS | 11.25 | 17.3,12.4,10.7, 9 µg/L (FB1), 11.8,17.2, 9, 10 µg/L (FB2) | Oat, soy,rice and bird seed milk | FB1,FB2 | [138] |
| Acquity BEH C18 column | UPLC | Water (ammonium acetate )- MeOH (formic acid) | MS/MS | 15 | 0.20, 0.15 µg/kg | *Alpinia oxyphylla* | FB1,FB2 | [124] |
| Eclipse Plus C8 RRHD column | MA-D- µ-SPE with | Water containing 0.1% formic acid-acetonitrile | MS | 9 | 0.0068, 0.013, | Peach seed, milk powder, corn flour | FB1 | [125] |

| | | | | | | | | |
|---|---|---|---|---|---|---|---|---|
| | UHPLC-Q-TOF/MS | | | | 0.0074, 0.0030 µg/kg | | | |
| C18 column Phenomenex Kinetex | UPLC-MS/MS | Water containing 0.5 mM $NH_4Ac$ – MeOH with 0.1% formic acid | MS/MS | 15 | 0.25 & 0.1 (FB2) µg/kg | Lotus seed | FB1, FB2 | [126] |
| ZORBAX RRHD Eclipse Plus C18 | UHPLC | 0.1% formic acid solution – acetonitrile ( formic acid) | MS | 12 | 1 µg/L | Grape and wines | FB1 | [127] |
| Gemini® C18-column | LC | Methanol/water (with acetic acid and ammonium acetate | MS/MS | - | 1 µg/kg | Dried date palm fruits | FB2 | [139] |
| Acquity UPLC HSS T3 column | UPLC | (Formic acid & ammonium formate) water-acetonitrile | MS/MS | 10 | 0.15, 0.09, 0.04, 0.03, 0.17 µg/L | Broiler chicken plasma | FB1, FB2, pHFB1a, pHFB1b, HFB1 | [147] |
| Silica based particles bonded with C18-penta fluorophenyl functions | LC-HRMS | Water- acetonitrile (both with formic acid) – MeOH | MS | 26 | 0.5 µg/L | Tea | FB1, FB2 | [137] |
| Gemini-NX LC-column | LC | Water – methanol acidified (both with ammonium formate +formic acid) | MS/MS | 39 | 1.5, 0.3 (vegetables) µg/kg | Ready-to-eat food (cereals, fish, legumes, vegetables, meat) | FB1, FB2 | [128] |
| Scherzo Sm-C18 column | HPLC | Acetonitrile (ammonium acetate) – acetonitrile (formic acid) | MS/MS | 26 | 2.4, 2.3 µg/kg | Corn derived products | FB1, FB2 | [129] |
| Acquity HSS T3 column | LC | Water-I (both acidified with Hac) | MS/MS | 25 | 0.001 µg/L | Human urine | FB1 | [130] |
| Waters ACQUITY HSS T3 column | UPLC | 0.1% formic acid and 5 mM ammonium formate (phase A) -methanol (phase B). | MS/MS | 13 | 0.22 µg/L | Beer | FB1, FB1 | [131] |
| Zorbax CX | UHPLC | Methanol/water (1:1 v/v) with 0.1% acetic acid | MS/MS | 3.6 (chromatogram time) | 51.5, 45.3 µg/kg | Rice | FB1, FB2 | [93] |
| Kinetex Core-shell C18 | LC | Water- methanol (both with ammonium formate and formic acid ) | MS/MS | 25.5 | 8.3 µg/kg | Green coffee | FB1, FB2 | [150] |
| Kinetex Biphenyl column | LC | 37.19 M ammonium acetate + 0.1% of acetic acid in water/ MeOH – 0.01 M ammonium acetate+ 0.1% of acetic acid in water/MeOH | MS/MS | 16 | 0.50, 1.56 µg/kg | Animal feed | FB1, FB2 | [132] |
| UPLC HSS T3 | LC | Aqueous ammonium formate 1mM and formic acid 1% (phase A)-Ammonium formate 1mM and formic acid 1% in methanol:water(95:3.9) | MS/MS | 11 | 20 µg/kg | Nixtamalized Maize | FB1, FB2 | [144] |
| Kinetex 2.6 µm C18 100A | UHPLC | Aqueous acetic acid 0.5% (phase A)-Acetic acid 0.5% and isopropanol 99.5% (phase B) | MS/MS | 11 | 0.03, 0.01 µg/L | Kankankan | FB1, FB2 | [145] |
| Gemini C18-column | LC-ESI | Ammonium acetate 5 mM with methanol/water/acetic acid 10:89:1 (phase A) and 97:2:1 (phase B) | MS/MS | 18.5 | 2.39, 1.68, 8.55 µg/kg | Dried Turkish figs | FB1, FB2, FB3 | [135] |

[1] Abbreviations: **HRMS:** High-resolution mass spectrometry; **SPE:** Solid-phase extraction; **UFLC:** Ultra-fast liquid chromatography; **UHPLC:** Ultra-high-performance liquid chromatography

**Table 3.** Immuno-based assays for the determination of FB1[1]

| Support | Method | Labelling/Substrate | Measurement | Assay Time (min) | LOD | Sample | Fumonisin | Ref |
|---|---|---|---|---|---|---|---|---|
| 96-well immunoplates | ELISA | HRP | Optical density | 150 | 0.2 µg/L | Corn | FB1 | [112] |
| ELISA kit | AgraQuant Total Fumonisin Assay Protocol | Methanol-water | Intensity of colour | 20 | 200 µg/kg | Corn | FBs | [109] |
| 96-well plate | ELISA (RIDASCREEN ®) | HRP | Optical density | 55 | 25 µg/kg, | Tunisian foods and feed | FB1+FB2 | [82] |
| Test kit | ELISA | Antigen | OD | 20 | 200 µg/kg | Maize | FB1+FB2 | [146] |
| Optical fibre | DC assay | FITC | Fluorescence | 24 | 10 µg/L | Corn | FB1 | [190] |
| Sample cell | SPR | Gold film | Reflected light intensity | 10 | 50 µg/L | PBS | FB1 | [191] |
| Protein-A coated capillary column | Liposome-amplified competitive assay | Liposome | Fluorescence | <11 | 1 µg/L | TBS | FB1 | [192] |
| Glass culture tube | Competition of unlabelled fumonisin | Fluorescein | Fluorescence Polarization | 2 | 500 µg/kg | Maize | FB1 | [193] |
| Borosilicate glass slides | Competitive assay | Biotin | Fluorescence | ~8 | 250 µg/L | PBSTB | FB1 | [151] |
| 96-well microplate | ECL-ELISA | HRP | Fluorescence | 60 | 0.09 µg/L | Cereals | FB1 | [152] |
| DMA-NAS-MAPS treated glass | Competitive immunoassay | Streptavidin-AP/ NBT/BCIP | Colorimetric | 65 | 43 µg/L | Binding buffer | FB1 | [194] |
| NC membrane | LFIA | Colloidal Gold | Line intensity | 4 | 199 µg/kg | Maize | FB1 | [162] |
| Luminex 100 microspheres | Indirect competitive fluid array | Biotin | Fluorescence cytometry | 60 | 0.3 µg/L | Grain Products | FB1 | [195] |
| SPGE | DC assay | HRP-TMB | Chronoamperometry | 45 | 5 µg/L | Corn | FB1,FB2 | [79] |
| NC membrane | LFIA | Colloidal Gold | Line intensity | 10 | 120 µg/L | Maize | FB1 | [163] |
| Aldehydelized glass slides | Specific competitive reactions | Ag conjugates | Fluorescence | 90 | 109.06 µg/L | Wheat | FB1 | [196] |
| NC strip | Competitive lateral flow immunoassay | HRP | CL | 15 | 2.5 µg/L | Maize | FB1,FB2 | [172] |
| NC membrane strip | One-step competitive immunochromatographic | AuNP | Colour density | 10 | 2.5 µg/L | Maize | FB1+FB2+FB3 | [164] |
| NC membrane | LFIA | Protein A-gold | Line intensity | 30 | 3200 µg/kg | Maize | FB1 | [165] |
| 96-well microplate | IC ELISA | HRP | Absorbance | 70 | 8.32 µg/kg | Corn | FB1 | [197] |
| Paramagnetic beads | Inhibition immunoassay | Mycotoxin-R-Phycoerythrin | Dose–response cytometry (Fluorescence) | 50 | 170, 1270 µg/kg | Maize, wheat | FB1+FB2 | [183] |
| NC membrane | LFDIA | Colloidal Gold | Line intensity | 30 | 5.23 µg/L | Corn | FB1 | [166] |
| NC membrane | Immunochromatographic strip | Colloidal gold | Visual detection | 3 | 5 µg/L | Cereal | FB1 | [99] |
| PrG functionalized magnetic beads | DC multi-channel electrochemical immunoassay | HRP | Current | 40 | 0.58 µg/L | Cereals | FB1 | [189] |
| SPCEs | | | | | | | | |
| GCE/PT | Impedimetric immunosensor | PDMA-MWCNT | EIS | - | 0.00000046 µg/L | Methanol | FB1 | [97] |
| | | | | | 14 µg/kg | Corn | FB1 | |
| | | | | | 11 µg/kg | Corn | FB2+FB3 | |
| NC strip | LFIA | HRP | CL | 30 | 6 µg/kg | Maize | FB1 | [167] |
| SWNTs/CS electrode | Indirect competitive binding | Alkaline phosphatase | Electrochemical | 180.11 | 0.002 µg/L | Corn | FB1 | [160] |
| SPCEs-Magnetic beads | Competitive multi- immunoassay | HRP | Amperometric | 60 | 0.33 µg/L | CRM, beer | FB1,FB2,FB3 | [182] |
| 96-well microplate | Biopanning | Ab2β Nb /HRP | OD | ~60 | 0.15 µg/L | PBS | FB1,FB2 | [198] |
| Microplate reader | FPIA | FITC | Fluorescence Polarization | <30 | 157.4, 290.6 µg/kg | Maize | FB1, $FB2_2$ | [184] |
| NC membrane | Competitive small molecule detection | UGNs | Colour intensity | <5 | 5 µg/L | Grains | FB1 | [84] |
| NC membrane | Competitive small molecule detection | AuNP | Colour intensity | <5 | 20 µg/L | Grains | FB1 | [84] |
| Ppy/ErGO SPE | Label-free electrochemical immunosensing | AuNP | Current | 40 | 4.2 µg/kg | Corn | FB1 | [199] |
| GCE | Electrochemical impedance spectroscopy | PDMA-MWCNT | Electron transfer resistance | - | 0.0000038 µg/L | Corn | FB1 | [98] |
| NC membrane | Immunochromatographic strip test | DR-AuNP | Visual detection | 10 | 1000 µg/kg | Maize flour | FB1 | [178] |
| Hi-Flow Plus membranes | Competitive reaction | AuNP | Coloration | 15 | 0.6 µg/L | Maize | FB1 | [200] |
| Microbead | Flow immunocytometry | Phycoerythrin | Fluorescence | 45 | 116 µg/kg | Maize | FB1 | [185] |
| NC strips | Competitive assay | Colloidal gold | Colour intensity | 10 | 0.24 µg/L | Agricultural products | FB1 | [168] |
| Plates | IC ELISA | IgG-HRP | Absorbance | 68 | 0.08 µg/L | Agricultural products | FB1 | [168] |
| Mimotope on ARChip Epoxy slides | Competitive binding inhibition | Alexa Fluor 647- IgG | Fluorescence | 210 | 11.1 µg/L | Maize, wheat | FB1 | [201] |
| NC high-flow plus membranes | Competitive binding inhibition | AuNP/ HRP-labelled IgG | Colour | 10 | 25 µg/L | Corn | FB1 | [179] |
| Nitrocellulose membrane | LFIA | AuNP/ CdSe/ZnS QD | Fluorescence | 15 | 62.5 µg/kg | Maize flour | FB1, FB2 | [169] |
| 96-well microplates | Competitive assay | AuNF@FeTPPCl + TMB | Colour | 40 | 0.05 µg/L | Buffer | FB1 | [188] |
| Mycotoxin-protein conjugates on chip (MZI) | Primary (mycotoxin/protein conjugates – anti-mycotoxin specific mAbs) and secondary immunoreaction (immune adsorbed mAbs- IgG antibody) | Label-free | Phase shift | 12 | 5.6 µg/L | Beer | FB1 | [186] |

| | | | | | | | | |
|---|---|---|---|---|---|---|---|---|
| 96-well plates with protein G-coated AuNPs (bulk) | Competitive immunoassay | YFP-tagged FB1-mimotope | Fluorescence | 45 | 1.1 µg/L | Wheat | FB1, FB2 | [187] |
| NC membrane | Competitive inhibition reaction | Antibody- AuNP conjugates, FB1-BSA, IgG | Visual detection | 10 | 30 µg/L | Corn | FB1 | [170] |
| Anti-FB1 mAbs on plate well | Competitive fluorescence ELISA | CAT-regulated-fluorescence quenching of MPA-QD | Fluorescence | 75n | 0.33 µg/L | Corn | FB1 | [202] |
| Gold coated magnetic NP | Competitive CLIA | HRP-LUMINOL | Fluorescence | 150 | 0.027 µg/L | Cereals | FB1 | [203] |
| Microplate | IC-ELISA | IgG-HRP | Absorbance | 120 | 0.078 µg/L | Corn | FB1,FB2,FB3 | [204] |
| Microplate | DC-pELISA | AuNP | Absorbance | 120 | 12.5 µg/L | Corn | FB1 | [205] |
| Test column | IATC | HRP | Color intensity | 5.5 | 20 µg/kg | Maize | FB1,FB2,FB3 | [180] |
| Au nanopillars | Surface-enhanced Raman scattering | Malachite green isothiocyanate-AuNP | Raman intensity | 120 | 0.00511 µg/mL | Standard curve | FB | [161] |
| NC membrane | Direct competition | Streptavidin-horseradish peroxidase | Enhanced chemiluminescence | 45 | 0.24 µg/L | Corn samples | FB1 | [173] |
| Anti- FB1 mAb in microtiter wells | Non-competitive idiometric nanobodies phage ELISA | HRP conjugated anti-M13 antibody-TMB | Absorbance | 130 | 0.19 µg/L | Corn | FB1 | [157] |
| ITO coated glass integrated with PDMS microfluidic channel. | Three-electrode electrochemical sensor | AuNP-Ab | Current | 50 | 0.097 µg/L | Corn | FB1 | [206] |
| Superparamagnetic carboxylated xMAP® microspheres | Quadplex FCIA | R-PE conjugated goat anti-mouse antibody | Fluorescence | 60 | 2.45 µg/L | Milk | FB1 | [158] |
| NC membranes | Multiplex lcr assay | QD nanobeads | Fluorescence | 10 | 20 µg/L | Maize | FB1 | [181] |
| GONC on DEP electrodes | Electroactivity reduction with biorecognition. | Label-free | CV/DPV | 65 | 294 µg/L | PBS-T | FB1 | [207] |
| 96 well plates with protein-G and BSA | Competitive Plasmonic ELISA | Glucose oxidase-FB1 | Absorbance | 180 | 0.31 µg/L | Maize | FB1 | [154] |
| NC membrane | Competitive multiplex lcr Assay | Quantum dot nanobeads-Mab | Fluorescence (test line/ control line) | 18 | 1.58 µg/L | Cereals | FB1 | [174] |
| NC membrane | lcr strip | Flower-like AuNP | Color intensity | 5 | 5 µg/L | Chinese traditional medicine | FB1 | [85] |
| NC membrane | Multiplex lcr test | AuNP | Color intensity | - | 60 µg/L | Wheat and corn | FB1 | [171] |
| Nanomagnetic beads | Competitive solid-phase assay | Biotin NHS-Streptavidin-HRP | OD | 22 | 0.21 µg/L | Maize | FB1 | [153] |
| NC membrane | Competitive lcr strip | Colloidal gold-scFv | Color Intensity | 10 | 2.5 µg/L | Maize | FB1 | [155] |
| NC membrane | Smartphone-based multiplex LFIA | AuNP and TRFMs | Ratio T/C line color & fluorescence | 8 | 0.59 µg/kg CAN 0.42 µg/kg (F) | Maize, wheat, bran | FB1 | [177] |
| Microplate-OVA-FB1 | Competitive immunoreaction | Cysteamine on mAb-RBITC-AuNPs | Fluorescence | 46 | 0.023 µg/L | Maize | FB1, FB2, FB3 | [156] |
| NC membrane | Competitive lcr strip | QDNBs-mAb | Fluorescence | 25 | 60 µg/L | Wheat. Corn | FB1 | [175] |
| NC-membrane | Immunochromatographic assay | Eu-FM-mAB | Time-resolved fluorescence | 7 | 8.26 µg/kg | Corn, corn flour, wheat, rice, brown rice | FB1 | [176] |

[1] Abbreviations: **Ab2β Nb:** Anti-idiotypic nanobody; **AP**/**NBT**/**BCIP:** Alkaline phosphatase/ nitro blue tetrazolium chloride/5-Bromo-4-chloro-3-indolyl phosphate toluidine salt; **AuNP**: Gold nanoparticles(spherical)**; BSA:** Bovine serum albumin; **CAT:** Catalase; **CL:** Chemiluminescence; **CLIA:** Chemiluminescence immunoassay; **CV:** Cyclic voltammetry; **DC:** direct competitive; **DEP:** Disposable electrical printed; **DMA-NAS-MAPS**: Copoplymer (N,Ndimethylacrylamide)- N,N-acryloyloxysuccinimide-[3-(methacryloyl-oxy)propyl] trimethoxysilyl; **DPV:** Differential pulse voltammetry; **DR:** Desert rose-like; **ECL:** Enhanced chemiluminescent; **EIS:** Electrochemical impedane spectroscopy; **ErGO:** Electrochemically reduced graphene oxide; **Eu-FM:** Europium Fluorescent Nanosphere; **FCIA**: Flow cytometric immunoassay; **FeTPPC:** Iron porphyrins; **FITC:** Fluorescein isothiocyanate; **FPIA:** Fluorescence polarization immunoassay; **GCE:** Glassy carbon electrode; **GONC:** Graphene oxide nanocolloids; **HRP:** Horseradish peroxidase; **IATC**: Immunoaffinity test column; **IC:** Indirect competitive; **lcr:** immunochromatographic; **IgG:** Goat anti-mouse immunoglobullin; **ITO:** Indium tin oxide; **LFIA:** Lateral flow immunoassay; **mAb:** Monoclonal antibody; **MPA-QD:** mercaptopropionic acid-modified CdTe quantum dots; **MZI:** Mach-Zehnder interferometers; **NC:** Nitrocellulose; **NHS:** *N*-Hydroxysuccinimide; **NP:** Nanoparticles; **OD:** Optical density; **p:**plasmonic; **PDMA-MWCNT:** Poly(2,5-dimethoxyaniline) multi-walled carbon nanotube composite; **PDMS:** Polydimethylsiloxane**; Ppy:** Polypyrrole; **PrG:** Recombinant Protein G; **QD:** Quantum dot; **QDNBs:** Quantum dots nanobeads; **RBITC:** Rhodamine B isothiocyanate; **R-PE:** R-phycoerythrin; **scFv:** single-chain variable fragment; **SPCEs:** Screen -printed carbon electrode; **SPE:** Screen-printed carbon electrode; **SPGE:** Bare gold screen-printed electrode; **SPR:** Surface plasmon resonance; **SWNTs**/**CS:** Single-walled carbon nanostructure/ Chitosan; **TMB:** 3,3',5,5'-tetramethylbenzidine dihydrochloride; **TRFMs:** Time resolved fluorescence microspheres; **UGNs:** Urchin-like gold nanoparticles; **YFP:** Yellow fluorescent protein

**Table 4.** Other methods for FB1 determination [1]

| Support | Method | Labelling/ Substrate | Bioreceptor | Measurement | Assay Time (min) | LOD | Sample | Fumonisin Type | Ref |
|---|---|---|---|---|---|---|---|---|---|
| Quartz plate | Surface-enhanced Raman spectroscopy | Ag Dendrites | SPR | Raman signal | <1 | >5000 µg/kg (not reported as LOD) | Maize | FB1,FB2, FB3 | [94] |
| Polymer-coated microplates | MIP | HRP-conjugate | nanoMIPs | Absorbance | 70 | 0.0044 µg/L | PBS | FB2 | [208] |
| GCE-AuNPs-Ru@$SiO_2$-Chitosan | SEECL | MIP containing FB1 + MAA+ EDMA+AIBN | MIP-Amino group | ECL | 5 | 0.00035 µg/L | Milk, maize | FB1 | [211] |
| 96-well microplates+EGMP, NIPAm, NAPMA, TBAm | Direct competitive assay based on | HRP–FB1 conjugate + TMB | MINA | Color | 5.16 | 0.00137 µg/L | PBS buffer | FB1 | [159] |
| ITO electrode surface coated with GO/CdS/CS | MIP-Photoelectrochemical sensor | MIP including FB1, MAA, EDMA and AIBN | MIP | Photocurrent | 15 | 0.0047 µg/L | Maize meal and milk | FB1 | [212] |
| Polymer-coated microplates (EGMP,NIPAm,BIS, NAPMA) | MINA | HRP-conjugate + TMB | nanoMIPs | Absorbance | 70 | 0.001 µg/L | Maize | FB1 | [209] |
| Cys-AuNPs | Aggregation based colorimetric detection | AuNPs | HFB1 | Absorbance | 65 | 0.90 µg/kg | Corn | FB1 | [210] |
| Syringe SPE (Nylon membrane) | Solid-phase fluorescence spectrometry | RhB-Cl | Derivatization | Relative Intensity (Fluorescence) | 4 | 0.119 µg/L | Maize | FB1 | [100] |
| nanoMIPSs-Ppy/ZnP-Pt Electrode | Electrochemical sensor | MIP+FB1+NIPAM+BIS+TBAm+EGMP+NAPMA | MIP | EIS, DPV | 5 | 0.0000000216, 0.0000005 µg/L | Maize | FB1 | [86] |
| Fused silica capillary | CE | Ammonium formate/ammonia+ CAN 10% (Background electrolyte) | - | MS | 40 | 156 µg/L | Rice, *Fusarium* microconidia | FB1, FB2 | [217] |

[1]Abbreviations: **CAN:** Acetonitrile; **AIBN:** Azodiisobutyronitrile; **AuNP:** Gold nanoparticles; **BIS:** N,N'- methylene-bis-acrylamide; **CE:** Capillary electrophoresis; **Cys-AuNPs:** Cysteamine-capped gold nanoparticles; **DPV:** Differential pulse voltammetry; **ECL:** Electrochemiluminescence; **EDMA:** Ethylene glycol dimethacrylate; **EIS:** Electrochemical impedance spectroscopy; **EGMP**: Ethylene glycol methacrylate; **GCE:** Glassy carbon electrode; **GO:** graphene oxide; **HFB1**: Alkaline hydrolysis of FB1; **HRP:** Horseradish peroxidase; **ITO:** Indium tin oxide; **MAA:** Methacrylic acid; **MINA:** Molecularly imprinted polymer nanoparticles; **MIP:** Molecularly imprinted polymer; **NAPMA:** N-(3-Aminopropyl) methacrylamide hydrochloride; **NIPAm:** N-isopropylacrylamide; **Ppy**/**ZnP:** Polypyrrole-zinc porphyrin; **RhB-Cl:** 9-[2-(Chlorocarbonyl)phenyl]-3,6-bis(diethylamino) xanthylium; **SEECL:** Surface-enhanced electrochemiluminescence; **SPE:** Solid Phase Extraction; **SPR:** Surface plasmon resonance; **TBAm:** N-tert-butylacrylamide; **TMB:** 3,3′,5,5′-tetramethylbenzidine

**Table 5.** Aptasensors for the determination of FB1[1]

| Support | Labelling | Measurement | Detection Time (min) | Extraction Time (min) | Sample Preparation Steps | LOD µg/L | Sample | Specificity Test[2] | Ref |
|---|---|---|---|---|---|---|---|---|---|
| GO | UCNPs with Er and Tm | Fluorescence spectra | 200 | - | - | 0.1 | PBS | **OTA**, AFB1, AFB2, AFG1, AFG2, FB2, ZEN | [81] |
| Carboxilated MNPs/MB | UCNPs | Fluorescence | 100 | >2 | 7 | 0.01 | Maize | - | [232] |
| Centrifuge tubes | AuNP-cDNA | Absorbance | 35 | 30 | 3 | 0.125 | Beer | - | [241] |
| SPCMs | FITC-Complementary DNA | Fluorescence | 60 | 135 | 3 | 0.00016 | Cereal | AFB1, **OTA**, FB2 | [234] |
| cDNA modified Au electrode | Au NPs–Ir | ECL | 120.41 | - | 5 | 0.27 | Wheat flour | OTA, AFT, L-cystein, BSA | [230] |
| GCE-AuNPs | Label free | EIS | 30 | 745 | 8 | 0.0014 | Maize | AFB1, ZEN, T-2 toxin | [222] |
| Au coated silicon cantilever beams | Label Free | Deflection | 30 | - | - | 33 | Buffer | OTA, DON | [148] |
| GCE-AuNPs-capture DNA | GS-TH | CV | 25.11 | - | - | 0.001 | Ultra-pure water | AFB1, OTA, ZEN, DON | [240] |
| cDNA (Corning® Costar® 96-Well Cell Culture Plates) | PicoGreen | Fluorescence intensity | 25 | - | 2 | 0.1 | Milk | CTN,OTA, AFB1, ZEN | [90] |
| SPCE- PDMS microcell | AuNPs | Impedance signal | 30 | 735 | 7 | 0.0034 | Corn | FB2, OTA, AFB1 | [231] |
| SPCM | cy3 modified aptamer | Fluorescence | 90 | 751 | 7 | 0.01104 | Cereals | AFB1, **OTA** | [235] |
| $SiO_2$ spheres/ $Fe_3O_4$@Au Magnetic Beads-cDNA | PbS QD | SWV (current) | 65 | 15 | 4 | 0.02 | Maize | **OTA**, OTB, AFB1 | [236] |
| Reduce graphene/Ni/ Pt NPs micromotors | Fluorescein amidine (FAM) labelled aptamer | Fluorescence intensity | 15 | Maize: 30<br>Beer: 20<br>Whine: - | 4,1,1 | 0.4 | Maize, Beer | **OTA** | [237] |
| Graphene modified GCE | Label free | Impedimetric signal | 30 | - | - | 0.0123 | Tris buffer | - | [223] |
| Centrifuge tube | FAM-Complementary DNA | Fluorescence | 21 | - | - | 7.21 | Buffer | AFB1, AFB2, OTA, FB2 (response) | [243] |
| $TiO_2$ modified porous silicon | Cy3 labelled aptamer-BHQ2 labelled anti aptamer | Fluorescence Intensity | 720 | 751 | 7 | 0.00021 | Cereal (Rice, Wheat, Corn) | **OTA, AFB1** | [80] |
| GONC on DEP carbon electrodes | GONC | Peak current intensity | 65 | - | - | 10.82 | Tris buffer | OTA, Thrombin | [91] |
| Reduced graphene/ Pt NPs micromotors | FAM labelled aptamer | Fluoresecence | 17 | 30, 20 | 3,2 | 0.70 | Maize. Beer | **OTA** | [238] |
| GO-cDNA (probe1)& $Fe_3O_4$/GO-cDNA (probe 2) | Allochroic dyes (thymolphthalein)-alkaline conditions | Absorbance | 90 | 40 | 7 | 100 (lowest value explored) | Peanut | **OTA, AFB1, microcystin-LR** | [242] |
| Amine funtionalized $Fe_3O_4$ magnetic particles | $NaYF_4$: Ce/Tb nanoparticles-cDNA | Fluorescence decrease | 60 | >2 | 7 | 0.000019 | Maize | **OTA**<br>T-2, AFB1, OTB, ZEN | [95] |
| GO/$Fe_3O_4$ nanocomposites | Aptamer-Red QDs | Fluorescence inensity | 60 | - | 3 | 0.0162 | Peanut | OTA, **AFB1**, OTB. AFM1, AFB2 | [239] |
| cDNA on AuE | Methylene blue | Peak current | 40 | 45 (Corn) | 3 (Corn)<br>1 | 0.00015 | Corn<br>Beer | OTA, ZEN, AFB1 | [227] |
| $MoS_2$-Au modified GCE | FC6S -Au-cDNA | Current difference | 15 | - | - | 0.0005 | PBS | **ZEN**<br>α-ZOL, AFB1, DON, T-2, OTA | [228] |
| cDNA on AuE | AuNRs-Fc | DPV | 10 | - | 4 | 0.00026 | Beer | **OTA**, ZEN, AFB1 | [229] |
| cDNA on AuNR | Cy5.5-aptamer | SERS/ Fluorescence | 45 | 735 | 8 | 0.0003/ 0.0005 | Corn | AFB1, ZEN, PAT, OTA, FB2, FB3 | [87] |
| Streptavidin coated microplate | TMB | Absorbance | 73 | 30 | 11 | 0.3 | Beer<br>Corn | AFB, DON, OTA, ZEN | [233] |
| cDNA2 on AuNR | UCNPs-Hibridized TAMRA-cDNA1& Aptamer | Fluorescence | 50 | 735 | 7 | 0.000003 | Corn | **ZEN**, AFB1, OTA, PAT, OTB | [96] |
| Aptamer-Magnetic Beads | cDNA-AgNP | Ag intensity (ICP-MS) | 121 | 42 | 8 | 0.3 | Wheat Flour | **OTA**, AFB1, DON, ZEN, FB2 | [149] |
| Aptamer-AuNP-UCNP-AuNP-cDNA | 4-MBA | SERS | 121 | 735 | 9 | 0.00002 | Corn | **ZEN, OTA**, AFB1, PAT, T-2 | [88] |
| ITO electrodes | Silver-Au-Aptamer-cDNA-$Fe_3O_4$ & Prussian Blue | Color change of ITO (Mobile phone) | 62 | - | - | 0.01 | Corn | DON, OTA | [226] |
| AuNP | AuNP | UV-Vis | 192.2 | - | - | 0.000056 | $MgCl_2$ 1mM Buffer | OTA, AFB1 | [89] |
| GO-Au-Thionine on GCE | Label-Free | CV | 25 | 10 min | 4 | 0.01 | Corn | Mycotoxins | [244] |

[1] Abbreviations: **AFB1:** Aflatoxin B1; **AFB2:** Aflatoxin B2; **AFG1:** Aflatoxin G1; **AFG2:** Aflatoxin G2; **AgNP:** Silver nanoparticles; **AuE:** Gold electrode; **AuNP:** Gold nanoparticles; **AuNRs:** Gold nanorods; **BHQ2:** Black hole quencher; **cDNA:** complementary DNA; **CTN:** Citrinin; **Cy:** Cyanine; **CV:** Cyclic voltammetry; **DEP:** Disposable electrical printed; **DON:** Deoxynivalenol; **DPV:** Differential pulse voltammetry; **FAM:** Fluorescein amidine; **FB2:** Fumonisin B2; **Fc:** Thiol modified ferrocene; **FC6S:** 6-(Ferrocenyl)hexanethiol; **FITC:** Fluorescein isothiocyanate; **GCE:** Glassy carbon electrode; **GO:** Graphene oxide; **GONC:** Graphene oxide nanocolloids; **GS:** Graphenes; **ICP-MS:** Inductively coupled plasma mass spectrometry; **ITO:** Indium Tin Oxide; **MB:** Molecular beacon; **MBA:** Mercaptobenzoic acid ; **MNP:** Magnetic nanoparticles; **$MoS_2$:** Molybdenum disulfide; **NP:** Nanoparticles; **PDMS:** Polydimethylsiloxane; **OTA:** Ochratoxin A; **OTB:** Ochratoxin B; **QD:** Quantum dots; **SERS:** Surface-enhanced Raman spectroscopy; **SPCE:** Screen-printed carbon electrode; **SPCM:** Silica photonic crystal microsphere; **TAMRA:** Carboxytetramethylrhodamine; **TH:** Thionine; **TMB:** 3,3',5,5'-tetramethylbenzidine; **UCNPs:** Upconversion fluorescent nanoparticles; **ZEN:** Zearalenone; **ZOL:** Zearalenol; **PAT:** Patulin

[2] Mycotoxins highlighted in bold indicate a multiplex assay

**Table 6** DNA sequences utilized for different aptasensor and their binding conditions[1]

| Aptamer Modification | cDNA | Other | Binding Buffer | Incubation | Ref |
|---|---|---|---|---|---|
| **5′-ATA CCA GCT TAT TCA ATT AAT CGC ATT ACC TTA TAC CAG CTT ATT CAA TTA CGT CTG CAC ATA CCA GCT TAT TCA ATT AGA TAG TAA GTG CAA TCT-3′** | | | | | [69] |
| 5′-Biotin-$(CH_2)_6$- | - | - | Tris-HCl buffer (10 mM containing 100 mM NaCl, pH 7.4) | 37 °C Overnight (conjugation in BB)<br>37 °C, 2 h (Binding)<br>37 °C, 80 min (Incubation with GO) | [81] |
| 5′-Biotin-$(CH_2)_6$- | 5′-AAT TGA ATA AGC TGG-3 | Molecular Beacon<br>5′-SH-$(CH_2)_6$-GCT CG CCA GCT TAT TCA ATT CGA GC-$(CH_2)_6$-$H_2$N-3′ | 10 mM PBS | 37 °C 12 h (immobilization on MNPs)<br>37 °C, 30 min (hibridization aptamer-cDNA)<br>37 °C, 30–40 min (incubation)<br>37 °C, 30 min (hibridization cDNA-MB) | [232] |
| None | 5′ -SH-AAT TGA ATA AGC TGG TA-3′ | 5′-SH TAC CAG CTT ATT CAA TT-3′ | 10 mM PB containing 1% SDS by mass pH 7.4 (DNA dilution)<br>500 Mm NaCl cDNA1<br>300 mM NaCl cDNA2<br>1 x PCR amplification buffer (Conjugate dilution)<br>20 mM NaCl + 10 mM PB | 37 °C, shaking for 12 h (funtionalization)<br>RT, overnight salt aging<br>95 °C, 5 min (hibridization cDNA1-cDNA2)<br>Cool down RT | [241] |
| -$(CH_2)_6$-$NH_2$-3′ | 5′-FITC-AAT TGA ATA AGC TGG TA-3′ | - | TE solution (100 mM Tris-HCl + 10 mM EDTA)<br>5× saline sodium citrate (hibridization)<br>10mM Tris-HCl (pH 8.0), 120 mM NaCl, 20 mM $CaCl_2$, 5 mM KCl, 20 mM $MgCl_2$ (binding) | 4 °C, 12 h. (Immobilization on SPCMs in TE solution)<br>37 °C, 1 h. (blocking with 1B% BSA PBS)<br>37 °C, 2 h. (hibridization)<br>37 °C, 1 h (binding) | [234] |
| 5′-SH-$(CH_2)_6$- | -SH-$(CH_2)_6$-AAT TGA ATA AGC TGG TAT | - | Methanol 50% | 80 °C, 5 min (hibridization)<br>Cooled to RT<br>37 °C, 2 h (binding) | [230] |
| 5′-SH-$(CH)_6$- | - | - | 10 mM Tris–HCl, 100 mM NaCl,<br>100 mM TCEP, pH 7.4 (immobilization)<br>10 mM Tris–HCl, 100 mM NaCl pH 7.4. (binding) | 3 h, 25 °C (Functionalization)<br>1 h, 25 °C with MCH (blocking)<br>10 min, 25 °C, (Incubation) | [148] |
| None | 5′-SH-$(CH_2)_6$-AAT TGA ATA AGC TGG TA-3′ | - | 10 mM Tris-HCl buffer pH 7.4 (hibridization)<br>PBS (pH 7.4). (binding) | 24 h, RT (cDNA immobilization)<br>37 °C, 2 h. (hibridization)<br>Room temperature, 25 min (binding) | [240] |
| 5′-AAT CGC ATT ACC TTA TAC CAG CTT ATT CAA TTA CGT CTG CAC ATA CCA GCT TAT TCA ATT-3′ | 5′-AAT TGA ATA AGC TGG TAT GTG CAG ACG TAA TTG AAT AAG CTG GTA TAA GGT AAT GCG ATT-3′ | - | 10 mmol/L Tris, 120 mmol/L NaCl, 5 mmol/L KCl、20 mmol/L $CaCl_2$ (pH 8.5) | 95 ℃, 5 min (denaturation)<br>10 min on ice<br>25 ℃, 20 min (Incubation)<br>25 ℃, 5 min (hibridization) | [90] |
| FB139t3: F- ATA CCA GCT TAT TCA ATT AAT CGC ATT ACC TTA TAC CAG CTT ATT CAA TTA CGT CTG CAC ATA CCA GCT TAT TCA ATT<br>FB139t3-5: F- AAT CGC ATT ACC TTA TAC CAG CTT ATT CAA TTA CGT CTG CAC ATA CCA GCT TAT TCA ATT | - | - | 100 mM NaCl, 20 mM Tris, 2 mM $MgCl_2$, 5 mM KCl, 1 mM $CaCl_2$, pH 7.6 (selection buffer) | Dnase I assay: 30 min, RT (Incubation with FB1)<br>Magnetic beads assay:<br>90 °C, 10 min (pre-heating)<br>RT, 30 min<br>RT, 60 min (Incubation) | [221] |
| 5′-SH-$(CH_2)_6$- | - | - | Aptamer stock: 50 mM Tris-HCl buffer (ph 7.4, 0.1M NaCl, 0.2M KCl, 5 mM $MgCl_2$ and 1 mM EDTA)<br>Activation Buffer: 50 mM Tris-HCl with 100 mM TCEP<br>Activated aptamer: 50 mM Tris-HCl pH 7.4 with 1.0 mM EDTA)<br>PBS 0.1M, pH 7.4<br>Binding buffer: TE buffer containing 0.1 M NaCl, 0.2 M KCl, and 5.0 mM $MgCl_2$ | Room temperature, 1 h (activation)<br>6 h and 4 °C (SPCE modification with activated aptamer)<br>1 h, RT (Blocking with MCH)<br>Room temperature, 30 min h (binding) | [231] |
| 5′-$NH_2$-$(CH_2)_6$-reverse sequence-Cy3-*3′ | 5′-BHQ2-TAT GGT CGA ATA AGT TAA-3′ | - | Binding buffer: Tris-HCl, 0.01 M, pH 8.0, NaCl 120 mM, $CaCl_2$ 20 mM, KCl, 5 mM, $MgCl_2$ 20 mM | 60 min and 37 °C (hibridization)<br>Room Temperature 12 h (Immobilization on microspheres)<br>90 min and 45 °C (binding) | [235] |
| –$NH_2$–3′ | 5′-TTG AAT AAG CTG GTA TAA GGT AAT GCG ATT AAT TGA ATA AGC TGG TAT–SH–3′ | - | 10 mM Tris-HCl, 1 mM EDC, 1 mM NHS (aptamer conjugation)<br>10 mM Tris-HCl with 100 mM TCEP (cDNA activation) | 37 °C, overnight (aptamer conjugation)<br>37 °C, 1 h. (cDNA activation)<br>37 °C, 30 min (cDNA incubation with MBs )<br>RT, 1 h (blocking with MCH)<br>37 °C, 2 h. (hibridization)<br>37 °C, 1 h (binding) | [236] |
| 5′-FAM- | | - | Tris-HCl pH 7.5; 10 mM<br>PBST: 100 mM PBS (pH 7.5) with 0.01% Tween (Aptamer dilution) | 25 ℃, 15 min (Incubation) | [237] |

| | | | | | |
|---|---|---|---|---|---|
| None | FAM- AATAAGCTGGTATGT | - | 20 mM Tris, 0.1 M NaCl, 2 mM $MgCl_2$, 5 mM KCl, 1 mM $CaCl_2$ pH 7.6 (Binding buffer) | 95 °C, 5 min (Heating)<br>5 min on ice<br>37 °C, 1 h. (hibridization) | [243] |
| 5′-$NH_2$–$(CH_2)_6$- reverse sequence-Cy3-3’ | 5′-BHQ2-TAT GGT CGA ATA AGT TAA-3′ | - | Binding buffer: Tris-HCl 10 mM (pH 8.0), NaCl 120 mM, $CaCl_2$ 20 mM, KCl 5 mM,$MgCl_2$ 20 mM) | 88 °C, 5 min (Heating in BB)<br>25 °C, 2 h (aptamer-antiaptamer mixture and incubation)<br>37 °C, 12 h (hibridization-immobilization)<br>37 °C, 12 h (Binding) | [80] |
| 5’-FAM- | - | - | 10 mM Tris-HCl pH 7.5 (aptamer reconstitution/ incubation)<br>SDS 1% v/v (aptamer capture)<br>PBS 100 mM pH 7.5 with Milli-Q water and 0.01% of Tween (PBS-T) (Aptamer dilution) | 25 °C, 15 min (Incubation)<br>RT, 2 min (Aptamer capture) | [238] |
| None | 5’-GTG TGT GTG TGT GTG TGT GTG TGT GTG TGT AGA TTG CAC TTA CTA TCT AAT TGA ATA AGC TGG TAT GTG CAG ACG TAA-3’ | 5’-TTG AAT AAG CTG GTA TAA GGT AAT GCG ATT AAT TGA ATA AGC TGG TAT GTG TGT GTG TGT GTG TGT GTG TGT-3’ | PBS, ($Na_2HPO_4$–$NaH_2PO_4$, 0.1 M) | RT, 2 h (DNA1 binding on GO)<br>RT, 24 h (DNA2 immobilization on $Fe_3O_4$/GO)<br>RT, 12 h (hibridization)<br>37 °C, 1.5 h (Incubation) | [242] |
| 5′-biotin-$(CH_2)_6$- | 5′-biotin-$(CH_2)_6$-TCT AAT TGA ATA AGC TGG TAT GTG CAG ACG-3′ | - | PBS (10 mM $Na_2HPO_4$, 137 mM NaCl, 2.7 mM KCl, 2 mM $KH_2PO_4$, pH 7.4) | 37 °C, 1 h (Incubation) | [95] |
| –$NH_2$–3′ | - | - | PBS 0.1M (pH 7.4) | RT, overnight (bio-probe)<br>RT, overnight (Immobilization)<br>37 °C, 1 h (Incubation) | [239] |
| None | 5′-SH-GAG GGG TGG GCG GGA GGG AGA TTG CAC GGA CTA TCT AAT TGA ATA AGC-3′ | | Tris–HCl buffer (containing 0.05 M Tris, 0.2 M NaCl and 0.001 M EDTA) | 37 °C (cDNA Immobilization)<br>37 °C, 2 h (hibridization)<br>37 °C, 10 min (Incubation FB1)<br>37 °C, 30 min (Incubation Exo-I) | [227] |
| 5′-SH-$(CH_2)_6$ | 5′-SH-$(CH_2)_6$-AATTGAATAAGCTGG-3′ | | TE Buffer (solutions, washing)<br>PBS (0.1 M, ph 6.0) | 95 °C, 5 min (Heating)<br>RT 1h (Cooling)<br>37 °C, 2 h (Ap conjugation to electrode)<br>37 °C, 2 h (hibridization)<br>15 min (Incubation) | [228] |
| 5′-SH- | 5′-SH-GAG GGG TGG AGA TTG CAC TTA CTA TCT AAT TGA GGG GGG TGT CCG ATG CTC-3′ | | 50 mM Tris-HCl | 2 h (Conjugation to AuNRs)<br>37 °C , 2 h (cDNA Immobilization on electrode)<br>37 °C, 2 h (hibridization)<br>37 °C, 10 min (Incubation) | [229] |
| 5’-biotin | 5’-biotin- AGA TTG CAC TTA CTA TCT AAT TGA ATA AGC TGG TAT GTG CAG ACG TAA TTG AAT AAG CTG GTA TAA GGT AAT GCG ATT AAT TGA ATA AGC TGG TAT -30. | | PBS buffer (10 mmol/L $Na_2HPO_4$, 2 mmol/L $KH_2PO_4$, 2.7 mmol/L KCl, 137 mmol/L NaCl, pH 7.4)<br>PBS-T (Washing) | 37 °C, 30 min (Immobilization)<br>25 °C, 60 min (Immobilization) | [233] |
| 5’-biotin | 5’-biotin-GAT AGG AGT CGT GTG GGA TAG TGT GGG AGA TTG CAC TTA CTA TCT AAT TGA ATA AGC TGG TAT GTG CAG ACG TAA-3’ | | Tris-HCl buffer 20 mmol/L with 0.5 mol/L NaCl,1 mmol/L EDTA (Washing)<br>20 mM Tris-HCl pH 7.4 (Dissolving/Target Incubation)<br>100 mM Tris-HCl pH 7.4 (Re-dispersion) | 37 °C, 120 min (Functionalization of magnetic beads)<br>37 °C, 90 min (Labelling of Ag NPs)<br>37 °C, 120 min (Hibridization)<br>37 °C, 120 min (Target Incubation) | [149] |
| 5′-SH-$C_6$- | 5-$NH_2$-C6-AAT TGA ATA AGC TGG TA-3’ | 5-SH-$C_6$-GTTGGTGAGTCCAACCACACCA-3’ (Control DNA) | PBS, pH 7.4, 1× (Washing, redispersion, AuNP stability)<br>Tris-HCl buffer 0.01 M,<br>pH 7.4 (Hibridization, target incubation) | 37 °C, 120 min (Functionalization of $Fe_3O_4$)<br>37 °C, 30 min (Hibridization)<br>37 °C, 30 min (Target Incubation) | [226] |
| None | - | - | $MgCl_2$ 1mM | 37 °C, 30 min (Target Incubation)<br>RT, 60 min (Functionalization of AuNP) | [89] |
| 5’-SH- | - | - | PBS pH 7.4 (Eletrochemical measurements/Sample dilution)<br>Tris-HCl buffer(Washing) | RT, 25 min (Incubation) | [244] |
| **5’-AGC AGC ACA GAG GTC AGA TGC GAT CTG GAT ATT ATT TTT GAT ACC CCT TTG GGG AGA CAT CCT ATG CGT GCT ACC GTG AA-3’** | | | | | [70] |
| 5′-SH-$(CH_2)_6$- | - | - | pH 7.4, 100 mM NaCl, 20 mM Tris–HCl, 2 mM $MgCl_2$, 5 mM KCl, 1 mM $CaCl_2$ | 37 °C, 6 h (electrode modification)<br>94 °C, 5 min followed by 15 min cooling with ice (folding)<br>Room temperature, 30 min (binding) | [222] |
| 5’-C GAT CTG GAT ATT ATT TTT GAT ACC CCT TTG GGG AGA CAT- 3’ | - | - | PBS pH 7.0 (aptamer solution)<br>Tris buffer pH 8.2(FB1 solution) | 60 °C, 15 min (aptamer dropcasting)<br>37 °C, 30 min (Incubation) | [223] |
| 5’-C GAT CTG GAT ATT ATT TTT GAT ACC CCT TTG GGG AGA CAT- 3’ | - | - | Aptamer dilution: PBS (10 mM $Na_2HPO_4$; 100 mM NaCl; pH 7.2)<br>FB1 dilution: Tris (25 mM Tris; 300 mM NaCl; pH 8.2). | 60 °C, 10 min (cast on GONC)<br>25 °C, 5 min (washing in PBS)<br>37 °C, 1 h (Incubation) | [91] |

**NOT SPECIFIED SEQUENCES**

| | | | | | |
|---|---|---|---|---|---|
| Cy5.5 | cDNA | - | 10 mM Tris-HCl, 100 mM NaCl, 1 mM EDTA, pH 8.0 (hibridization buffer)<br>50 mM TE buffer pH 7.4 (Extract adjustment) | 37 °C, 1 h (Hibridization)<br>37 °C, 45 min (Incubation/Hibridization) | [87] |
| None | cDNA1 | cDNA2 | PBS containing 0.9% NaCl (Hybridization buffer) | RT, 12 h (cDNA2 attachment on AuNR)<br>RT, 12 h (UCNPs funtionalization with aptamers)<br>RT, 12 h (Addition of cDNA1 to aptamer-UCNPs)<br>60 °C, 50 min (Hibridization with cDNA2-AuNR)<br>37 °C, 50 min (Cooling)<br>37 °C, 50 min (Incubation) | [96] |
| NS | cDNA | | Hybridization buffer (not specified)<br>PBS buffer(redispersion)<br>50 mM TE buffer pH 7.4 (pH adjustement) | 37 °C, 12 h (Hibridization)<br>37 °C, 2 h (Target Incubation) | [88] |

[1] Abbreviations: **AuNRs:** Gold nanorods; **BB:** Binding buffer; **BSA:** Bovine serum albumin; **cDNA:** Complementary DNA; **GO:** Graphene oxide; **GONC:** Graphene oxide nanocolloids; **MCH:** 6-mercapto-1-hexanol; **NS:** Not specified; **RT:** Room temperature; **SPCE:** Screen-printed carbon electrode; **SPCM:** Silica photonic crystal microsphere; **UCNPs:** Upconversion fluorescent nanoparticles

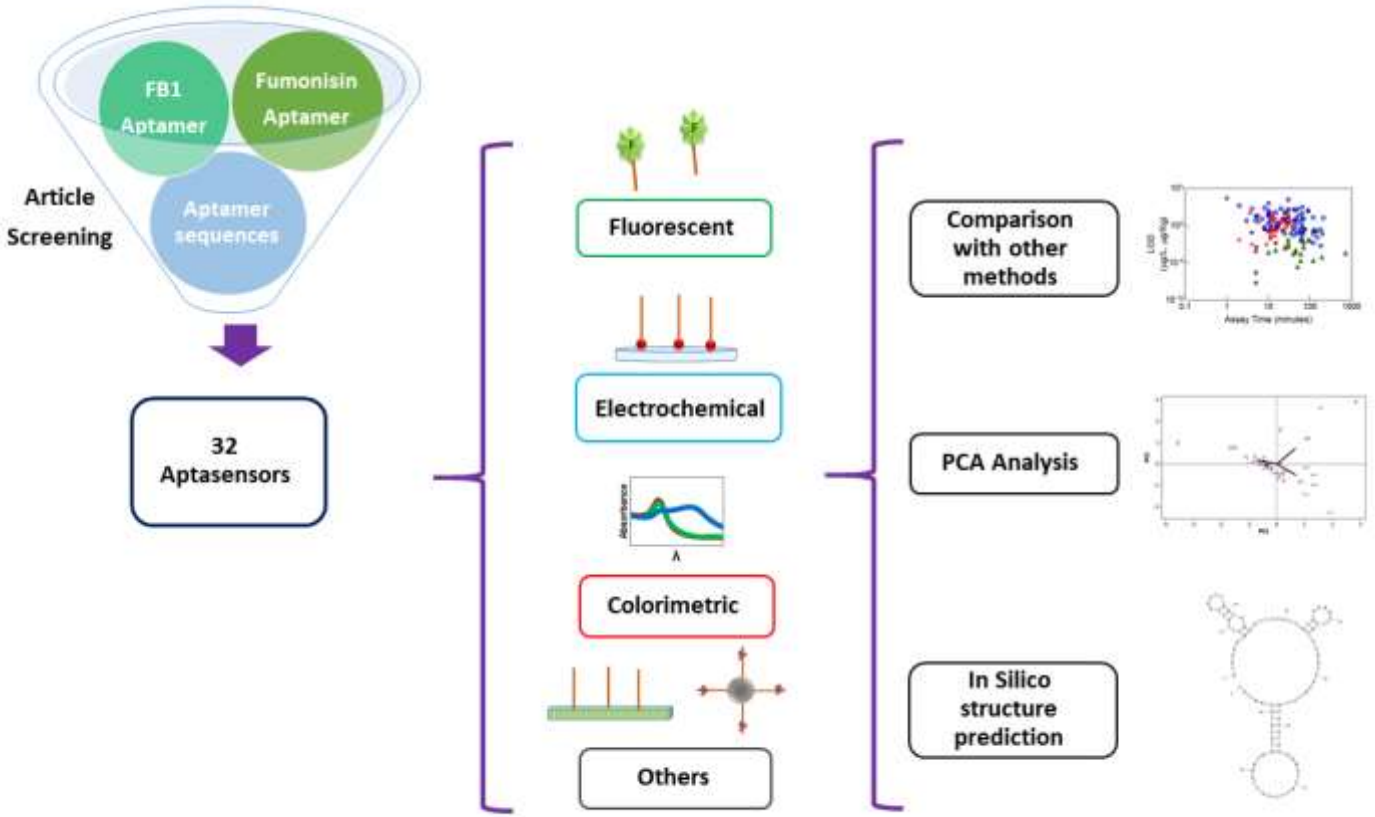


**Graphical Abstract**